PB91-100545

Performance of Jointed Concrete Pavements

Volume III Summary of Research Findings

Publication No. FHWA-RD-89-138
November 1990

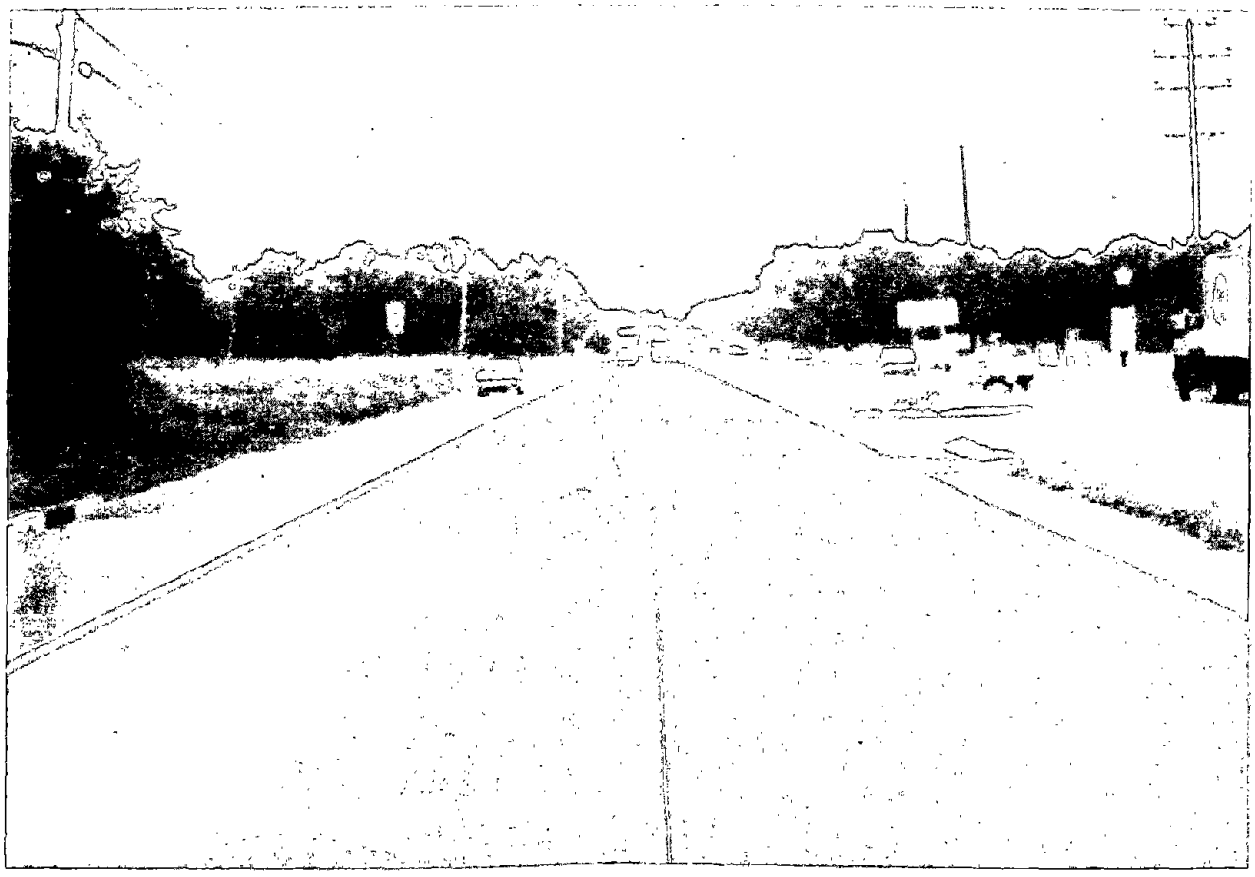

NJ Route 130 10-in. JRCP 12-in. gravel base 36 Years 35 Million ESAL's PSR - 3.8

REPRODUCED BY
U.S. DEPARTMENT OF COMMERCE
NATIONAL TECHNICAL
INFORMATION SERVICE
SPRINGFIELD, VA 22161

U.S. Department of Transportation
Federal Highway Administration

Office of Research and Development
Turner-Fairbank Highway Research Center
6300 Georgetown Pike
McLean, Virginia 22101-2296

FOREWORD

This report is the final report for a six-volume set of reports documenting the performance of 95 experimental or other in-service pavements in the United States or Canada (Interim Reports - Volumes I, IV and V) and describing the evaluation of various design and analysis models and the development of improved prediction models (Interim Reports - Volumes II and VI). The five interim reports have previously been distributed.

This report (Volume III) summarizes the data collection procedures and describes the evaluation of the effect of slab thickness, base type, slab length, slab reinforcement, joint orientation, joint load transfer, dowel bar coatings, longitudinal joint design, joint sealing, tied shoulders, widened traffic lanes, and subdrainage on pavement performance. Various concrete pavement design and analysis models are generally described and selected analysis models are evaluated using case studies from one State in each of the four general environmental regions. New prediction models were then developed using data from this project and from NCHRP Report 277 (COPES) data. The cost effectiveness of various newer design features of 15 recently constructed projects (seven years old or less) were then generally evaluated.

This comprehensive evaluation will be of interest to those involved in the design, construction, maintenance, rehabilitation or performance evaluation of jointed concrete pavements.

Sufficient copies of this report are being distributed by FHWA memorandum to provide five copies to each FHWA Region office, two copies to each FHWA Division office and four copies to each State Highway Agency. Direct distribution is being made to the Division offices. Additional copies for the public are available from the National Technical Information Service (NTIS), U.S. Department of Commerce, 5285 Port Royal Road, Springfield, Virginia 22161. A small charge will be imposed for each copy ordered from NTIS.

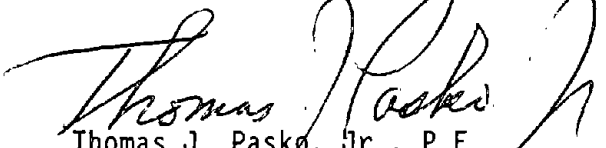

Thomas J. Pasko, Jr., P.E.
Director, Office of Engineering and
Highway Operations Research and Development

NOTICE

This document is disseminated under the sponsorship of the Department of Transportation in the interest of information exchange. The United States Government assumes no liability for its contents or use thereof. The contents of this report reflect the views of the contractor, who is responsible for the accuracy of the data presented herein. The contents do not necessarily reflect the official policy of the Department of Transportation. This report does not constitute a standard, specification, or regulation.

The United States Government does not endorse products or manufacturers. Trade or manufacturers' name appear herein only because they are considered essential to the object of this document.

Technical Report Documentation Page

1. Report No.	2. Government Accession No.	3.
FHWA-RD-89-138		PB91-100545

4. Title and Subtitle	5. Report Date
PERFORMANCE OF JOINTED CONCRETE PAVEMENTS, Volume III - Summary of Research Findings	November 1990
	6. Performing Organization Code
7. Author(s)	8. Performing Organization Report No.
K.D. Smith, D.G. Peshkin, M.I. Darter, A.L. Mueller	
9. Performing Organization Name and Address	10. Work Unit No. (TRAIS)
ERES Consultants, Inc. 1401 Regency Drive East Savoy, Illinois 61874	3C1A2012
	11. Contract or Grant No. DTFH61-86-C-00079
	13. Type of Report and Period Covered
12. Sponsoring Agency Name and Address	Final Report Oct. 1986 - March 1990
Office of Engineering & Highway Operations R&D Federal Highway Administration 6300 Georgetown Pike McLean, VA 22101-2296	14. Sponsoring Agency Code

15. Supplementary Notes

FHWA COTR:
Roger M. Larson, HNR-20

16. Abstract

A major national field and analytical study has been conducted into the effect of various design features on the performance of jointed concrete pavements. Extensive design, construction, traffic, and performance data were obtained from numerous experimental and other concrete pavement sections throughout the country. Field data collected and analyzed included distress, drainage, roughness, present serviceability rating (PSR), deflections, destructive testing (coring and boring), and weigh-in-motion (WIM) on selected sites. This information was compiled into a comprehensive microcomputer database. Projects were evaluated on an individual basis and then compared at a national level to identify performance trends. The performance data was used to evaluate and modify several concrete pavement design procedures and analysis models.

This volume provides a broad overview of the work performed in this study. Summaries of the effect of various design features on concrete pavement performance are reviewed and performance trends identified. The accuracy of various prediction models and analysis methods are examined using the field performance data. From that evaluation, new prediction models were developed and a cost-effectiveness evaluation was performed.

This volume is the third in a series. The other volumes are:

FHWA Report No.	Vol. No.	Short Title
FHWA-RD-89-136	I	Evaluation of Concrete Pavement Performance and Design Features
FHWA-RD-89-137	II	Evaluation and Modification of Concrete Pavement Design and Analysis Models
FHWA-RD-89-139	IV	Appendix A - Project Summary Reports and Summary Tables
FHWA-RD-89-140	V	Appendix B - Data Collection and Analysis Procedures
FHWA-RD-89-141	VI	Appendix C - Synthesis of Concrete Pavement Design Methods and Analysis Models
		Appendix D - Summary of Analysis Data for the Evaluation of Predictive Models

17. Key Words	18. Distribution Statement
concrete, concrete pavement, pavement performance, pavement evaluation, pavement design, nondestructive testing, slab thickness, base type, joint spacing, reinforcement, subdrainage	No restrictions. This document is available through the National Technical Information Service, 5285 Port Royal Road, Springfield, VA 22161

19. Security Classif. (of this report)	20. Security Classif. (of this page)	21. No. of Pages	22. Price
Unclassified	Unclassified	145	

Form DOT F 1700.7 (8-72) Reproduction of completed page authorized

SI* (MODERN METRIC) CONVERSION FACTORS

APPROXIMATE CONVERSIONS TO SI UNITS

Symbol	When You Know	Multiply By	To Find	Symbol
LENGTH				
in	inches	25.4	millimetres	mm
ft	feet	0.305	metres	m
yd	yards	0.914	metres	m
mi	miles	1.61	kilometres	km
AREA				
in^2	square inches	645.2	millimetres squared	mm^2
ft^2	square feet	0.093	metres squared	m^2
yd^2	square yards	0.836	metres squared	m^2
ac	acres	0.405	hectares	ha
mi^2	square miles	2.59	kilometres squared	km^2
VOLUME				
fl oz	fluid ounces	29.57	millilitres	mL
gal	gallons	3.785	litres	L
ft^3	cubic feet	0.028	metres cubed	m^3
yd^3	cubic yards	0.765	metres cubed	m^3

NOTE: Volumes greater than 1000 L shall be shown in m^3.

MASS				
oz	ounces	28.35	grams	g
lb	pounds	0.454	kilograms	kg
T	short tons (2000 lb)	0.907	megagrams	Mg
TEMPERATURE (exact)				
°F	Fahrenheit temperature	5(F-32)/9	Celcius temperature	°C

APPROXIMATE CONVERSIONS FROM SI UNITS

Symbol	When You Know	Multiply By	To Find	Symbol
LENGTH				
mm	millimetres	0.039	inches	in
m	metres	3.28	feet	ft
m	metres	1.09	yards	yd
km	kilometres	0.621	miles	mi
AREA				
mm^2	millimetres squared	0.0016	square inches	in^2
m^2	metres squared	10.764	square feet	ft^2
ha	hectares	2.47	acres	ac
km^2	kilometres squared	0.386	square miles	mi^2
VOLUME				
mL	millilitres	0.034	fluid ounces	fl oz
L	litres	0.264	gallons	gal
m^3	metres cubed	35.315	cubic feet	ft^3
m^3	metres cubed	1.308	cubic yards	yd^3
MASS				
g	grams	0.035	ounces	oz
kg	kilograms	2.205	pounds	lb
Mg	megagrams	1.102	short tons (2000 lb)	T
TEMPERATURE (exact)				
°C	Celcius temperature	1.8C + 32	Fahrenheit temperature	°F

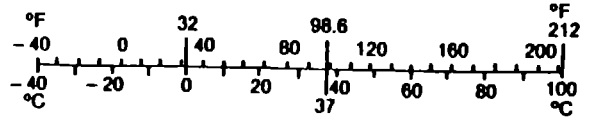

* SI is the symbol for the International System of Measurement

(Revised April 1989)

TABLE OF CONTENTS

VOLUME I EVALUATION OF CONCRETE PAVEMENT PERFORMANCE AND DESIGN FEATURES

Chapter		Page
1	INTRODUCTION	1
	1. OBJECTIVES	1
	2. BACKGROUND AND RESEARCH APPROACH	2
	3. SEQUENCE OF REPORT	3
2	DESCRIPTION OF PROJECTS IN STUDY	4
	1. INTRODUCTION	4
	2. DESCRIPTION OF EXPERIMENTAL AND SINGLE PAVEMENT SECTIONS	6
	Dry-Freeze Environmental Region	6
	Minnesota 1	6
	Minnesota 2	6
	Minnesota 3	6
	Minnesota 4	6
	Minnesota 6	8
	Dry-Nonfreeze Environmental Region	8
	Arizona 1	8
	Arizona 2	8
	California 1	8
	California 2	8
	California 6	11
	California 7	11
	California 8	11
	Wet-Freeze Environmental Region	11
	Michigan 1	11
	Michigan 3	13
	Michigan 4	13
	Michigan 5	13
	New York 1	13
	New York 2	13
	Ohio 1	15
	Ohio 2	15
	Ontario 1	15
	Ontario 2	15
	Pennsylvania 1	15
	New Jersey 2	18
	New Jersey 3	18
	Wet-Nonfreeze Environmental Region	18
	California 3	18
	North Carolina 1	21
	North Carolina 2	21
	Florida 2	21
	Florida 3	21
	3. GENERAL DATA COLLECTION EFFORTS	21

TABLE OF CONTENTS (continued)

VOLUME I EVALUATION OF CONCRETE PAVEMENT PERFORMANCE AND DESIGN FEATURES (continued)

Chapter		Page
3	PERFORMANCE EVALUATION OF PROJECTS	25
	1. INTRODUCTION	25
	2. DRY-FREEZE ENVIRONMENTAL REGION	25
	Minnesota 1	27
	Observations	27
	Conclusions	27
	Minnesota 2	31
	Observations	31
	Conclusions	34
	Minnesota 3	35
	Minnesota 4	35
	Minnesota 6	37
	3. DRY-NONFREEZE ENVIRONMENTAL REGION	37
	Arizona 1	37
	Observations	40
	Conclusions	40
	Arizona 2	41
	California 1	41
	Observations	44
	Conclusions	44
	California 2	45
	Observations	45
	Conclusions	48
	California 6	48
	California 7	50
	Observations	50
	Conclusions	50
	California 8	51
	4. WET-FREEZE ENVIRONMENTAL REGION	51
	Michigan 1	51
	Observations	54
	Conclusions	55
	Michigan 3	56
	Michigan 4	56
	Observations	56
	Conclusions	60
	Michigan 5	61
	Observations	61
	Conclusions	61
	New York 1	63
	Observations	63
	Conclusions	63
	New York 2	65
	Observations	65
	Conclusions	68
	Ohio 1	69

TABLE OF CONTENTS (continued)

VOLUME I EVALUATION OF CONCRETE PAVEMENT PERFORMANCE AND DESIGN FEATURES (continued)

Chapter		Page
	Observations	69
	Conclusions	72
	Ohio 2	72
	Observations	73
	Conclusions	75
	Ontario 1	75
	Observations	78
	Conclusions	79
	Ontario 2	79
	Observations	80
	Conclusions	80
	Pennsylvania 1	80
	Observations	80
	Conclusions	84
	New Jersey 2	85
	Observations	85
	Conclusions	85
	New Jersey 3	85
	Observations	88
	Conclusions	89
5.	**WET-NONFREEZE ENVIRONMENTAL REGION**	89
	California 3	89
	Observations	89
	Conclusions	92
	North Carolina 1	92
	Observations	93
	Conclusions	96
	North Carolina 2	96
	Observations	97
	Conclusions	97
	Florida 2	97
	Florida 3	97
	Observations	99
	Conclusions	101
4	**EFFECT OF DESIGN FEATURES ON PAVEMENT PERFORMANCE**	102
1.	**INTRODUCTION**	102
2.	**SLAB THICKNESS**	102
	Minnesota 1 and Minnesota 2	102
	Arizona 1	102
	California 1	104
	Ohio 2	104
	Ontario 1	104
	North Carolina 2	104
	Summary of the Effects of Slab Thickness	104
3.	**BASE TYPE**	106

TABLE OF CONTENTS (continued)

VOLUME I EVALUATION OF CONCRETE PAVEMENT PERFORMANCE AND DESIGN FEATURES (continued)

Chapter		Page
	Minnesota 1	106
	Minnesota 6	107
	Arizona 1	107
	California 1	107
	California 2	107
	California 6	109
	Michigan 1	109
	Michigan 3	109
	Michigan 5	109
	New York 1	111
	Ohio 1	111
	Ontario 1	111
	Pennsylvania 1	111
	New Jersey 3	113
	North Carolina 1	113
	North Carolina 2	113
	Florida 3	113
	Summary of the Effects of Base Type	115
4.	**JOINT SPACING**	117
	Minnesota 1	117
	Minnesota 2	121
	California 1	121
	Michigan 1	121
	New York 1	121
	New York 2	123
	Ohio 1	123
	New Jersey 2	123
	North Carolina 1	123
	Florida 3	123
	Summary of the Effects of Joint Spacing	123
5.	**REINFORCEMENT DESIGN**	133
	Minnesota 1	133
	Ohio 1	135
	New Jersey 2 and New Jersey 3	135
	Other Sections	135
	Summary of the Effects of Reinforcement	135
6.	**JOINT ORIENTATION**	135
	New York 1	137
	North Carolina 1	137
	Summary of the Effects of Joint Orientation	137
7.	**TRANSVERSE JOINT LOAD TRANSFER**	137
	Doweled and Nondoweled Comparisons	139
	Minnesota 1	139
	North Carolina 1	139
	Nondoweled Sections	141
	Other Doweled Sections	141
	Summary of the Effects of Load Transfer	144

TABLE OF CONTENTS (continued)

VOLUME I EVALUATION OF CONCRETE PAVEMENT PERFORMANCE AND DESIGN FEATURES (continued)

Chapter		Page
	8. DOWEL BAR COATINGS	144
	Michigan 1	144
	Michigan 5	144
	Ohio 1	145
	New York 2	145
	New Jersey 2	145
	Summary of the Effects of Dowel Coatings	145
	9. LONGITUDINAL JOINT DESIGN	145
	Summary of the Effects of Longitudinal Joint Design	148
	10. TRANSVERSE JOINT SEALANT	148
	Direct Sealant Comparisons	148
	California 3	148
	Minnesota 2	149
	Nonsealed Joints in California	149
	Preformed Compression Seals	149
	Other Sealant Types	150
	Summary of the Effects of Joint Sealing	150
	11. TIED PCC SHOULDERS/WIDENED LANES	150
	Minnesota 2	150
	Arizona 1	151
	Michigan 1	151
	Michigan 4	151
	New York 2	151
	Ohio 2	153
	Ontario 1	153
	California 3	153
	Widened Lanes	153
	Summary of the Effects of Tied PCC Shoulders/ Widened Lanes	153
	12. SUBDRAINAGE	154
	Michigan 1	154
	Michigan 5	156
	Arizona 1	156
	California 2	156
	Pennsylvania 1	156
	New Jersey 3	156
	Summary of the Effects of Subdrainage	156
5	SUMMARY AND CONCLUSIONS	159
	1. SUMMARY OF THE EFFECT OF DESIGN FEATURES	159
	2. FUTURE RESEARCH	164
	3. SUGGESTIONS FOR FUTURE DATA COLLECTION AND TESTING	165
6	BIBLIOGRAPHY	166

TABLE OF CONTENTS (continued)

VOLUME II EVALUATION AND MODIFICATION OF CONCRETE PAVEMENT DESIGN AND ANALYSIS MODELS

Chapter		Page
1	INTRODUCTION	1
	1. INTRODUCTION	1
	2. PROJECT BACKGROUND	2
	Selection of Models	2
	Research Approach	3
	3. SEQUENCE OF REPORT	4
2	DESCRIPTION OF PAVEMENT SECTIONS	5
	1. DRY-FREEZE ENVIRONMENTAL REGION	5
	2. DRY-NONFREEZE ENVIRONMENTAL REGION	6
	3. WET-FREEZE ENVIRONMENTAL REGION	6
	4. WET-NONFREEZE ENVIRONMENTAL REGION	9
	5. OVERALL DISTRIBUTION OF DESIGN FEATURES	9
	Base Type	9
	Slab Thickness	12
	Joint Spacing/Pavement Type	12
	Load Transfer	12
	Shoulder Type/Widened Lanes	17
3	ANALYSIS OF THE ACCURACY OF SELECTED PREDICTION MODELS	19
	1. INTRODUCTION	19
	2. DESCRIPTION OF PREDICTION MODELS	19
	AASHTO Design Model	20
	PEARDARP Prediction Models	25
	Spalling Model	26
	PSI Model	26
	Roughness Model	26
	Pumping Models	27
	Cracking Model	29
	Faulting Models	30
	COPES Prediction Models	31
	JPCP Pumping Model	31
	JRCP Pumping Model	32
	JPCP Joint Faulting Model	32
	JRCP Joint Faulting Model	33
	JPCP Joint Deterioration Model	33
	JRCP Joint Deterioration Model	34
	JPCP Slab Cracking Model	35
	JRCP Slab Cracking Model	35
	JPCP Present Serviceability Rating (PSR) Model	36
	JRCP Present Serviceability Rating (PSR) Model	36
	PFAULT Faulting Prediction Models	37
	Doweled Jointed Concrete Pavements	37

TABLE OF CONTENTS (continued)

VOLUME II EVALUATION AND MODIFICATION OF CONCRETE PAVEMENT DESIGN AND ANALYSIS MODELS (continued)

Chapter		Page
	Nondoweled Jointed Concrete Pavements	37
	3. STATISTICAL ANALYSIS OF PREDICTION MODELS	39
	4. ABILITY OF MODELS TO PREDICT THE PERFORMANCE OF INSERVICE PAVEMENTS	41
	AASHTO	43
	PEARDARP	46
	PSI Model	46
	Roughness Model	46
	Pumping Model	49
	Spalling Model	49
	Faulting Models	50
	Cracking Model	51
	COPES	52
	Pumping Models	52
	Faulting Models	56
	Joint Deterioration Models	57
	Cracking Models	59
	Present Serviceability Rating (PSR) Models	61
	PFAULT Faulting Models	62
	5. SUMMARY	65
4	CASE STUDIES	67
	1. INTRODUCTION	67
	Climatic Model	67
	Drainage Model	68
	Structural Analysis Models	68
	Design Method	69
	Shoulder Analysis and Design	69
	2. PRESENTATION OF SECTIONS FOR CASE STUDIES	69
	Minnesota 1	69
	California 1	71
	Michigan 1	71
	North Carolina 1	71
	3. EVALUATION OF THE CMS PROGRAM	75
	Introduction	75
	Brief Technical Description	75
	Analysis of Results	78
	Rothsay, Minnesota	78
	Tracy, California	85
	Clare, Michigan	89
	Rocky Mount, North Carolina	99
	Conclusions and Recommendations	101
	4. EVALUATION OF LIU-LYTTON DRAINAGE MODELS	104
	Introduction	104
	Brief Technical Description	104
	Analysis of Results	105

TABLE OF CONTENTS (continued)

VOLUME II EVALUATION AND MODIFICATION OF CONCRETE PAVEMENT DESIGN AND ANALYSIS MODELS (continued)

Chapter		Page
	Rothsay, Minnesota	107
	Tracy, California	114
	Clare, Michigan	119
	Rocky Mount, North Carolina	125
	Conclusions and Recommendations	128
5.	**ANALYSIS OF JSLAB AND ILLISLAB**	131
	Introduction	131
	Analysis of Results	132
	Analysis of the Edge Loading Condition	137
	Analysis of the Corner Loading Condition	137
	Analysis of a Temperature Gradient Through the Slab	138
	Conclusions	138
6.	**EVALUATION OF THE ILLISLAB PROGRAM**	139
	Introduction	139
	Brief Technical Description	140
	Analysis of Results	141
	Analysis of the Edge Loading Condition	141
	Analysis of the Corner Loading Condition	144
	Analysis of Voids Beneath the Slab	146
	Analysis of a Temperature Gradient Through a Slab	149
	Conclusions and Recommendations	153
7.	**EVALUATION OF THE PMARP PROGRAM**	153
	Introduction	153
	Brief Technical Description	154
	Analysis of Results	156
	Analysis of the Edge Loading Condition	158
	Analysis of the Corner Loading Condition	160
	Conclusions and Recommendations	161
8.	**EVALUATION OF THE ZERO-MAINTENANCE DESIGN PROCEDURE**	162
	Introduction	162
	Brief Technical Description	162
	Analysis of Results	165
	Conclusions and Recommendations	168
9.	**EVALUATION OF JCS-1**	168
	Brief Technical Description	168
	Analysis of Results	169
	Conclusions and Recommendations	170
10.	**EVALUATION OF BERM**	171
	Brief Technical Description	171
	Analysis of Results	172
	Conclusions and Recommendations	173
11.	**SUMMARY AND CONCLUSIONS**	173
5	**DEVELOPMENT OF NEW PREDICTION MODELS**	175
1.	**INTRODUCTION**	175

TABLE OF CONTENTS (continued)

VOLUME II EVALUATION AND MODIFICATION OF CONCRETE PAVEMENT DESIGN AND ANALYSIS MODELS (continued)

Chapter		Page
2.	NEW PREDICTION MODELS	175
	Present Serviceability Rating (PSR)	175
	Jointed Plain Concrete Pavements	175
	Jointed Reinforced Concrete Pavements	176
	Longitudinal Cracking	177
	Transverse Joint Faulting	178
	Doweled Concrete Pavements	181
	Nondoweled Concrete Pavements	183
	Transverse Cracking	191
	Applied n	191
	Allowable N	192
	JPCP Cracking Model	196
	Transverse Joint Spalling	200
	JPCP Joint Spalling Model	200
	JRCP Joint Spalling Model	202
6	EVALUATION OF THE COST-EFFECTIVENESS OF SELECTED PAVEMENT DESIGN FEATURES	207
1.	INTRODUCTION	207
2.	ANALYSIS PROCEDURE	207
	Cost Information	209
	Life Prediction	209
	Cost-Effectiveness	209
3.	RESULTS	210
	Arizona	210
	Comparative Design 1	210
	Comparative Design 2	210
	Comparative Design 3	212
	California	212
	Comparative Design 1	212
	Comparative Design 2	212
	Comparative Design 3	215
	Comparative Design 4	215
	Comparative Design 5	215
	Comparative Design 6	215
	Michigan	216
	Comparative Design 1	216
	Comparative Design 2	216
	Comparative Design 3	219
	Comparative Design 4	219
	Comparative Design 5	219
	Comparative Design 6	219
	Minnesota	220
	Comparative Design 1	220
	Comparative Design 2	220
	Comparative Design 3	220

TABLE OF CONTENTS (continued)

VOLUME II EVALUATION AND MODIFICATION OF CONCRETE PAVEMENT DESIGN AND ANALYSIS MODELS (continued)

Chapter		Page
	Comparative Design 4	223
	Comparative Design 5	223
	North Carolina	223
	Comparative Design 1	223
	Comparative Design 2	225
	Comparative Design 3	225
	4. SUMMARY	225
7	SUMMARY AND CONCLUSIONS	228
	APPENDIX A — PAVEMENT DESIGNS FOR COST-EFFECTIVENESS EVALUATION	230
	REFERENCES	239

VOLUME III SUMMARY OF RESEARCH FINDINGS

Chapter		Page
1	INTRODUCTION	1
	STUDY OBJECTIVES	1
	BACKGROUND AND RESEARCH SCOPE	2
	DESCRIPTION OF REPORTS	2
2	STUDY SECTIONS AND DATA COLLECTION	3
	STUDY SECTIONS	3
	DRY-FREEZE ENVIRONMENTAL REGION	3
	DRY-NONFREEZE ENVIRONMENTAL REGION	3
	WET-FREEZE ENVIRONMENTAL REGION	8
	WET-NONFREEZE ENVIRONMENTAL REGION	8
	OVERALL DISTRIBUTION OF DESIGN FEATURES	8
	BASE TYPE	8
	SLAB THICKNESS	8
	JOINT SPACING/PAVEMENT TYPE	12
	LOAD TRANSFER	12
	SHOULDER TYPE/WIDENED LANES	12
	SINGLE PAVEMENT SECTIONS	12
	FIELD DATA COLLECTION	12
	PAVEMENT CONDITION SURVEY	17
	DRAINAGE SURVEY	17
	PHOTO SURVEY	18
	FALLING WEIGHT DEFLECTOMETER (FWD)	18
	PAVEMENT ROUGHNESS	18

TABLE OF CONTENTS (continued)

VOLUME III SUMMARY OF RESEARCH FINDINGS (continued)

Chapter		Page
	WEIGH-IN-MOTION (WIM)	18
	CORING AND BORING	18
	DATA BASE DESCRIPTION	19
3	SUMMARY OF THE EFFECTS OF DESIGN FEATURES	21
	PROJECT SUMMARIES	21
	EFFECTS OF PAVEMENT DESIGN FEATURES	21
	SLAB THICKNESS	21
	BASE TYPE	21
	SLAB LENGTH	23
	SLAB REINFORCEMENT	24
	JOINT ORIENTATION	26
	JOINT LOAD TRANSFER	26
	DOWEL BAR COATINGS	27
	LONGITUDINAL JOINT DESIGN	27
	JOINT SEALING	27
	TIED SHOULDERS	28
	WIDENED TRAFFIC LANES	28
	SUBDRAINAGE	29
	SUMMARY	29
4	CONCRETE PAVEMENT DESIGN AND ANALYSIS MODELS	30
	SYNTHESIS AND SELECTION OF INITIAL MODELS	30
	ANALYSIS OF THE ACCURACY OF SELECTED PREDICTION MODELS	30
	STATISTICAL ANALYSIS OF PREDICTION MODELS	31
	AASHTO PAVEMENT DESIGN MODEL	31
	PEARDARP	32
	NCHRP 277 (COPES)	35
	PFAULT FAULTING MODELS	35
	OVERALL EVALUATION OF THE PREDICTION MODELS	40
	CASE STUDIES FOR SELECTED ANALYSIS MODELS	40
	EVALUATION OF THE CMS PROGRAM	41
	EVALUATION OF THE LIU-LYTTON DRAINAGE MODELS	42
	EVALUATION OF THE ILLISLAB PROGRAM	43
	ANALYSIS OF JSLAB AND ILLISLAB	44
	Analysis of the Edge Loading Condition	45
	Analysis of the Corner Loading Condition	45
	Analysis of a Temperature Gradient Through the Slab	46
	Conclusions	47
	EVALUATION OF THE PMARP PROGRAM	47
	EVALUATION OF THE ZERO-MAINTENANCE DESIGN PROCEDURE	49
	EVALUATION OF JCS-1	49
	EVALUATION OF BERM	50
	SUMMARY AND CONCLUSIONS	51

TABLE OF CONTENTS (continued)

VOLUME III SUMMARY OF RESEARCH FINDINGS (continued)

Chapter		Page
5	DEVELOPMENT OF NEW PREDICTION MODELS	53
	INTRODUCTION	53
	PRESENT SERVICEABILITY RATING (PSR)	54
	LONGITUDINAL CRACKING	54
	TRANSVERSE JOINT FAULTING	55
	DOWELED CONCRETE PAVEMENTS	57
	NONDOWELED CONCRETE PAVEMENTS	57
	TRANSVERSE CRACKING	60
	TRANSVERSE JOINT SPALLING	62
	JPCP JOINT SPALLING MODEL	65
	JRCP JOINT SPALLING MODEL	65
	USE OF MODELS IN DESIGN	65
	ACCURACY OF MODELS	68
	SUMMARY	71
6	COST EFFECTIVENESS EVALUATION OF SELECTED PAVEMENT DESIGN FEATURES	73
	INTRODUCTION	73
	ANALYSIS PROCEDURE	73
	RESULTS	75
	SUMMARY OF COST EVALUATION	75
APPENDIX A	PARTIAL LISTING OF CANDIDATE SECTIONS	78
APPENDIX B	NEW PREDICTION MODELS	82
	PRESENT SERVICEABILITY RATING	82
	JOINTED PLAIN CONCRETE PAVEMENTS	82
	JOINTED REINFORCED CONCRETE PAVEMENTS	83
	TRANSVERSE JOINT FAULTING	84
	DOWELED CONCRETE PAVEMENTS	84
	NONDOWELED CONCRETE PAVEMENTS	87
	TRANSVERSE CRACKING - JOINTED PLAIN CONCRETE PAVEMENTS	90
	TRANSVERSE JOINT SPALLING	91
	JPCP JOINT SPALLING MODEL	91
	JRCP JOINT SPALLING MODEL	92
REFERENCES		93

TABLE OF CONTENTS (continued)

VOLUME IV APPENDIX A - PROJECT SUMMARY REPORTS AND SUMMARY TABLES

Chapter		Page
1	INTERSTATE 94 -- ROTHSAY, MINNESOTA	1
	1. INTRODUCTION	1
	2. CLIMATE	1
	3. TRAFFIC	1
	4. MAINTENANCE AND REHABILITATION	2
	5. PHYSICAL TESTING RESULTS	2
	6. DRAINABILITY OF PAVEMENT SECTIONS	3
	7. DETERIORATION OF PAVEMENT SECTIONS	6
	Joint Spalling	6
	Best Performance	6
	Worst Performance	6
	Joint Faulting	6
	Best Performance	7
	Worst Performance	7
	Transverse Cracking	7
	Best Performance	8
	Worst Performance	8
	Longitudinal Cracking	8
	Best Performance	8
	Worst Performance	9
	Present Serviceability Rating (PSR) and Roughness	9
	Other Distress Types	9
	8. EFFECT OF DESIGN FEATURES ON PAVEMENT PERFORMANCE	9
	Base Type	9
	Joint Load Transfer	9
	Slab Thickness	10
	Joint Spacing	10
	9. COMPARISON OF OUTER LANE AND INNER LANE PERFORMANCE	10
	10. SUMMARY AND CONCLUSIONS	11
	11. ADDITIONAL READING	12
2	INTERSTATE 90 -- ALBERT LEA, MINNESOTA	13
	1. INTRODUCTION	13
	2. CLIMATE	13
	3. TRAFFIC	13
	4. MAINTENANCE AND REHABILITATION	13
	5. PHYSICAL TESTING RESULTS	14
	6. DRAINABILITY OF PAVEMENT SECTIONS	15
	7. DETERIORATION OF PAVEMENT SECTIONS	15
	Joint Spalling	15
	Joint Faulting	17
	Transverse Cracking	17
	Longitudinal Cracking	17
	Present Serviceability Rating (PSR) and Roughness	18
	Overall Shoulder Condition	18

TABLE OF CONTENTS (continued)

VOLUME IV APPENDIX A - PROJECT SUMMARY REPORTS AND SUMMARY TABLES (continued)

Chapter		Page
	8. EFFECT OF DESIGN FEATURES ON PAVEMENT PERFORMANCE	18
	Pavement Type	19
	Joint Spacing	19
	Slab Thickness	19
	Shoulder Type	19
	Widened Inside Lanes	20
	9. COMPARISON OF OUTER LANE AND INNER LANE PERFORMANCE	20
	10. SUMMARY AND CONCLUSIONS	20
	11. ADDITIONAL READING	22
3	INTERSTATE 90 – AUSTIN, MINNESOTA	23
	1. INTRODUCTION	23
	2. DESIGN	23
	3. CLIMATE	23
	4. TRAFFIC	23
	5. DRAINABILITY AND OTHER PHYSICAL TESTING RESULTS	23
	6. MAINTENANCE AND REHABILITATION	24
	7. PAVEMENT PERFORMANCE	24
	8. CONCLUSIONS	24
4	TRUNK HIGHWAY 15 – NEW ULM, MINNESOTA	25
	1. INTRODUCTION	25
	2. DESIGN	25
	3. CLIMATE	25
	4. TRAFFIC	25
	5. DRAINABILITY AND OTHER PHYSICAL TESTING RESULTS	25
	6. MAINTENANCE AND REHABILITATION	26
	7. PAVEMENT PERFORMANCE	26
	8. CONCLUSIONS	26
5	TRUNK HIGHWAY 15 – TRUMAN, MINNESOTA	27
	1. INTRODUCTION	27
	2. DESIGN	27
	3. CLIMATE	27
	4. TRAFFIC	27
	5. DRAINABILITY AND OTHER PHYSICAL TESTING RESULTS	27
	6. MAINTENANCE AND REHABILITATION	28
	7. PAVEMENT PERFORMANCE	28
	8. CONCLUSIONS	28
6	STATE ROUTE 360 (SUPERSTITION FREEWAY) – PHOENIX, ARIZONA	29
	1. INTRODUCTION	29

TABLE OF CONTENTS (continued)

VOLUME IV APPENDIX A - PROJECT SUMMARY REPORTS AND SUMMARY TABLES (continued)

Chapter		Page
	2. CLIMATE	29
	3. TRAFFIC	29
	4. MAINTENANCE AND REHABILITATION	30
	5. PHYSICAL TESTING RESULTS	30
	6. DRAINABILITY OF PAVEMENT SECTIONS	31
	7. DETERIORATION OF PAVEMENT SECTIONS	31
	Joint Spalling	34
	Joint Faulting	34
	Transverse Cracking	34
	Longitudinal Cracking	34
	Present Serviceability Rating (PSR) and Roughness	35
	8. EFFECT OF DESIGN FEATURES ON PAVEMENT PERFORMANCE	35
	Base Type	35
	Load Transfer Devices	35
	Slab Thickness	36
	Shoulder Type	36
	Subdrainage	36
	9. COMPARISON OF OUTER LANE AND MIDDLE LANE PERFORMANCE	36
	10. SUMMARY AND CONCLUSIONS	37
	11. ADDITIONAL READING	37
7	INTERSTATE 10 -- PHOENIX, ARIZONA	38
	1. INTRODUCTION	38
	2. DESIGN	38
	3. CLIMATE	38
	4. TRAFFIC	38
	5. DRAINABILITY AND OTHER PHYSICAL TESTING RESULTS	38
	6. MAINTENANCE AND REHABILITATION	39
	7. PAVEMENT PERFORMANCE	39
	8. CONCLUSIONS	39
8	INTERSTATE 5 -- TRACY, CALIFORNIA	41
	1. INTRODUCTION	41
	2. CLIMATE	41
	3. TRAFFIC	41
	4. MAINTENANCE AND REHABILITATION	42
	5. PHYSICAL TESTING RESULTS	42
	6. DRAINABILITY OF PAVEMENT SECTIONS	43
	7. DETERIORATION OF PAVEMENT SECTIONS	44
	Joint Spalling	44
	Joint Faulting	44
	Best Performance	47
	Worst Performance	47
	Transverse Cracking	47
	Best Performance	47

TABLE OF CONTENTS (continued)

VOLUME IV APPENDIX A - PROJECT SUMMARY REPORTS AND SUMMARY TABLES (continued)

Chapter		Page
	Worst Performance	48
	Longitudinal Cracking	48
	Present Serviceability Rating (PSR) and Roughness	48
	8. EFFECT OF DESIGN FEATURES ON PAVEMENT PERFORMANCE	49
	Base Type	49
	Joint Spacing	49
	High Strength Concrete	50
	Slab Thickness	50
	9. COMPARISON OF OUTER AND INNER LANE PERFORMANCE	50
	10. SUMMARY AND CONCLUSIONS	51
	11. ADDITIONAL READING	51
9	INTERSTATE 210 -- LOS ANGELES, CALIFORNIA	52
	1. INTRODUCTION	52
	2. CLIMATE	52
	3. TRAFFIC	52
	4. MAINTENANCE AND REHABILITATION	52
	5. PHYSICAL TESTING RESULTS	53
	6. DRAINABILITY OF PAVEMENT SECTIONS	53
	7. DETERIORATION OF PAVEMENT SECTIONS	54
	Joint Spalling	54
	Joint Faulting	54
	Transverse Cracking	56
	Longitudinal Cracking	56
	Present Serviceability Rating (PSR) and Roughness	56
	Other Pavement Distress	56
	8. EFFECT OF DESIGN FEATURES ON PAVEMENT PERFORMANCE	56
	9. COMPARISON OF OUTER AND MIDDLE LANE PERFORMANCE	57
	10. SUMMARY AND CONCLUSIONS	57
	11. ADDITIONAL READING	58
10	ROUTE 14 -- SOLEMINT, CALIFORNIA	59
	1. INTRODUCTION	59
	2. DESIGN	59
	3. CLIMATE	59
	4. TRAFFIC	59
	5. DRAINABILITY AND OTHER PHYSICAL TESTING RESULTS	59
	6. MAINTENANCE AND REHABILITATION	60
	7. PAVEMENT PERFORMANCE	60
	8. CONCLUSIONS	60
11	INTERSTATE 5 -- SACRAMENTO, CALIFORNIA	61
	1. INTRODUCTION	61
	2. DESIGN	61

TABLE OF CONTENTS (continued)

VOLUME IV APPENDIX A - PROJECT SUMMARY REPORTS AND SUMMARY TABLES (continued)

Chapter		Page
	3. CLIMATE	61
	4. TRAFFIC	61
	5. DRAINABILITY AND OTHER PHYSICAL TESTING RESULTS	62
	6. MAINTENANCE AND REHABILITATION	62
	7. PAVEMENT PERFORMANCE	62
	8. CONCLUSIONS	63
12	U.S. 101 -- THOUSAND OAKS, CALIFORNIA	64
	1. INTRODUCTION	64
	2. DESIGN	64
	3. CLIMATE	64
	4. TRAFFIC	64
	5. DRAINABILITY AND OTHER PHYSICAL TESTING RESULTS	64
	6. MAINTENANCE AND REHABILITATION	65
	7. PAVEMENT PERFORMANCE	65
	8. CONCLUSIONS	65
13	U.S. 10 -- CLARE, MICHIGAN	66
	1. INTRODUCTION	66
	2. CLIMATE	66
	3. TRAFFIC	66
	4. MAINTENANCE AND REHABILITATION	67
	5. PHYSICAL TESTING RESULTS	67
	6. DRAINABILITY OF PAVEMENT SECTIONS	68
	7. DETERIORATION OF PAVEMENT SECTIONS	69
	Joint Spalling	69
	Best Performance	72
	Worst Performance	72
	Joint Faulting	72
	Best Performance	73
	Worst Performance	73
	Transverse Cracking	73
	Best Performance	74
	Worst Performance	74
	Longitudinal Cracking	74
	Present Serviceability Rating (PSR) and Roughness	74
	8. EFFECT OF DESIGN FEATURES ON PAVEMENT PERFORMANCE	75
	Base Type	75
	Joint Load Transfer	75
	Subdrainage	75
	Joint Spacing	76
	Concrete Acceleration Ramp	76
	9. COMPARISON OF OUTER AND INNER LANE PERFORMANCE	76
	10. SUMMARY AND CONCLUSIONS	77
	11. ADDITIONAL READING	78

TABLE OF CONTENTS (continued)

VOLUME IV APPENDIX A - PROJECT SUMMARY REPORTS AND SUMMARY TABLES (continued)

Chapter		Page
14	INTERSTATE 94 -- MARSHALL, MICHIGAN	79
	1. INTRODUCTION	79
	2. DESIGN	79
	3. CLIMATE	79
	4. TRAFFIC	79
	5. DRAINABILITY AND OTHER PHYSICAL TESTING RESULTS	79
	6. MAINTENANCE AND REHABILITATION	80
	7. PAVEMENT PERFORMANCE	80
	8. CONCLUSIONS	80
15	INTERSTATE 69 -- CHARLOTTE, MICHIGAN	81
	1. INTRODUCTION	81
	2. CLIMATE	82
	3. TRAFFIC	82
	4. MAINTENANCE AND REHABILITATION	82
	5. PHYSICAL TESTING RESULTS	82
	6. DRAINABILITY OF PAVEMENT SECTIONS	83
	7. DETERIORATION OF PAVEMENT SECTIONS	84
	Joint Spalling	84
	Joint Faulting	84
	Transverse Cracking	84
	Transverse Crack Faulting	86
	Longitudinal Cracking	86
	Present Serviceability Rating and Roughness	86
	Shoulder Condition	87
	8. EFFECT OF DESIGN FEATURES ON PAVEMENT PERFORMANCE	87
	9. COMPARISON OF OUTER AND INNER LANE PERFORMANCE	88
	10. SUMMARY AND CONCLUSIONS	89
	11. ADDITIONAL READING	90
16	INTERSTATE 94 -- PAW PAW, MICHIGAN	91
	1. INTRODUCTION	91
	2. DESIGN	91
	3. CLIMATE	91
	4. TRAFFIC	91
	5. DRAINABILITY AND OTHER PHYSICAL TESTING RESULTS	91
	6. MAINTENANCE AND REHABILITATION	92
	7. PAVEMENT PERFORMANCE	92
	8. CONCLUSIONS	92
	9. ADDITIONAL READING	93
17	ROUTE 23 -- CATSKILL, NEW YORK	94
	1. INTRODUCTION	94
	2. CLIMATE	94

TABLE OF CONTENTS (continued)

VOLUME IV APPENDIX A - PROJECT SUMMARY REPORTS AND SUMMARY TABLES (continued)

Chapter		Page
	3. TRAFFIC	95
	4. MAINTENANCE AND REHABILITATION	95
	5. PHYSICAL TESTING RESULTS	95
	6. DRAINABILITY OF PAVEMENT SECTIONS	96
	7. DETERIORATION OF PAVEMENT SECTIONS	99
	Joint Spalling	99
	Best Performance	99
	Worst Performance	99
	Joint Faulting	99
	Best Performance	99
	Worst Performance	100
	Transverse Cracking	100
	Best Performance	100
	Worst Performance	100
	Longitudinal Cracking	100
	Present Serviceability Rating (PSR) and Roughness	101
	8. EFFECT OF DESIGN FEATURES ON PAVEMENT PERFORMANCE	101
	Base Type	101
	Load Transfer Devices	101
	Joint Spacing	102
	Joint Orientation	102
	9. COMPARISON OF OUTER LANE AND INNER LANE PERFORMANCE	102
	10. SUMMARY AND CONCLUSIONS	103
	11. ADDITIONAL READING	103
18	INTERSTATE 88 -- OTEGO, NEW YORK	104
	1. INTRODUCTION	104
	2. CLIMATE	105
	3. TRAFFIC	105
	4. MAINTENANCE AND REHABILITATION	105
	5. PHYSICAL TESTING RESULTS	105
	6. DRAINABILITY OF PAVEMENT SECTIONS	107
	7. DETERIORATION OF PAVEMENT SECTIONS	107
	Joint Spalling	107
	Joint Faulting	107
	Transverse Cracking	107
	Longitudinal Cracking	110
	Present Serviceability Rating (PSR) and Roughness	111
	Concrete Shoulder Distress Summary	111
	8. EFFECT OF DESIGN FEATURES ON PAVEMENT PERFORMANCE	111
	9. COMPARISON OF OUTER LANE AND INNER LANE PERFORMANCE	112
	10. SUMMARY AND CONCLUSIONS	112
19	U.S. 23 -- CHILLICOTHE, OHIO	114
	1. INTRODUCTION	114

TABLE OF CONTENTS (continued)

VOLUME IV APPENDIX A - PROJECT SUMMARY REPORTS AND SUMMARY TABLES (continued)

Chapter		Page
	2. CLIMATE	114
	3. TRAFFIC	114
	4. MAINTENANCE AND REHABILITATION	114
	5. PHYSICAL TESTING RESULTS	115
	6. DRAINABILITY OF PAVEMENT SECTIONS	116
	7. DETERIORATION OF PAVEMENT SECTIONS	116
	Joint Spalling	116
	Joint Faulting	119
	Best Performance	119
	Worst Performance	119
	Transverse Cracking	120
	Best Performance	120
	Worst Performance	120
	Longitudinal Cracking	120
	Present Serviceability Rating (PSR) and Roughness	120
	8. EFFECT OF DESIGN FEATURES ON PAVEMENT PERFORMANCE	121
	Base Type	121
	Joint Spacing	121
	Dowel Coating	121
	9. COMPARISON OF OUTER AND INNER LANE PERFORMANCE	122
	10. SUMMARY AND CONCLUSIONS	122
	11. ADDITIONAL READING	123
20	STATE ROUTE 2 -- VERMILION, OHIO	124
	1. INTRODUCTION	124
	2. CLIMATE	124
	3. TRAFFIC	124
	4. MAINTENANCE AND REHABILITATION	124
	5. PHYSICAL TESTING RESULTS	125
	6. DRAINABILITY OF PAVEMENT SECTIONS	125
	7. DETERIORATION OF PAVEMENT SECTIONS	125
	Joint Spalling	125
	Joint Faulting	127
	Transverse Cracking	127
	Longitudinal Cracking	127
	Present Serviceability Rating (PSR) and Roughness	127
	Other Pavement Distress	128
	"D" Cracking	128
	Pumping	128
	Longitudinal Joint Spalling	128
	8. EFFECT OF DESIGN FEATURES ON PAVEMENT PERFORMANCE	129
	9. COMPARISON OF OUTER AND INNER LANE PERFORMANCE	129
	10. SUMMARY AND CONCLUSIONS	130
	11. ADDITIONAL READING	131
21	HIGHWAY 3N -- RUTHVEN, ONTARIO	132

TABLE OF CONTENTS (continued)

VOLUME IV APPENDIX A - PROJECT SUMMARY REPORTS AND SUMMARY TABLES (continued)

Chapter		Page
	1. INTRODUCTION	132
	2. CLIMATE	132
	3. TRAFFIC	133
	4. MAINTENANCE AND REHABILITATION	133
	5. PHYSICAL TESTING RESULTS	133
	6. DRAINABILITY OF PAVEMENT SECTIONS	134
	7. DETERIORATION OF PAVEMENT SECTIONS	135
	Joint Spalling	135
	Joint Faulting	135
	Transverse Cracking	137
	Longitudinal Cracking	137
	Present Serviceability Rating (PSR) and Roughness	137
	Shoulder Condition	138
	Other Distresses	138
	8. EFFECT OF DESIGN FEATURES ON PAVEMENT PERFORMANCE	138
	Base Type	138
	Shoulder Type	139
	Slab Thickness	139
	Base Drainability	139
	9. COMPARISON OF LANE PERFORMANCE BY DIRECTION	140
	10. SUMMARY AND CONCLUSIONS	140
22	HIGHWAY 27 -- TORONTO, ONTARIO	142
	1. INTRODUCTION	142
	2. DESIGN	142
	3. CLIMATE	142
	4. TRAFFIC	142
	5. DRAINABILITY AND OTHER PHYSICAL TESTING RESULTS	142
	6. MAINTENANCE AND REHABILITATION	142
	7. PAVEMENT PERFORMANCE	143
	8. CONCLUSIONS	143
23	ROUTES 66 AND 422 -- KITTANNING, PENNSYLVANIA	144
	1. INTRODUCTION	144
	2. CLIMATE	145
	3. TRAFFIC	145
	4. MAINTENANCE AND REHABILITATION	145
	5. PHYSICAL TESTING RESULTS	145
	6. DRAINABILITY OF PAVEMENT SECTIONS	147
	7. DETERIORATION OF PAVEMENT SECTIONS	147
	Joint Spalling	150
	Joint Faulting	150
	Transverse Cracking	150
	Longitudinal Cracking	150
	Present Serviceability Rating (PSR) and Roughness	150

TABLE OF CONTENTS (continued)

VOLUME IV APPENDIX A - PROJECT SUMMARY REPORTS AND SUMMARY TABLES (continued)

Chapter		Page
	8. EFFECT OF DESIGN FEATURES ON PAVEMENT PERFORMANCE	150
	9. COMPARISON OF OUTER AND INNER LANE PERFORMANCE	151
	10. SUMMARY AND CONCLUSIONS	151
	11. ADDITIONAL READING	152
24	ROUTE 130 -- YARDVILLE, NEW JERSEY	153
	1. INTRODUCTION	153
	2. DESIGN	153
	3. CLIMATE	153
	4. TRAFFIC	153
	5. DRAINABILITY AND OTHER PHYSICAL TESTING RESULTS	153
	6. MAINTENANCE AND REHABILITATION	154
	7. PAVEMENT PERFORMANCE	154
	8. CONCLUSIONS	154
	9. ADDITIONAL READING	154
25	INTERSTATE 676 -- CAMDEN, NEW JERSEY	155
	1. INTRODUCTION	155
	2. CLIMATE	155
	3. TRAFFIC	155
	4. MAINTENANCE AND REHABILITATION	156
	5. PHYSICAL TESTING RESULTS	156
	6. DRAINABILITY OF PAVEMENT SECTIONS	157
	7. DETERIORATION OF PAVEMENT SECTIONS	157
	Joint Spalling	157
	Joint Faulting	159
	Transverse Cracking	159
	Longitudinal Cracking	159
	Present Serviceability Rating (PSR) and Roughness	159
	8. EFFECT OF DESIGN FEATURES ON PAVEMENT PERFORMANCE	159
	9. COMPARISON OF OUTER AND MIDDLE LANE PERFORMANCE	160
	10. SUMMARY AND CONCLUSIONS	160
	11. ADDITIONAL READING	161
26	U.S. 101 -- GEYSERVILLE, CALIFORNIA	162
	1. INTRODUCTION	162
	2. CLIMATE	162
	3. TRAFFIC	162
	4. MAINTENANCE AND REHABILITATION	163
	5. PHYSICAL TESTING RESULTS	163
	6. DRAINABILITY OF PAVEMENT SECTIONS	164
	7. DETERIORATION OF PAVEMENT SECTIONS	164
	Joint Spalling	164
	Joint Faulting	167

TABLE OF CONTENTS (continued)

VOLUME IV APPENDIX A - PROJECT SUMMARY REPORTS AND SUMMARY TABLES (continued)

Chapter		Page
	Transverse Cracking	167
	Longitudinal Cracking	168
	Present Serviceability Rating (PSR) and Roughness	168
	Other Pavement Distress	168
	8. EFFECT OF DESIGN FEATURES ON PAVEMENT PERFORMANCE	168
	Tied Concrete Shoulders	168
	Joint Sealant	169
	9. COMPARISON OF OUTER AND INNER LANE PERFORMANCE	169
	10. SUMMARY AND CONCLUSIONS	170
	11. ADDITIONAL READING	171
27	INTERSTATE 95 -- ROCKY MOUNT, NORTH CAROLINA	172
	1. INTRODUCTION	172
	2. CLIMATE	172
	3. TRAFFIC	172
	4. MAINTENANCE AND REHABILITATION	172
	5. PHYSICAL TESTING RESULTS	172
	6. DRAINABILITY OF PAVEMENT SECTIONS	174
	7. DETERIORATION OF PAVEMENT SECTIONS	174
	Joint Spalling	174
	Joint Faulting	174
	Best Performance	177
	Worst Performance	177
	Transverse Cracking	177
	Longitudinal Cracking	178
	Best Performance	178
	Worst Performance	178
	Present Serviceability Rating (PSR) and Roughness	178
	8. EFFECT OF DESIGN FEATURES ON PAVEMENT PERFORMANCE	179
	Base Type	179
	Joint Load Transfer	179
	Pavement Type/Joint Spacing	179
	Joint Orientation	180
	9. COMPARISON OF OUTER LANE AND INNER LANE PERFORMANCE	180
	10. SUMMARY AND CONCLUSIONS	181
	11. ADDITIONAL READING	182
28	INTERSTATE 85 -- GREENSBORO, NORTH CAROLINA	183
	1. INTRODUCTION	183
	2. DESIGN	183
	3. CLIMATE	183
	4. TRAFFIC	183
	5. DRAINABILITY AND OTHER PHYSICAL TESTING RESULTS	183
	6. MAINTENANCE AND REHABILITATION	184
	7. PAVEMENT PERFORMANCE	184

TABLE OF CONTENTS (continued)

VOLUME IV APPENDIX A - PROJECT SUMMARY REPORTS AND SUMMARY TABLES (continued)

Chapter		Page
	8. CONCLUSIONS	184
	9. ADDITIONAL READING	185
29	I-75 -- TAMPA, FLORIDA (HILLSBOROUGH COUNTY)	186
	1. INTRODUCTION	186
	2. DESIGN	186
	3. CLIMATE	186
	4. TRAFFIC	186
	5. DRAINABILITY AND OTHER PHYSICAL TESTING RESULTS	186
	6. MAINTENANCE AND REHABILITATION	187
	7. PAVEMENT PERFORMANCE	187
	8. CONCLUSIONS	187
30	INTERSTATE 75 -- TAMPA, FLORIDA (MANATEE COUNTY)	188
	1. INTRODUCTION	188
	2. DESIGN	188
	3. CLIMATE	188
	4. TRAFFIC	188
	5. DRAINABILITY AND OTHER PHYSICAL TESTING RESULTS	188
	6. MAINTENANCE AND REHABILITATION	189
	7. PAVEMENT PERFORMANCE	189
	8. CONCLUSIONS	191
	9. ADDITIONAL READING	191
31	KEY TO PROJECT SUMMARY TABLES	192
	1. GENERAL AND ENVIRONMENTAL DATA	192
	2. DESIGN DATA	193
	3. MONITORING DATA	199
	4. PERFORMANCE DATA	203
32	SUMMARY OF PROJECT DATA	205
33	REFERENCES	246

VOLUME V APPENDIX B - DATA COLLECTION AND ANALYSIS PROCEDURES

Chapter		Page
1	FIELD DATA COLLECTION PROCEDURES	1
	1. INTRODUCTION	1

TABLE OF CONTENTS (continued)

VOLUME V APPENDIX B - DATA COLLECTION AND ANALYSIS PROCEDURES (continued)

Chapter		Page
	2. CONDITION SURVEY	1
	Measurements	1
	Mapped Distresses	5
	Evaluated Conditions	6
	Noted Conditions	6
	3. PHOTO SURVEY	6
	4. DRAINAGE SURVEY	8
	5. FIELD TESTING	9
	Falling Weight Deflectometer (FWD)	9
	Coring and boring	9
	Roughness/PSR	14
	Traffic Control	14
	6. WEIGH-IN-MOTION DATA COLLECTION	14
	7. SUGGESTIONS FOR FUTURE DATA COLLECTION AND TESTING	16
2	WEIGH-IN-MOTION DATA COLLECTION PROCEDURES	17
	1. INTRODUCTION	17
	2. SITE SETUP AND CALIBRATION	17
	3. ACCURACY OF WIM DATA	19
3	TRAFFIC ANALYSIS	23
	1. INTRODUCTION	23
	2. INPUTS FOR PROCEDURE	23
	Average Daily Traffic, ADT	23
	Percentage of Heavy Trucks, TKS	23
	Directional Distribution, DD	24
	Lane Distribution, LD	24
	Average Truck Factor, TF	24
	3. CALCULATION PROCEDURE	25
	4. SUMMARY	25
4	DRAINAGE ANALYSIS AND DETERMINATION OF DRAINAGE COEFFICIENTS	26
	1. INTRODUCTION	26
	2. AASHTO DRAINAGE CRITERIA	27
	Roadbed Soils	27
	Cross Section	27
	3. MAD INDEX	28
	Base Drainability	29
	Climatic Moisture	29
	Subgrade	29
	MAD Index Categories	29
	Base Drainage	29
	Subgrade Drainage	30

TABLE OF CONTENTS (continued)

VOLUME V APPENDIX B - DATA COLLECTION AND ANALYSIS PROCEDURES (continued)

Chapter			Page
		Climatic Moisture Availability	30
	4.	DEVELOPING A DRAINAGE COEFFICIENT	32
		Time of Saturation	32
		Base Drainability	35
		Subgrade Drainability	37
		Combining Base and Subgrade	37
		Cross Section	37
	5.	DRAINAGE COEFFICIENTS FOR SECTIONS	39
		Arizona 1	40
		Arizona 2	40
		California 1	41
		California 2	41
		California 3	42
		California 6	43
		California 7	43
		California 8	44
		Florida 2	44
		Florida 3	44
		Michigan 1	44
		Michigan 3	45
		Michigan 4	46
		Michigan 5	46
		Minnesota 1	47
		Minnesota 2	48
		Minnesota 3	49
		Minnesota 4	49
		Minnesota 5	49
		Minnesota 6	50
		New Jersey 2	50
		New Jersey 3	51
		New York 1	51
		New York 2	52
		North Carolina 1	53
		North Carolina 2	54
		Ohio 1	54
		Ohio 2	55
		Ontario 1	55
		Ontario 2	56
		Pennsylvania 1	56
5		BACKCALCULATION METHODOLOGY	58
	1.	INTRODUCTION	58
	2.	FUNDAMENTAL CONCEPTS	58
	3.	OUTLINE OF BACKCALCULATION PROCEDURE	63
	4.	APPLICATION OF CLOSED-FORM BACKCALCULATION PROCEDURE	64
	5.	VARIABILITY AND RELIABILITY OF TESTING AND	

TABLE OF CONTENTS (continued)

VOLUME V APPENDIX B - DATA COLLECTION AND ANALYSIS PROCEDURES (continued)

Chapter		Page
	BACKCALCULATED VALUES	65
	Plate Theory	66
	Deflection Measurement	69
	Finite Element Analysis	70
	6. ADVANTAGES OF CLOSED-FORM BACKCALCULATION PROCEDURE	75
6	DATABASE DESCRIPTION	77
7	REFERENCES	82
8	ANNOTATED BIBLIOGRAPHY	85
	1. EXPERIMENTAL PROJECTS AND PAVEMENT PERFORMANCE	85
	2. SUBDRAINAGE	102
	3. LOAD TRANSFER	109
	4. JOINTS AND JOINT SEALING	111
	5. CONCRETE SHOULDERS	116
	6. PAVEMENT DESIGN	119
	7. PAVEMENT ANALYSIS	123
	8. LIFE CYCLE COSTS	125
	9. WEIGH-IN-MOTION	126

VOLUME VI APPENDIX C AND APPENDIX D

APPENDIX C - SYNTHESIS OF CONCRETE PAVEMENT DESIGN METHODS AND ANALYSIS MODELS

Chapter		Page
PART I.	REVIEW OF SELECTED DESIGN AND ANALYSIS MODELS	1
1.	INTRODUCTION	1
2.	EVALUATION OF THE ANALYSIS AND DESIGN MODELS	1
3.	CAPABILITIES AND LIMITATIONS OF ANALYSIS MODELS	2
	ILLISLAB	2
	Capabilities	2
	Limitations	3
	JSLAB	4
	Capabilities	4
	Limitations	4
	WESLIQID	5
	Capabilities	5
	Limitations	5
	WESLAYER	6
	Capabilities	6
	Limitations	6

TABLE OF CONTENTS (continued)

VOLUME VI APPENDIX C AND APPENDIX D

APPENDIX C - SYNTHESIS OF CONCRETE PAVEMENT DESIGN METHODS AND ANALYSIS MODELS (continued)

Chapter		Page
	PMARP	7
	Capabilities	7
	Limitations	7
	RISC	9
	Capabilities	9
	Limitations	10
	H51	10
	Capabilities	10
	Limitations	11
	CMS	11
	Capabilities	11
	Limitations	12
	Liu-Lytton Drainage Models	12
	Capabilities	13
	Limitations	13
	JRCP4	14
	Capabilities	14
	Limitations	14
4.	**CAPABILITIES AND LIMITATIONS OF DESIGN AND PREDICTION MODELS**	15
	PREDICT	15
	Capabilities	15
	Limitations	16
	PEARDARP	16
	Capabilities	16
	Limitations	17
	JCP-1	17
	Capabilities	17
	Limitations	18
	DNPS86	19
	Capabilities	19
	Limitations	19
	RPS-3	20
	Capabilities	20
	Limitations	21
	PCA Design Procedure	22
	Capabilities	22
	Limitations	22
	California Rigid Pavement Design Procedure	23
	Capabilities	23
	Limitations	23
	BERM	24
	Capabilities	24
	Limitations	25
	JCS-1	25

TABLE OF CONTENTS (continued)

VOLUME VI APPENDIX C AND APPENDIX D

APPENDIX C - SYNTHESIS OF CONCRETE PAVEMENT DESIGN METHODS AND ANALYSIS MODELS (continued)

Chapter		Page
	Capabilities	25
	Limitations	26
5.	OVERALL PROGRAM EVALUATION	26
	Structural Analysis Models	27
	Drainage/Climatic Analysis Models	27
	Pavement Design Methods	28
6.	RECOMMENDATIONS	28
	Structural Analysis Model	28
	Prediction Models	30
	Drainage/Climatic Model	30
	Design Method	30
PART II.	STANDARD PAVEMENT SECTION AND VARIABLES UNDER CONSIDERATION	32
PART III.	SUMMARY OF INPUT AND OUTPUT VARIABLES	51
PART IV.	RESULTS OF SENSITIVITY ANALYSIS	79

APPENDIX D - SUMMARY OF ANALYSIS DATA FOR THE EVALUATION OF PREDICTIVE MODELS

Chapter		Page
1.	INTRODUCTION	115
2.	DESCRIPTION OF TABLES AND FIGURES	115
REFERENCES		329

LIST OF FIGURES

VOLUME I EVALUATION OF CONCRETE PAVEMENT PERFORMANCE AND DESIGN FEATURES

Figure	Title	Page
1.	States and Provinces participating in study	5
2.	Experimental design matrix for Minnesota 1	7
3.	Experimental design matrix for Minnesota 2	7
4.	Experimental design matrix for Arizona 1	9
5.	Experimental design matrix for California 1	10
6.	Experimental design matrix for California 2	10
7.	Experimental design matrix for Michigan 1	12
8.	Experimental design matrix for Michigan 4	12
9.	Experimental design matrix for New York 1	14
10.	Experimental design matrix for New York 2	14
11.	Experimental design matrix for Ohio 1	16
12.	Experimental design matrix for Ohio 2	16
13.	Experimental design matrix for Ontario 1	17
14.	Experimental design matrix for Pennsylvania 1	19
15.	Experimental design matrix for New Jersey 3	20
16.	Experimental design matrix for California 3	20
17.	Experimental design matrix for North Carolina 1	22
18.	Outer lane performance data for Minnesota 1 (Age = 17 years, ESAL's = 5.5 million)	29
19.	Outer lane performance data for Minnesota 2 (Age = 10 years, ESAL's = 2.8 million)	33
20.	Outer lane performance data for Arizona 1	39
21.	Outer lane performance data for California 1 (Age = 16 years, ESAL's = 7.6 million)	43
22.	Outer lane performance data for California 2 (Age = 7 years, ESAL's = 4.4 million)	47
23.	Outer lane performance data for Michigan 1 (Age = 12 years, ESAL's = 0.89 million)	53
24.	Outer lane performance data for Michigan 4 (Age = 17 years, ESAL's = 4.4 million)	58
25.	Outer lane performance data for New York 1 (Age = 19 years, ESAL's = 3.1 million)	64
26.	Outer lane performance data for New York 2 (Age = 12 years, ESAL's = 1.4 million)	67
27.	Outer lane performance data for Ohio 1 (Age = 14 years, ESAL's = 3.4 million)	71
28.	Outer lane performance data for Ohio 2 (Age = 13 years, ESAL's = 3.3 million)	74
29.	Performance data by direction for Ontario 1 (Age = 5 years, ESAL's = 1.0 million)	77
30.	Outer lane performance data for Pennsylvania 1	83
31.	Outer lane performance data for New Jersey 3 (Age = 8 years, ESAL's = 4.2 million)	87
32.	Outer lane performance data for California 3 (Age = 12 years, ESAL's = 3.6 million)	91
33.	Outer lane performance data for North Carolina 1 (Age = 20 years, ESAL's 9.1 million)	95

LIST OF FIGURES (continued)

VOLUME I EVALUATION OF CONCRETE PAVEMENT PERFORMANCE AND DESIGN FEATURES (continued)

Figure	Title	Page
34.	Percent cracked slabs vs. L/l for California 1 (Tracy) sections	131
35.	Percent cracked slabs vs. L/l for all sections with cement-treated and lean concrete bases	132
36.	Percent cracked slabs vs. L/l for all sections with aggregate bases	134

VOLUME II EVALUATION AND MODIFICATION OF CONCRETE PAVEMENT DESIGN AND ANALYSIS MODELS

Figure	Title	Page
1.	Distribution of base type by environmental region	13
2.	Distribution of slab thickness by environmental region	14
3.	Distribution of joint spacing and pavement type by environmental region (P=JPCP, R=JRCP)	15
4.	Distribution of load transfer method by environmental region	16
5.	Distribution of shoulder type by environmental region	18
6.	Scattergram of actual field-measured faulting versus faulting as predicted using the COPES faulting models for the dry-freeze region	42
7.	Experimental design matrix for Minnesota 1	70
8.	Experimental design matrix for California 1	72
9.	Experimental design matrix for Michigan 1	73
10.	Experimental design matrix for North Carolina 1	74
11.	Use of CMS in the design process	77
12.	Temperature profile versus depth through the slab on July 15, 1987, Rothsay, Minnesota	81
13.	Change in 6 a.m. thermal gradient in June 1987, Rothsay, Minnesota	82
14.	Change in 3 p.m. thermal gradient in June 1987, Rothsay, Minnesota	82
15.	Temperature profile versus depth through the slab on July 15, 1987, Tracy, California	86
16.	Change in 6 a.m. thermal gradient from January through June 1987, Tracy, California	88
17.	Change in 6 a.m. thermal gradient from July through December 1987, Tracy, California	88
18.	Change in 3 p.m. thermal gradient from January through June 1987, Tracy, California	90
19.	Change in 3 p.m. thermal gradient from July through December 1987, Tracy, California	90
20.	Temperature profile versus depth through the slab on July 15, 1987, Clare, Michigan	91
21.	Change in 6 a.m. thermal gradient in April 1987, Clare, Michigan	92
22.	Change in 3 p.m. thermal gradient in April 1987, Clare, Michigan	92
23.	Change in 6 a.m. thermal gradient in June 1987, Clare, Michigan	93
24.	Change in 3 p.m. thermal gradient in June 1987, Clare, Michigan	93

LIST OF FIGURES (continued)

VOLUME II EVALUATION AND MODIFICATION OF CONCRETE PAVEMENT DESIGN AND ANALYSIS MODELS (continued)

Figure	Title	Page
25.	Change in 6 a.m. thermal gradient in August 1987, Clare, Michigan	94
26.	Change in 3 p.m. thermal gradient in August 1987, Clare, Michigan	94
27.	Change in 6 a.m. thermal gradient in December 1987, Clare Michigan	95
28.	Change in 3 p.m. thermal gradient in December 1987, Clare Michigan	95
29.	Frostline versus depth in January, 1987, Clare, Michigan	96
30.	Temperature profile versus depth through the slab on July 15, 1987, Rocky Mount, North Carolina	100
31.	Change in 6 a.m. thermal gradient in July 1987, Rocky Mount, North Carolina	102
32.	Change in 3 p.m. thermal gradient in April 1987, Clare, Michigan	102
33.	Percent drainage versus time for MN 1-1, MN 1-5, and MN 1-9	108
34.	Percent saturation versus base course modulus for MN 1-1, MN 1-2, MN 1-3, and MN 1-4	111
35.	Percent saturation versus subgrade modulus for MN 1-1, MN 1-2, MN 1-3, and MN 1-4	113
36.	Percent drainage versus time for CA 1-1, CA 1-7, and CA 1-9	115
37.	Percent saturation versus subbase modulus for CA 1-1, CA 1-7, and CA 1-9	117
38.	Percent saturation versus subgrade modulus for CA 1-1, CA 1-7, and CA 1-9	118
39.	Percent drainage versus time for MI 1-1a, MI 1-4a, and MI 1-10b	120
40.	Percent saturation versus base or subbase modulus for MI 1-1a, MI 1-10a, and MI 1-10b	122
41.	Percent saturation versus subgrade modulus for MI 1-1a, MI 1-4a, and MI 1-10b	123
42.	Percent drainage versus time for NC 1-1, NC 1-2, and NC 1-7	126
43.	Percent saturation versus base modulus for NC 1-1, NC 1-7, and NC 1-8	127
44.	Percent saturation versus subgrade modulus for NC 1-1, NC 1-7, and NC 1-8	129
45.	Example finite element mesh for the edge loading condition	136
46.	FWD sensor location at the approach joint	148
47.	Measured deflection basin and calculated deflection basin from void analysis	150
48.	Finite element mesh for a 15-ft (4.6 m) slab used in the PMARP evaluation of the corner loading condition	157
49.	Original zero-maintenance fatigue damage curve supplemented with projects from current study	167
50.	Predicted versus actual faulting for doweled joint faulting model	184
51.	Sensitivity of doweled joint faulting model to dowel diameter	185
52.	Sensitivity of doweled joint faulting model to drainage and shoulder type	186
53.	Predicted versus actual faulting for nondoweled joint faulting model	189
54.	Sensitivity of doweled and nondoweled faulting models to drainage and shoulder type	190
55.	Relation between deflection load transfer efficiency and stress load transfer efficiency	195
56.	Percent slabs cracked versus accumulated fatigue damage	197
57.	Sensitivity of cracking model to shoulder type	198
58.	Sensitivity of cracking model to joint spacing	199
59.	Sensitivity of cracking model to slab thickness	201
60.	Sensitivity of JPCP joint spalling model to sealant type	203

LIST OF FIGURES (continued)

VOLUME II EVALUATION AND MODIFICATION OF CONCRETE PAVEMENT DESIGN AND ANALYSIS MODELS (continued)

Figure	Title	Page
61.	Sensitivity of JRCP joint spalling model to climate	204
62.	Sensitivity of JRCP joint spalling model to sealant type	206

VOLUME III SUMMARY OF RESEARCH FINDINGS

Figure	Title	Page
1.	States participating in study	4
2.	Distribution of base type by climatic region	11
3.	Distribution of slab thickness by climatic region	13
4.	Distribution of joint spacing/pavement type by climatic region	14
5.	Distribution of load transfer mechanism by climatic region	15
6.	Distribution of shoulder type (and widened lanes) by climatic region	16
7.	Percent slab cracking as a function of L/*l* for sections with aggregate bases	25
8.	Percent slab cracking as a function of L/*l* for sections with LCB and CTB bases	25
9.	Sensitivity of doweled faulting model to dowel diameter	58
10.	Sensitivity of doweled faulting model to drainage and shoulder type	58
11.	Sensitivity of faulting models to dowels, drainage, and shoulder type	59
12.	Percent slab cracking as a function of accumulated fatigue damage	59
13.	Sensitivity of JPCP cracking model to shoulder type	63
14.	Sensitivity of JPCP cracking model to joint spacing	63
15.	Sensitivity of JPCP cracking model to slab thickness	64
16.	Sensitivity of JPCP spalling model to joint sealant type	64
17.	Sensitivity of JPCP spalling model to climate	66
18.	Sensitivity of JRCP spalling model to joint sealant type	66

VOLUME IV APPENDIX A - PROJECT SUMMARY REPORTS AND SUMMARY TABLES

Figure	Title	Page
1.	Outer lane performance data for Minnesota 1	4
2.	Inner lane performance data for Minnesota 1	5
3.	Outer and inner lane performance data for Minnesota 2	16
4.	Outer lane performance data for Arizona 1	32
5.	Inner lane performance data for Arizona 1	33
6.	Outer lane performance data for California 1	45
7.	Inner lane performance data for California 1	46
8.	Outer and middle lane performance data for California 2	55
9.	Outer lane performance data for Michigan 1	70
10.	Inner lane performance data for Michigan 1	71
11.	Outer and inner lane performance data for Michigan 4	85
12.	Outer lane performance data for New York 1	97

LIST OF FIGURES (continued)

VOLUME IV APPENDIX A - PROJECT SUMMARY REPORTS AND SUMMARY TABLES (continued)

Figure	Title	Page
13.	Inner lane performance data for New York 1	98
14.	Outer lane performance data for New York 2	108
15.	Inner lane performance data for New York 2	109
16.	Outer lane performance data for Ohio 1	117
17.	Inner lane performance data for Ohio 1	118
18.	Outer and inner lane performance data for Ohio 2	126
19.	Performance data by direction for Ontario 1	136
20.	Outer lane performance data for Pennsylvania 1	148
21.	Inner lane performance data for Pennsylvania 1	149
22.	Outer and middle lane performance data for New Jersey 3	158
23.	Outer lane performance data for California 3	165
24.	Inner lane performance data for California 3	166
25.	Outer lane performance data for North Carolina 1	175
26.	Inner lane performance data for North Carolina 1	176

VOLUME V APPENDIX B - DATA COLLECTION AND ANALYSIS PROCEDURES

Figure	Title	Page
1.	General field survey sheet	2
2.	Drainage field survey sheet	3
3.	Field data collection form	4
4.	Project photographic record	7
5.	Layout for FWD testing of projects with AC shoulders	10
6.	Layout for FWD testing of projects with PCC shoulders	11
7.	Layout for FWD testing of projects with widened lanes	12
8.	Raw data file from the Dynatest model 8000	13
9.	Sample raw output from Mays Roughness Meter	15
10.	Climatic zones for AASHTO and FHWA procedures	31
11.	Plot of monthly rainfall and potential evapotranspiration for Clare, Michigan	34
12.	Procedure to combine drainabilities of base and subgrade	38
13.	Variation in deflection basin AREA with radius of relative stiffness	60
14.	Variation in dimensionless deflections with radius of relative stiffness for the dense liquid foundation	61
15.	Variation in dimensionless deflections with radius of relative stiffness for the elastic solid foundation	62
16.	Deflection basin as measured by the FWD and as calculated using the closed-form procedure	71
17.	Deflection basin as measured by the FWD and as calculated using the closed-form procedure	72
18.	Deflection basin as measured by the FWD and as calculated using the closed-form procedure	73
19.	Eh**3 versus kl**4 for all Phase I sections	74
20.	Main UNIFY database menu	79
21.	Inventory database menu	80
22.	Monitoring database menu	81

LIST OF FIGURES (continued)

VOLUME VI APPENDIX C AND APPENDIX D

APPENDIX C - SYNTHESIS OF CONCRETE PAVEMENT DESIGN METHODS AND ANALYSIS MODELS

Figure	Title	Page
1.	Assumed standard pavement section	33
2.	ILLISLAB and JSLAB finite element mesh for standard pavement section analysis	38
3.	ILLISLAB and JSLAB finite element mesh for 10-ft joint spacing analysis	39
4.	ILLISLAB and JSLAB finite element mesh for 20-ft joint spacing analysis	40
5.	ILLISLAB and JSLAB finite element mesh for widened lane analysis	41
6.	WESLIQID and WESLAYER finite element mesh for standard pavement analysis using a four-slab system	42
7.	WESLIQID and WESLAYER finite element mesh for standard pavement analysis using a two-slab system	43
8.	WESLIQID and WESLAYER finite element mesh for 10-ft joint spacing analysis	44
9.	WESLIQID and WESLAYER finite element mesh for 20-ft joint spacing analysis	45
10.	WESLIQID and WESLAYER finite element mesh for widened lane analysis	46
11.	PMARP finite element mesh for standard pavement section	47
12.	PMARP finite element mesh for widened lane analysis	48
13.	PMARP finite element mesh for 20-ft joint spacing analysis	49
14.	Wheel configuration used for H-51 analysis	50
15.	Temperature gradient as measured by CMS	93
16.	Climatic zones based on Thornthwaite potential evapotranspiration and moisture index and their interaction with performance, with similar performance expected in similar climatic regions (5)	98

APPENDIX D - SUMMARY OF ANALYSIS DATA FOR THE EVALUATION OF PREDICTIVE MODELS

Figure	Title	Page
17.	Actual ESAL's (based on ADT) versus ESAL's as predicted using the AASHTO design equation for all Phase I sections	119
18.	Actual ESAL's (based on ADT) versus ESAL's as predicted using the AASHTO design equation for the dry-freeze region	122
19.	Actual ESAL's (based on ADT) versus ESAL's as predicted using the AASHTO design equation for the dry-nonfreeze region	122
20.	Actual ESAL's (based on ADT) versus ESAL's as predicted using the AASHTO design equation for the wet-freeze region	126
21.	Actual ESAL's (based on ADT) versus ESAL's as predicted using the AASHTO design equation for the wet-nonfreeze region	126

LIST OF FIGURES (continued)

VOLUME VI APPENDIX C AND APPENDIX D

APPENDIX D - SUMMARY OF ANALYSIS DATA FOR THE EVALUATION OF PREDICTIVE MODELS (continued)

Figure	Title	Page
22.	Actual PSR as determined by a panel of users versus PSI as predicted by the PEARDARP PSI model for all Phase I sections	130
23.	Actual PSR as determined by a panel of users versus PSI as predicted by the PEARDARP PSI model for the dry-freeze region	133
24.	Actual PSR as determined by a panel of users versus PSI as predicted by the PEARDARP PSI model for the dry-nonfreeze region	133
25.	Actual PSR as determined by a panel of users versus PSI as predicted by the PEARDARP PSI model for the wet-freeze region	137
26.	Actual PSR as determined by a panel of users versus PSI as predicted by the PEARDARP PSI model for the wet-nonfreeze region	137
27.	Actual field measured roughness versus roughness as predicted using the PEARDARP roughness model for all Phase I sections	141
28.	Actual field measured roughness versus roughness as predicted using the PEARDARP roughness model for the dry-freeze region	144
29.	Actual field measured roughness versus roughness as predicted using the PEARDARP roughness model for the dry-nonfreeze region	144
30.	Actual field measured roughness versus roughness as predicted using the PEARDARP roughness model for the wet-freeze region	148
31.	Actual field measured roughness versus roughness as predicted using the PEARDARP roughness model for the wet-nonfreeze region	148
32.	Actual field measured spalling versus spalling as predicted using the PEARDARP spalling model for all Phase I sections	155
33.	Actual field measured spalling versus spalling as predicted using the PEARDARP spalling model for the dry-freeze region	158
34.	Actual field measured spalling versus spalling as predicted using the PEARDARP spalling model for the dry-nonfreeze region	158
35.	Actual field measured spalling versus spalling as predicted using the PEARDARP spalling model for the wet-freeze region	162
36.	Actual field measured spalling versus spalling as predicted using the PEARDARP spalling model for the wet-nonfreeze region	162
37.	Actual field measured faulting versus faulting as predicted using the PEARDARP faulting models for all Phase I sections	166
38.	Actual field measured faulting versus faulting as predicted using the PEARDARP faulting models for the dry-freeze region	168
39.	Actual field measured faulting versus faulting as predicted using the PEARDARP faulting models for doweled pavements for the dry-freeze region	171
40.	Actual field measured faulting versus faulting as predicted using the PEARDARP faulting models for nondoweled pavements for the dry-freeze region	171
41.	Actual field measured faulting versus faulting as predicted using the PEARDARP faulting models for the dry-nonfreeze region	173

LIST OF FIGURES (continued)

VOLUME VI APPENDIX C AND APPENDIX D

APPENDIX D - SUMMARY OF ANALYSIS DATA FOR THE EVALUATION OF PREDICTIVE MODELS (continued)

Figure	Title	Page
42.	Actual field measured faulting versus faulting as predicted using the PEARDARP faulting models for the wet-freeze region	176
43.	Actual field measured faulting versus faulting as predicted using the PEARDARP faulting models for doweled pavements for the wet-freeze region	179
44.	Actual field measured faulting versus faulting as predicted using the PEARDARP faulting models for nondoweled pavements for the wet-freeze region	179
45.	Actual field measured faulting versus faulting as predicted using the PEARDARP faulting models for the wet-nonfreeze region	181
46.	Actual field measured faulting versus faulting as predicted using the PEARDARP faulting models for doweled pavements for the wet-nonfreeze region	184
47.	Actual field measured faulting versus faulting as predicted using the PEARDARP faulting models for nondoweled pavements for the wet-nonfreeze region	184
48.	Actual field measured cracking versus cracking as predicted using the PEARDARP cracking models for all Phase I sections	188
49.	Actual field measured cracking versus cracking as predicted using the PEARDARP cracking model for the dry-freeze region	191
50.	Actual field measured cracking versus cracking as predicted using the PEARDARP cracking model for the dry-nonfreeze region	191
51.	Actual field measured cracking versus cracking as predicted using the PEARDARP cracking model for the wet-freeze region	195
52.	Actual field measured cracking versus cracking as predicted using the PEARDARP cracking model for the wet-nonfreeze region	195
53.	Actual field observed pumping versus pumping as predicted using COPES pumping models for all Phase I sections	199
54.	Actual field observed pumping versus pumping as predicted using COPES pumping models for the dry-freeze region	201
55.	Actual field observed pumping versus pumping as predicted using COPES JPCP pumping model for the dry-freeze region	204
56.	Actual field observed pumping versus pumping as predicted using COPES JRCP pumping model for the dry-freeze region	204
57.	Actual field observed pumping versus pumping as predicted using COPES pumping model for the dry-nonfreeze region	206
58.	Actual field observed pumping versus pumping as predicted using COPES pumping model for the wet-freeze region	209
59.	Actual field observed pumping versus pumping as predicted using COPES JPCP pumping model for the wet-freeze region	212
60.	Actual field observed pumping versus pumping as predicted using COPES JRCP pumping model for the wet-freeze region	212
61.	Actual field observed pumping versus pumping as predicted using COPES pumping model for the wet-nonfreeze region	214

LIST OF FIGURES (continued)

VOLUME VI APPENDIX C AND APPENDIX D

APPENDIX D - SUMMARY OF ANALYSIS DATA FOR THE EVALUATION OF PREDICTIVE MODELS (continued)

Figure	Title	Page
62.	Actual field measured faulting versus faulting as predicted using the COPES faulting models for all Phase I sections	218
63.	Actual field measured faulting versus faulting as predicted using the COPES faulting models for the dry-freeze region	220
64.	Actual field measured faulting versus faulting as predicted using the COPES JPCP faulting model for the dry-freeze region	223
65.	Actual field measured faulting versus faulting as predicted using the COPES JRCP faulting model for the dry-freeze region	223
66.	Actual field measured faulting versus faulting as predicted using the COPES faulting models for the dry-nonfreeze region	225
67.	Actual field measured faulting versus faulting as predicted using the COPES faulting models for the wet-freeze region	228
68.	Actual field measured faulting versus faulting as predicted using the COPES JPCP faulting model for the wet-freeze region	231
69.	Actual field measured faulting versus faulting as predicted using the COPES JRCP faulting model for the wet-freeze region	231
70.	Actual field measured faulting versus faulting as predicted using the COPES faulting models for the wet-nonfreeze region	233
71.	Actual field measured spalling versus joint deterioration (spalling) as predicted using the COPES spalling models for all Phase I sections	237
72.	Actual field measured spalling versus joint deterioration (spalling) as predicted using the COPES spalling models for the dry-freeze region	239
73.	Actual field measured spalling versus joint deterioration (spalling) as predicted using the COPES JPCP joint deterioration model for the dry-freeze region	242
74.	Actual field measured spalling versus joint deterioration (spalling) as predicted using the COPES JRCP joint deterioration model for the dry-freeze region	242
75.	Actual field measured spalling versus joint deterioration (spalling) as predicted using the COPES spalling models for the dry-nonfreeze region	244
76.	Actual field measured spalling versus joint deterioration (spalling) as predicted using the COPES spalling models for the wet-freeze region	247
77.	Actual field measured spalling versus joint deterioration (spalling) as predicted using the COPES JPCP joint deterioration model for the wet-freeze region	250
78.	Actual field measured spalling versus joint deterioration (spalling) as predicted using the COPES JRCP joint deterioration model for the wet-freeze region	250

LIST OF FIGURES (continued)

VOLUME VI APPENDIX C AND APPENDIX D

APPENDIX D - SUMMARY OF ANALYSIS DATA FOR THE EVALUATION OF PREDICTIVE MODELS (continued)

Figure	Title	Page
79.	Actual field measured spalling versus joint deterioration (spalling) as predicted using the COPES spalling models for the wet-nonfreeze region	252
80.	Actual field measured cracking versus cracking as predicted by the COPES cracking models for all Phase I sections	256
81.	Actual field measured cracking versus cracking as predicted by the COPES cracking models for the dry-freeze region	258
82.	Actual field measured cracking versus cracking as predicted by the COPES JPCP cracking model for the dry-freeze region	261
83.	Actual field measured cracking versus cracking as predicted by the COPES JRCP cracking model for the dry-freeze region	261
84.	Actual field measured cracking versus cracking as predicted by the COPES cracking models for the dry-nonfreeze region	263
85.	Actual field measured cracking versus cracking as predicted by the COPES cracking models for the wet-freeze region	266
86.	Actual field measured cracking versus cracking as predicted by the COPES JPCP cracking models for the wet-freeze region	269
87.	Actual field measured cracking versus cracking as predicted by the COPES JRCP cracking models for the wet-freeze region	269
88.	Actual field measured cracking versus cracking as predicted by the COPES cracking models for the wet-nonfreeze region	271
89.	Actual PSR as determined by a panel of users versus PSR as predicted by the COPES PSR models for all Phase I sections	275
90.	Actual PSR as determined by a panel of users versus PSR as predicted by the COPES PSR models for the dry-freeze region	277
91.	Actual PSR as determined by a panel of users versus PSR as predicted by the COPES JPCP PSR model for the dry-freeze region	280
92.	Actual PSR as determined by a panel of users versus PSR as predicted by the COPES JRCP PSR model for the dry-freeze region	280
93.	Actual PSR as determined by a panel of users versus PSR as predicted by the COPES PSR models for the dry-nonfreeze region	282
94.	Actual PSR as determined by a panel of users versus PSR as predicted by the COPES PSR models for the wet-freeze region	285
95.	Actual PSR as determined by a panel of users versus PSR as predicted by the COPES JPCP PSR model for the wet-freeze region	288
96.	Actual PSR as determined by a panel of users versus PSR as predicted by the COPES JRCP PSR model for the wet-freeze region	288
97.	Actual PSR as determined by a panel of users versus PSR as predicted by the COPES PSR models for the wet-nonfreeze region	290
98.	Actual field measured faulting versus faulting as predicted using the PFAULT models for all Phase I sections	294
99.	Actual field measured faulting versus faulting as predicted using the PFAULT models for the dry-freeze region	296

LIST OF FIGURES (continued)

VOLUME VI APPENDIX C AND APPENDIX D

APPENDIX D - SUMMARY OF ANALYSIS DATA FOR THE EVALUATION OF PREDICTIVE MODELS (continued)

Figure	Title	Page
100.	Actual field measured faulting versus faulting as predicted using the PFAULT models for doweled pavements for the dry-freeze region	299
101.	Actual field measured faulting versus faulting as predicted using the PFAULT models for nondoweled pavements for the dry-freeze region	299
102.	Actual field measured faulting versus faulting as predicted using the PFAULT models for the dry-nonfreeze region	301
103.	Actual field measured faulting versus faulting as predicted using the PFAULT models for the wet-freeze region	304
104.	Actual field measured faulting versus faulting as predicted using the PFAULT models for doweled pavements for the wet-freeze region	307
105.	Actual field measured faulting versus faulting as predicted using the PFAULT models for nondoweled pavements for the wet-freeze region	307
106.	Actual field measured faulting versus faulting as predicted using the PFAULT models for the wet-nonfreeze region	309
107.	Actual field measured faulting versus faulting as predicted using the PFAULT models for doweled pavements for the wet-nonfreeze region	312
108.	Actual field measured faulting versus faulting as predicted using the PFAULT models for nondoweled pavements for the wet-nonfreeze region	312

LIST OF TABLES

VOLUME I EVALUATION OF CONCRETE PAVEMENT PERFORMANCE AND DESIGN FEATURES

Table	Title	Page
1.	Listing of critical distress values by pavement type	26
2.	Slab modulus and composite k-values for Minnesota 1	28
3.	Deflection testing results and drainage coefficients for Minnesota 1	28
4.	Slab modulus and composite k-values for Minnesota 2	32
5.	Deflection testing results and drainage coefficients for Minnesota 2	32
6.	Longitudinal lane-shoulder joint load transfer efficiency for Minnesota 2	32
7.	Design and performance data for the outer lane of Minnesota 3 (Age = 1 year, ESAL's = 1.5 million)	36
8.	Design and performance data for the outer lane of Minnesota 4 (Age = 1 year, ESAL's = 0.22 million)	36
9.	Design and performance data for the outer lane of Minnesota 6 (Age = 4 years, ESAL's = 0.85 million)	36
10.	Traffic information for Arizona 1	38
11.	Slab modulus and composite k-values for Arizona 1	38
12.	Deflection testing results and drainage coefficients for Arizona 1	38
13.	Longitudinal lane-shoulder joint load transfer efficiency for Arizona 1	38
14.	Design and performance data for the outer lane of Arizona 2 (Age = 4 years, ESAL's = 1.6 million)	42
15.	Slab modulus and composite k-values for California 1	42
16.	Deflection testing results and drainage coefficients for California 1	42
17.	Slab modulus and composite k-values for California 2	46
18.	Deflection testing results and drainage coefficients for California 2	46
19.	Design and performance data for the outer lane of California 6 (Age = 7 years, ESAL's = 4.4 million)	49
20.	Design and performance data for the outer lane of California 7 (Age = 8 years, ESAL's = 10.5 million)	49
21.	Design and performance data for the outer lane of California 8 (Age = 4 years, ESAL's = 5.3 million)	49
22.	Slab modulus and composite k-values for Michigan 1	52
23.	Deflection testing results and drainage coefficients for Michigan 1	52
24.	Design and performance data for the outer lane of Michigan 3 (Age = 1 year, ESAL's = 2.8 million)	57
25.	Slab modulus and composite k-values for Michigan 4	57
26.	Deflection testing results and drainage coefficients for Michigan 4	57
27.	Longitudinal lane-shoulder joint load transfer efficiency for Michigan 4	57
28.	Design and performance data for the outer lane of Michigan 5 (Age = 3 years, ESAL's = 3.1 million)	62
29.	Slab modulus and composite k-values for New York 1	62
30.	Deflection testing results and drainage coefficients for New York 1	62
31.	Slab modulus and composite k-values for New York 2	66
32.	Deflection testing results and drainage coefficients for New York 2	66
33.	Longitudinal lane-shoulder joint load transfer efficiency for New York 2	66
34.	Slab modulus and composite k-values for Ohio 1	67
35.	Deflection testing results and drainage coefficients for Ohio 1	75
36.	Deflection testing results and drainage coefficients for Ontario 1	76
37.	Design and performance data for the outer lane of Ontario 2 (Age = 16 years, ESAL's = 36 million)	81

LIST OF TABLES (continued)

VOLUME I EVALUATION OF CONCRETE PAVEMENT PERFORMANCE AND DESIGN FEATURES (continued)

Table	Title	Page
38.	Traffic information for Pennsylvania 1	82
39.	Slab modulus and composite k-values for Pennsylvania 1	82
40.	Deflection testing results and drainage coefficients for Pennsylvania 1	82
41.	Design and performance data for the outer lane of New Jersey 2 (Age = 36 years, ESAL's = 35 million)	86
42.	Slab modulus and composite k-values for New Jersey 3	86
43.	Deflection testing results and drainage coefficients for New Jersey 3	86
44.	Slab modulus and composite k-values for California 3	90
45.	Deflection testing results and drainage coefficients for California 3	90
46.	Longitudinal lane-shoulder joint load transfer efficiency for California 3	90
47.	Slab modulus and composite k-values for North Carolina 1	94
48.	Deflection testing results and drainage coefficients for North Carolina 1	94
49.	Design and performance data for the outer lane of North Carolina 2 (Age = 5 years, ESAL's = 5.8 million)	98
50.	Design and performance data for the outer lane of Florida 2 (Age = 1 year, ESAL's = 2.0 million)	98
51.	Design and performance data for the outer lane of Florida 3 (Age = 5 years, ESAL's = 4.1 million)	100
52.	Transverse cracking by lane for Florida 3	100
53.	Effect of slab length on cracking for Florida 3	100
54.	Outer lane performance data relative to slab thickness for Minnesota 1 (Age = 17 years, ESAL's = 5.5 million)	103
55.	Outer lane performance data relative to slab thickness for Minnesota 2 (Age = 10 years, ESAL's = 2.8 million)	103
56.	Outer lane performance data relative to slab thickness for Arizona 1	103
57.	Outer lane performance data relative to slab thickness for California 1 (Age = 16 years, ESAL's = 7.6 million)	105
58.	Outer lane performance data relative to slab thickness for Ontario 1 (Age = 5 years, ESAL's = 0.84 million)	105
59.	Outer lane performance data relative to base type for Minnesota 1 (Age = 17 years, ESAL's = 5.5 million)	108
60.	Outer lane performance data relative to base type for Arizona 1	108
61.	Outer lane performance data relative to base type for California 1 (Age = 16 years, ESAL's = 7.6 million)	108
62.	Outer lane performance data relative to base type for California 2 (Age = 7 years, ESAL's = 4.4 million)	108
63.	Outer lane performance data relative to base type for Michigan 1 (Age = 12 years, ESAL's = 0.9 million)	110
64.	Outer lane performance data relative to base type for New York 1 (Age = 22 years, ESAL's = 2.0 million)	112
65.	Outer lane performance data relative to base type for Ohio 1 (Age = 14 years, ESAL's = 3.4 million)	112
66.	Average performance data relative to base type for Ontario 1 (Age = 5 years, ESAL's = 0.84 million)	112
67.	Outer lane performance data relative to base type for North Carolina 1 (Age = 20 years, ESAL's = 9.1 million)	114
68.	Overall relative summary of the performance of base types	116

LIST OF TABLES (continued)

VOLUME I EVALUATION OF CONCRETE PAVEMENT PERFORMANCE AND DESIGN FEATURES (continued)

Table	Title	Page
69.	Gradation information for permeable bases required for filter criteria evaluation	118
70.	Evaluation of filter criteria	119
71.	Outer lane performance data relative to joint spacing for Minnesota 1 (Age = 17 years, ESAL's = 5.5 million)	120
72.	Outer lane performance data relative to joint spacing for Minnesota 2 (Age = 10 years, ESAL's = 2.8 million)	120
73.	Outer lane performance data relative to joint spacing for California 1 (Age = 16 years, ESAL's = 7.6 million)	122
74.	Outer lane performance data relative to joint spacing for Michigan 1 (Age = 12 years, ESAL's = 0.9 million)	122
75.	Outer lane performance data relative to joint spacing for New York 1 (Age = 22 years, ESAL's = 2.0 million)	122
76.	Outer lane performance data relative to joint spacing for New York 2 (Age = 12 years, ESAL's = 1.43 million)	122
77.	Outer lane performance data relative to joint spacing for Ohio 1 (Age = 14 years, ESAL's = 3.4 million)	124
78.	Summary of cracking by slab length for sections with random joint spacing	126
79.	Ratio of slab length to the radius of relative stiffness (L/l)	127
80.	Effect of joint spacing, slab thickness, and base type on transverse cracking for California 1	130
81.	Summary of performance data related to reinforcement design	136
82.	Outer lane performance data relative to joint orientation for New York 1 (Age = 22 years, ESAL's = 2.0 million)	138
83.	Outer lane performance data relative to joint orientation for North Carolina 1 (Age = 20 years, ESAL's = 9.1 million)	138
84.	Outer lane performance data relative to joint load transfer for Minnesota 1 (Age = 17 years, ESAL's = 5.5 million)	140
85.	Outer lane performance data relative to joint load transfer for North Carolina 1 (Age = 20 years, ESAL's = 9.1 million)	140
86.	Load transfer performance data for nondoweled pavement sections	142
87.	Load transfer performance data for doweled sections	143
88.	Outer lane performance data relative to dowel coating for Ohio 1 (Age = 14 years, ESAL's = 3.4 million)	146
89.	Summary of longitudinal cracking and related design data	147
90.	Influence of shoulder on performance of mainline pavement for Michigan 4 (Age = 15 years, ESAL's = 4.4 million)	152
91.	Performance data relative to drainage for Michigan 1 (Age = 12 years, ESAL's = 0.9 million)	155
92.	Summary of selected performance data related to C_d	158

LIST OF TABLES (continued)

VOLUME II EVALUATION AND MODIFICATION OF CONCRETE PAVEMENT DESIGN AND ANALYSIS MODELS

Table	Title	Page
1.	Listing of pavement sections in dry-freeze environmental region	7
2.	Listing of pavement sections in dry-nonfreeze environmental region	8
3.	Listing of pavement sections in wet-freeze environmental region	10
4.	Listing of pavement sections in wet-nonfreeze environmental region	11
5.	Recommended levels of reliability for various functional classifications (1)	22
6.	Values of the drainage coefficient for the design of rigid pavements as presented in the AASHTO Guide (1)	24
7.	Load transfer coefficients for various pavement types and design conditions as presented in the AASHTO Guide (1)	24
8.	Actual field-measured faulting versus faulting as predicted using the COPES faulting models for the dry-freeze region	40
9.	Summary of the statistical analysis of the AASHTO design model	44
10.	Summary of the statistical analyses of the PEARDARP prediction models	47
11.	Summary of the statistical analyses of the COPES prediction models	53
12.	Summary of the statistical analyses of the PFAULT faulting prediction models	63
13.	CMS inputs for use with concrete pavements	76
14.	Specific sections and analyses performed using the CMS program	79
15.	Summary of thermal gradients at specified times for MN 1-1 for July 15 through July 21, 1987	80
16.	Analysis of stiffness of the paving layers in the deep frost, thaw-recovery, and nonfrost periods for MN 1-1	84
17.	Summary of thermal gradients at specified times for CA 1-1 for July 15 through July 21, 1987	87
18.	Summary of thermal gradients at specified times for MI 1-10a for July 15 through July 21, 1987	97
19.	Summary of thermal gradients at specified times for NC 1-1 for July 15 through July 21, 1987	101
20.	Summary of the results of the Liu-Lytton percent drainage versus time analyses for MN 1	107
21.	Relationships used in the Liu-Lytton drainage program to determine the base strength based on the level of saturation	112
22.	Summary of the results of the Liu-Lytton percent drainage versus time analysis for CA 1	114
23.	Permeabilities and porosities of subbase and subgrade for CA 1	114
24.	Time required to reach an 85 percent saturation level for CA 1 sections	116
25.	Probability of a wet subbase course for the CA 1 sections	119
26.	Summary of the results of the Liu-Lytton percent drainage versus time analyses for MI 1	119
27.	Permeabilities and porosities of subbase and subgrade for MI 1	121
28.	Time required to reach an 85 percent saturation level for MI 1 sections	124
29.	Probability of a wet subbase course for the MI 1 sections	124
30.	Summary of the results of the Liu-Lytton percent drainage versus time analyses for NC 1	125
31.	Time required to reach an 85 percent saturation level for NC 1 sections	128
32.	Summary of maximum surface deflection as calculated by ILLISLAB and JSLAB for a 14.4 kip (64 kN) dual wheel load with a tire pressure of 120 psi (83 kPa) placed at the slab's edge	133

LIST OF TABLES (continued)

VOLUME II EVALUATION AND MODIFICATION OF CONCRETE PAVEMENT DESIGN AND ANALYSIS MODELS (continued)

Table	Title	Page
33.	Summary of maximum tensile stress as calculated by ILLISLAB and JSLAB for a 14.4 kip (64 kN) dual wheel load with a tire pressure of 120 psi (83 kPa) placed at the slab's edge	133
34.	Summary of maximum surface deflection as calculated by ILLISLAB and JSLAB for a 14.4 kip (64 kN) dual wheel load with a tire pressure of 120 psi (83 kPa) placed at the slab's corner	134
35.	Summary of maximum tensile stress as calculated by ILLISLAB and JSLAB for a 14.4 kip (64 kN) dual wheel load with a tire pressure of 120 psi (83 kPa) placed at the slab's corner	134
36.	Summary of maximum thermal stresses as calculated by ILLISLAB and JSLAB	135
37.	Summary of maximum surface deflection, maximum edge stress, and maximum subgrade distress as calculated by ILLISLAB for a 14.4 kip (64 kN) dual wheel load with a tire pressure of 120 psi (83 kPa) placed at the slab's edge	142
38.	Summary of deflection and stress load transfer efficiencies as calculated by ILLISLAB for a 14.4 kip (64 kN) dual wheel load with a tire pressure of 120 psi (83 kPa) placed at the slab corner	145
39.	Measured deflection basin under 13,000 lb (58 kN) load at STA 3+73 approach joint, MI 1-10a	147
40.	Finite element analysis for the void analysis performed for STA 3+73, MI 1-10a	147
41.	Maximum positive and minimum negative thermal gradient calculated by the CMS program for MN 1, CA 1, MI 1, and NC 1	151
42.	Stresses developing due to thermal gradients through the slab	152
43.	Summary of PMARP results for the edge loading condition employing a 9 kip (40 kN) dual wheel load with a tire pressure of 80 psi (55 kPa)	159
44.	Summary of PMARP results for the corner loading condition employing a 9 kip (40 kN) dual wheel load with a tire pressure of 80 psi (55 kPa)	160
45.	Summary of Miner's fatigue damage and transverse cracking for MN 2, CA 2, MI 1, and NC 1	166
46.	Shoulder fatigue damage analysis for AZ 1 and MI 4-1 using the JCS-1 program	170
47.	Shoulder fatigue analysis for NC 1 using the BERM program	172
48.	Mean longitudinal cracking for all sections included in COPES and RIPPER databases	179
49.	Distribution of pavement sections and designs used in development of faulting models	180
50.	Yearly average daytime thermal gradients used in curling computations(2)	193
51.	Critical distress levels, by pavement type (46)	208
52.	Cost-effectiveness evaluation for Arizona	211
53.	Cost-effectiveness evaluation for California	213
54.	Cost-effectiveness evaluation for Michigan	217
55.	Cost-effectiveness evaluation for Minnesota	221
56.	Cost-effectiveness evaluation for North Carolina	224
57.	Arizona designs for cost-effectiveness evaluation	231
58.	California designs for cost-effectiveness evaluation	232
59.	Michigan designs for cost-effectiveness evaluation	234
60.	Minnesota designs for cost-effectiveness evaluation	236
61.	North Carolina designs for cost-effectiveness evaluation	238

LIST OF TABLES (continued)

VOLUME III SUMMARY OF RESEARCH FINDINGS

Table	Title	Page
1.	General information for pavements included in study	5
2.	Listing of pavement sections in dry-freeze environmental region	6
3.	Listing of pavement sections in dry-nonfreeze environmental regions	7
4.	Listing of pavement sections in wet-freeze environmental region	9
5.	Listing of pavement sections in wet-nonfreeze environmental region	10
6.	Listing of major data items contained in the data base	20
7.	Analysis and design models evaluated in this study	30
8.	Summary of the statistical analysis of the AASHTO design model	32
9.	Summary of the statistical analyses of the PEARDARP prediction models	33
10.	Summary of the statistical analyses of the COPES prediction models	36
11.	Summary of the statistical analyses of the PFAULT faulting prediction models	39
12.	Summary of maximum edge deflection as calculated by ILLISLAB and JSLAB	45
13.	Summary of maximum thermal stress as calculated by ILLISLAB and JSLAB	46
14.	Mean longitudinal cracking for all sections included in COPES and RIPPER data bases	56
15.	Suggested design limits for use with prediction models	67
16.	Performance results for 12 "replicate" inservice pavement sections in Illinois[41]	69
17.	Computed coefficients of variation for replicate pavement sections[41]	70
18.	Critical distress levels by pavement type[39]	74
19.	Example of the cost-effectiveness evaluation for Arizona projects	76

VOLUME IV APPENDIX A - PROJECT SUMMARY REPORTS AND SUMMARY TABLES

Table	Title	Page
1.	Corner voids on MN 1 sections at Rothsay	3
2.	Drainage summary for MN 1 and MN 5 sections	3
3.	Transverse joint spalling, by design variable	6
4.	Transverse joint faulting, by design variable	7
5.	Transverse cracking, by design variable	7
6.	Longitudinal cracking, by design variable	8
7.	Comparison of performance by lane	10
8.	Composite k-values	14
9.	Load transfer efficiency and corners with voids	14
10.	Drainage summary for MN 2 sections	15
11.	Transverse joint spalling on MN 2 sections	15
12.	Longitudinal cracking at MN 2, by design variable	17
13.	Shoulder performance at MN 2 sections	18
14.	Comparison of performance by lane at MN 2	21
15.	Traffic summary of AZ 1 sections	30
16.	Summary of k-value by base type	30
17.	Drainage summary for AZ 1 sections	31
18.	Comparison of performance by lane at AZ 1	36

LIST OF TABLES (continued)

VOLUME IV APPENDIX A - PROJECT SUMMARY REPORTS AND SUMMARY TABLES (continued)

Table	Title	Page
19.	Comparison of performance by lane at AZ 2	39
20.	Backcalculated E-value by concrete type	42
21.	Composite k-value by base type	43
22.	Corners with voids and pumping severity by base type	43
23.	Drainage summary for CA 1 sections	43
24.	Transverse joint faulting	44
25.	Transverse cracking on CA 1 sections	47
26.	Longitudinal cracking on CA 1 sections	48
27.	Roughness and present serviceability on CA 1 sections	48
28.	Performance summarized by base type	49
29.	Performance summarized by joint spacing	49
30.	Performance summarized by slab thickness	50
31.	Comparison of performance by lane at CA 1	50
32.	Summary of composite k-values of CA 2	53
33.	Load transfer efficiencies and corners with voids at CA 2	53
34.	Drainage summary for CA 2 sections	54
35.	Transverse joint faulting at CA 2	54
36.	Roughness and present serviceability at CA 2	56
37.	Comparison of performance by lane at CA 2	57
38.	Comparison of performance by lane at CA 6	60
39.	Summary of performance by lane at CA 7	62
40.	Comparison of performance by lane at CA 8	65
41.	Summary of composite k-value by base type	67
42.	Corners with voids at MI 1	68
43.	Drainage summary for MI 1 sections	69
44.	Transverse joint spalling on MI 1 sections	69
45.	Transverse joint faulting on MI 1 sections	72
46.	Transverse joint faulting summarized by subdrainage	73
47.	Roughness and present serviceability at MI 1	74
48.	Faulting as a function of load transfer and drainage	75
49.	Comparison of performance by transverse joint spacing	76
50.	Comparison of performance by lane at MI 1	77
51.	Corner void detection on MI 4 sections	83
52.	Drainage summary for MI 4 sections	83
53.	Composite k-value by base type	95
54.	Load transfer efficiencies and corners with voids at NY 1	96
55.	Drainage summary for NY 1 sections	96
56.	Roughness and present serviceability on NY 1 sections	101
57.	Comparison of performance by lane at NY 1	102
58.	Composite k-values and average mid-slab deflections at NY 2	106
59.	Load transfer efficiencies and corners with voids at NY 2	106
60.	Drainage summary for NY 2 sections	107
61.	Transverse cracking summarized by lane and transverse joint spacing	110
62.	Longitudinal cracking summarized by lane and transverse joint spacing	110
63.	Roughness and present serviceability at NY 2	111
64.	Summary of slab cracking on sections with concrete shoulders	111
65.	Performance comparison of sections with 20-ft transverse joint spacing	112

LIST OF TABLES (continued)

VOLUME IV APPENDIX A - PROJECT SUMMARY REPORTS AND SUMMARY TABLES (continued)

Table	Title	Page
66.	Comparison of performance by lane and pavement type at NY 2	112
67.	Composite k-values at OH 1	115
68.	Load transfer efficiencies and corners with voids at OH 1	115
69.	Drainage summary for OH 1 sections	116
70.	Transverse joint faulting at OH 1	119
71.	Roughness and present serviceability at OH 1	120
72.	Comparison of performance by lane and base type of OH 1	122
73.	Drainage summary for OH 2 Sections	125
74.	Transverse joint spalling at OH 2	125
75.	Transverse joint performance at OH 2	127
76.	Roughness and present serviceability on OH 2 sections	128
77.	Summary of longitudinal joint spalling at OH 2	129
78.	Outer shoulder performance at OH 2	129
79.	Comparison of performance by lane at OH 2	130
80.	Load transfer efficiency and corners with voids at ONT 1	134
81.	Summary of drainage characteristics at ONT 1	134
82.	Summary of transverse joint faulting by direction of traffic	135
83.	Roughness and present serviceability at ONT 1	137
84.	Shoulder performance at ONT 1	138
85.	Comparison of performance by lane at ONT 1	140
86.	Summary of performance variables at ONT 2	143
87.	Traffic summary of PA 1 sections	145
88.	Summary of composite k-value by base type	146
89.	FWD deflection testing results at PA 1	146
90.	Drainage summary for PA 1 sections	147
91.	Roughness and present serviceability at PA 1	150
92.	Comparison of performance by lane at PA 1	151
93.	Comparison of performance by lane at NJ 2	154
94.	Summary of composite k-values at NJ 3	156
95.	Drainage summary for NJ 3	157
96.	Transverse joint faulting at NJ 3	159
97.	Roughness and present serviceability at NJ 3	159
98.	Comparison of performance by lane at NJ 3	160
99.	Composite k-values at CA 3	163
100.	FWD deflection testing results at CA 3	164
101.	Drainage summary for CA 3	164
102.	Transverse joint spalling at CA 3	167
103.	Transverse joint faulting at CA 3	167
104.	Transverse cracking at CA 3	167
105.	Roughness and present serviceability at CA 3	168
106.	Outer shoulder performance at CA 3	169
107.	Comparison of performance by lane at CA 3	169
108.	Composite k-values and load transfer efficiency at NC 1	173
109.	Percent corners with voids at NC 1	173
110.	Drainage summary for NC 1 sections	174
111.	Transverse joint faulting by load transfer type	177
112.	Longitudinal cracking at NC 1	178

LIST OF TABLES (continued)

VOLUME IV APPENDIX A - PROJECT SUMMARY REPORTS AND SUMMARY TABLES (continued)

Table	Title	Page
113.	Comparison of performance by transverse joint orientation	180
114.	Comparison of performance by lane and base type at NC 1	180
115.	Comparison of performance by lane for NC 2	184
116.	Pavement performance at FL 2	187
117.	Comparison of performance by lane for FL 3	189
118.	Transverse cracking at FL 3	189
119.	Slab cracking as a function of slab length at FL 3	190
120.	General information and design data for projects included in study	205
121.	Slab design data for projects in dry-freeze environmental zone	206
122.	Base, subbase, subgrade, and outer shoulder design data for projects in dry-freeze environmental zone	207
123.	Pavement joint data for projects in dry-freeze environmental zone	208
124.	Outer lane deflection data of projects in dry-freeze environmental zone	209
125.	Outer shoulder and drainage information for projects in dry-freeze environmental zone	210
126.	Traffic information for projects in dry-freeze environmental zone	211
127.	Outer lane performance data for projects in dry-freeze environmental zone	212
128.	Lane 2 performance data for projects in dry-freeze environmental zone	213
129.	Slab design for projects in dry-nonfreeze environmental zone	214
130.	Base, subbase, subgrade, and outer shoulder design data for projects in dry-nonfreeze environmental zone	215
131.	Pavement joint data for projects in dry-nonfreeze environmental zone	216
132.	Outer lane deflection data of projects in dry-nonfreeze environmental zone	217
133.	Outer shoulder and drainage information for projects in dry-nonfreeze environmental zone	218
134.	Traffic information for projects in dry-nonfreeze environmental zone	219
135.	Outer lane performance data for projects in dry-nonfreeze environmental zone	220
136.	Lane 2 performance data for projects in dry-nonfreeze environmental zone	221
137.	Slab design for projects in wet-freeze environmental zone	222
138.	Base, subbase, subgrade, and outer shoulder design data for projects in wet-freeze environmental zone	224
139.	Pavement joint data for projects in wet-freeze environmental zone	226
140.	Outer lane deflection data of projects in wet-freeze environmental zone	228
141.	Outer shoulder and drainage information for projects in wet-freeze environmental zone	230
142.	Traffic information for projects in wet-freeze environmental zone	232
143.	Outer lane performance data for projects in wet-freeze environmental zone	234
144.	Lane 2 performance data for projects in wet-freeze environmental zone	236
145.	Slab design for projects in wet-nonfreeze environmental zone	238
146.	Base, subbase, subgrade, and outer shoulder design data for projects in wet-nonfreeze environmental zone	239
147.	Pavement joint data for projects in wet-nonfreeze environmental zone	240
148.	Outer lane deflection data of projects in wet-nonfreeze environmental zone	241
149.	Outer shoulder and drainage information for projects in wet-nonfreeze environmental zone	242
150.	Traffic information for projects in wet-nonfreeze environmental zone	243

LIST OF TABLES (continued)

VOLUME IV APPENDIX A - PROJECT SUMMARY REPORTS AND SUMMARY TABLES (continued)

Table	Title	Page
151.	Outer lane performance data for projects in wet-nonfreeze environmental zone	244
152.	Lane 2 performance data for projects in wet-nonfreeze environmental zone	245

VOLUME V APPENDIX B - DATA COLLECTION AND ANALYSIS PROCEDURES

Table	Title	Page
1.	WIM project locations	18
2.	FHWA vehicle classification types (5)	18
3.	Field procedures for collection of WIM data	20
4.	Chart to calculate saturation time curve	36
5.	Eh^3 values for all Phase I sections	67
6.	Effect of deflection error on backcalculated E and k	69
7.	Listing of major data items contained in the database	78

VOLUME VI APPENDIX C AND APPENDIX D

APPENDIX C - SYNTHESIS OF CONCRETE PAVEMENT DESIGN METHODS AND ANALYSIS MODELS

Table	Title	Page
1.	Evaluation of analysis models and design methods	29
2.	Levels of design variables	34
3.	Parameters assumed for use in the analysis models and design methods (5)	35
4.	Traffic data assumed in design models (5)	36
5.	Loadometer data assumed in design models (5)	37
6.	ILLISLAB input and output variables	52
7.	JSLAB input and output variables	53
8.	WESLIQID input and output variables	54
9.	WESLAYER input and output variables	55
10.	RISC input and output variables	56
11.	PMARP input and output variables	57

LIST OF TABLES (continued)

VOLUME VI APPENDIX C AND APPENDIX D

APPENDIX C - SYNTHESIS OF CONCRETE PAVEMENT DESIGN METHODS AND ANALYSIS MODELS (continued)

Table	Title	Page
12.	H-51 input and output variables	58
13.	CMS input and output variables	59
14.	Liu-Lytton drainage models input and output variables	60
15.	PREDICT input and output variables	61
16.	PEARDARP input and output variables	62
17.	JCP-1 input and output variables	63
18.	DNPS86 input and output variables	64
19.	RPS-3 input and output variables	65
20.	PCA and California Rigid Pavement Design Procedure input and output variables	67
21.	JCS-1 and BERM input and output variables	68
22.	Method of obtaining input variables for ILLISLAB	69
23.	Methods of obtaining input variables for JSLAB	70
24.	Methods of obtaining input variables for CMS	71
25.	Methods of obtaining input variables for Liu-Lytton Drainage Models	72
26.	Method of obtaining input variables for PMARP	73
27.	Method of obtaining input variables for PEARDARP	74
28.	Method of obtaining input variables for PREDICT	75
29.	Method of obtaining input variables for BERM	76
30.	Method of obtaining input variables for JCS-1	77
31.	Method of obtaining input variables for JCP-1	78
32.	Effect of slab thickness on pavement responses as measured by ILLISLAB, JSLAB, WESLIQID, and WESLAYER	80
33.	Effect of shoulder parameters on pavement responses as measured by ILLISLAB, JSLAB, WESLIQID, and WESLAYER	81
34.	Effect of subgrade strength on pavement responses as measured by ILLISLAB, JSLAB, WESLIQID, and WESLAYER	82
35.	Effect of joint width and slab length on pavement responses as measured by ILLISLAB, JSLAB, WESLIQID, and WESLAYER	83
36.	Effect of load transfer on pavement responses as measured by ILLISLAB and JSLAB	84
37.	Effect of base type on pavement responses as measured by ILLISLAB and JSLAB	85
38.	Effect of slab length/joint width, slab thickness, and shoulder parameters on pavement responses as measured by PMARP	86
39.	Effect of void depth, drainage factor, rainfall factor, and subbase treatment factor on pavement responses as measured by PMARP	87
40.	ILLISLAB and JSLAB curling analysis	88
41.	WESLIQID and WESLAYER curling analysis	89
42.	Analysis of RISC	90
43.	Effect of subgrade strength and pavement thickness on pavement response as measured by H-51	91
44.	CMS capabilities	92
45.	Effect of subgrade strength and slab thickness on cracking and PSR of JPCP as measured by PREDICT	94

LIST OF TABLES (continued)

VOLUME VI APPENDIX C AND APPENDIX D

APPENDIX C - SYNTHESIS OF CONCRETE PAVEMENT DESIGN METHODS AND ANALYSIS MODELS (continued)

Table	Title	Page
46.	Effect of subgrade strength and slab thickness on pumping of JPCP as measured by PREDICT	95
47.	Effect of climatic region on distresses of JPCP as measured by PREDICT	96
48.	Specific variables for the nine climatic zones (5)	97
49.	Effect of climatic region on distresses of JRCP as measured by PREDICT	99
50.	Effect of climatic region on distress of JRCP as measured by PREDICT	100
51.	Effect of subdrainage on JRCP distress as measured by PREDICT	101
52.	Effect of subgrade strength on JPCP distress as measured by PEARDARP	102
53.	Effect of pavement thickness on JPCP distress as measured by PEARDARP	103
54.	Effect of various inputs on fatigue damage as measured by JCP-1	104
55.	Effect of various inputs on serviceability as measured by JCP-1	105
56.	Effect of various inputs on DNPS86 design outputs	106
57.	Effect of loss of support, drainage factor, and ESAL's on design using DNPS86	107
58.	Effect of various inputs on RPS-3 outputs	108
59.	Effect of subgrade strength and load transfer on PCA design outputs	109
60.	Effect of subgrade strength on California rigid pavement design outputs	110
61.	Effect of shoulder type and thickness on BERM shoulder design outputs	111
62.	Effect of various inputs on JCS-1 design outputs	112
63.	Effect of various inputs on the Liu-Lytton drainage models outputs	113
64.	Effect of various inputs on JRCP4 outputs	114

VOLUME VI APPENDIX C AND APPENDIX D

APPENDIX D - SUMMARY OF ANALYSIS DATA FOR THE EVALUATION OF PREDICTIVE MODELS

Table	Title	Page
65.	Actual ESAL's (based on ADT) versus ESAL's as predicted using the AASHTO design equation for all Phase I sections	116
66.	Actual ESAL's (based on ADT) versus ESAL's as predicted using the AASHTO design equation for the dry-freeze region	120
67.	Actual ESAL's (based on ADT) versus ESAL's as predicted using the AASHTO design equation for the dry-nonfreeze region	121
68.	Actual ESAL's (based on ADT) versus ESAL's as predicted using the AASHTO design equation for the wet-freeze region	123
69.	Actual ESAL's (based on ADT) versus ESAL's as predicted using the AASHTO design equation for the wet-nonfreeze region	125
70.	Actual PSR as determined by a panel of users versus PSI as predicted by the PEARDARP PSI model for all Phase I sections	127
71.	Actual PSR as determined by a panel of users versus PSI as predicted by the PEARDARP PSI model for the dry-freeze region	131
72.	Actual PSR as determined by a panel of users versus PSI as predicted by the PEARDARP PSI model for the dry-nonfreeze region	132

LIST OF TABLES (continued)

VOLUME VI APPENDIX C AND APPENDIX D

APPENDIX D - SUMMARY OF ANALYSIS DATA FOR THE EVALUATION OF PREDICTIVE MODELS (continued)

Table	Title	Page
73.	Actual PSR as determined by a panel of users versus PSI as predicted by the PEARDARP PSI model for the wet-freeze region	134
74.	Actual PSR as determined by a panel of users versus PSI as predicted by the PEARDARP PSI model for the wet-nonfreeze region	136
75.	Actual field measured roughness versus roughness as predicted using the PEARDARP roughness model for all Phase I sections	138
76.	Actual field measured roughness versus roughness as predicted using the PEARDARP roughness model for the dry-freeze region	142
77.	Actual field measured roughness versus roughness as predicted using the PEARDARP roughness model for the dry-nonfreeze region	143
78.	Actual field measured roughness versus roughness as predicted using the PEARDARP roughness model for the wet-freeze region	145
79.	Actual field measured roughness versus roughness as predicted using the PEARDARP roughness model for the wet-nonfreeze region	147
80.	Comparison of actual field observed pumping with the normalized pumping index, volume of pumping, number of joints pumping, and volume of undersealing material required as predicted by the PEARDARP pumping model for all Phase I sections	149
81.	Actual field measured spalling versus spalling as predicted using the PEARDARP spalling model for all Phase I sections	152
82.	Actual field measured spalling versus spalling as predicted using the PEARDARP spalling model for the dry-freeze region	156
83.	Actual field measured spalling versus spalling as predicted using the PEARDARP spalling model for the dry-nonfreeze region	157
84.	Actual field measured spalling versus spalling as predicted using the PEARDARP spalling model for the wet-freeze region	159
85.	Actual field measured spalling versus spalling as predicted using the PEARDARP spalling model for the wet-nonfreeze region	161
86.	Actual field measured faulting versus faulting as predicted using the PEARDARP faulting models for all Phase I sections	163
87.	Actual field measured faulting versus faulting as predicted using the PEARDARP faulting models for the dry-freeze region	167
88.	Actual field measured faulting versus faulting as predicted using the PEARDARP faulting models for doweled pavements for the dry-freeze region	169
89.	Actual field measured faulting versus faulting as predicted using the PEARDARP faulting models for nondoweled pavements for the dry-freeze region	170
90.	Actual field measured faulting versus faulting as predicted using the PEARDARP faulting models for the dry-nonfreeze region	172
91.	Actual field measured faulting versus faulting as predicted using the PEARDARP faulting models for the wet-freeze region	174
92.	Actual field measured faulting versus faulting as predicted using the PEARDARP faulting models for doweled pavements for the wet-freeze region	177

LIST OF TABLES (continued)

VOLUME VI APPENDIX C AND APPENDIX D

APPENDIX D - SUMMARY OF ANALYSIS DATA FOR THE EVALUATION OF PREDICTIVE MODELS (continued)

Table	Title	Page
93.	Actual field measured faulting versus faulting as predicted using the PEARDARP faulting models for nondoweled pavements for the wet-freeze region	178
94.	Actual field measured faulting versus faulting as predicted using the PEARDARP faulting models for the wet-nonfreeze region	180
95.	Actual field measured faulting versus faulting as predicted using the PEARDARP faulting models for doweled pavements for the wet-nonfreeze region	182
96.	Actual field measured faulting versus faulting as predicted using the PEARDARP faulting models for nondoweled pavements for the wet-nonfreeze region	183
97.	Actual field measured cracking versus cracking as predicted using the PEARDARP cracking models for all Phase I sections	185
98.	Actual field measured cracking versus cracking as predicted using the PEARDARP cracking model for the dry-freeze region	189
99.	Actual field measured cracking versus cracking as predicted using the PEARDARP cracking model for the dry-nonfreeze region	190
100.	Actual field measured cracking versus cracking as predicted using the PEARDARP cracking model for the wet-freeze region	192
101.	Actual field measured cracking versus cracking as predicted using the PEARDARP cracking model for the wet-nonfreeze region	194
102.	Actual field observed pumping versus pumping as predicted using COPES pumping models for all Phase I sections	196
103.	Actual field observed pumping versus pumping as predicted using COPES pumping models for the dry-freeze region	200
104.	Actual field observed pumping versus pumping as predicted using COPES JPCP pumping model for the dry-freeze region	202
105.	Actual field observed pumping versus pumping as predicted using COPES JRCP pumping model for the dry-freeze region	203
106.	Actual field observed pumping versus pumping as predicted using COPES pumping model for the dry-nonfreeze region	205
107.	Actual field observed pumping versus pumping as predicted using COPES pumping model for the wet-freeze region	207
108.	Actual field observed pumping versus pumping as predicted using COPES JPCP pumping model for the wet-freeze region	210
109.	Actual field observed pumping versus pumping as predicted using COPES JRCP pumping model for the wet-freeze region	211
110.	Actual field observed pumping versus pumping as predicted using COPES pumping model for the wet-nonfreeze region	213
111.	Actual field measured faulting versus faulting as predicted using the COPES faulting models for all Phase I sections	215
112.	Actual field measured faulting versus faulting as predicted using the COPES faulting models for the dry-freeze region	219
113.	Actual field measured faulting versus faulting as predicted using the COPES JPCP faulting model for the dry-freeze region	221

LIST OF TABLES (continued)

VOLUME VI APPENDIX C AND APPENDIX D

APPENDIX D - SUMMARY OF ANALYSIS DATA FOR THE EVALUATION OF PREDICTIVE MODELS (continued)

Table	Title	Page
114.	Actual field measured faulting versus faulting as predicted using the COPES JRCP faulting model for the dry-freeze region	222
115.	Actual field measured faulting versus faulting as predicted using the COPES faulting models for the dry-nonfreeze region	224
116.	Actual field measured faulting versus faulting as predicted using the COPES faulting models for the wet-freeze region	226
117.	Actual field measured faulting versus faulting as predicted using the COPES JPCP faulting model for the wet-freeze region	229
118.	Actual field measured faulting versus faulting as predicted using the COPES JRCP faulting model for the wet-freeze region	230
119.	Actual field measured faulting versus faulting as predicted using the COPES faulting models for the wet-nonfreeze region	232
120.	Actual field measured spalling versus joint deterioration (spalling) as predicted using the COPES spalling models for all Phase I sections	234
121.	Actual field measured spalling versus joint deterioration (spalling) as predicted using the COPES spalling models for the dry-freeze region	238
122.	Actual field measured spalling versus joint deterioration (spalling) as predicted using the COPES JPCP joint deterioration model for the dry-freeze region	240
123.	Actual field measured spalling versus joint deterioration (spalling) as predicted using the COPES JRCP joint deterioration model for the dry-freeze region	241
124.	Actual field measured spalling versus joint deterioration (spalling) as predicted using the COPES spalling models for the dry-nonfreeze region	243
125.	Actual field measured spalling versus joint deterioration (spalling) as predicted using the COPES spalling models for the wet-freeze region	245
126.	Actual field measured spalling versus joint deterioration (spalling) as predicted using the COPES JPCP joint deterioration model for the wet-freeze region	248
127.	Actual field measured spalling versus joint deterioration (spalling) as predicted using the COPES JRCP joint deterioration model for the wet-freeze region	249
128.	Actual field measured spalling versus joint deterioration (spalling) as predicted using the COPES spalling models for the wet-nonfreeze region	251
129.	Actual field measured cracking versus cracking as predicted by the COPES cracking models for all Phase I sections	253
130.	Actual field measured cracking versus cracking as predicted by the COPES cracking models for the dry-freeze region	257
131.	Actual field measured cracking versus cracking as predicted by the COPES JPCP cracking model for the dry-freeze region	259

LIST OF TABLES (continued)

VOLUME VI APPENDIX C AND APPENDIX D

APPENDIX D - SUMMARY OF ANALYSIS DATA FOR THE EVALUATION OF PREDICTIVE MODELS (continued)

Table	Title	Page
132.	Actual field measured cracking versus cracking as predicted by the COPES JRCP cracking model for the dry-freeze region	260
133.	Actual field measured cracking versus cracking as predicted by the COPES cracking models for the dry-nonfreeze region	262
134.	Actual field measured cracking versus cracking as predicted by the COPES cracking models for the wet-freeze region	264
135.	Actual field measured cracking versus cracking as predicted by the COPES JPCP cracking models for the wet-freeze region	267
136.	Actual field measured cracking versus cracking as predicted by the COPES JRCP cracking model for the wet-freeze region	268
137.	Actual field measured cracking versus cracking as predicted by the COPES cracking models for the wet-nonfreeze region	270
138.	Actual PSR as determined by a panel of users versus PSR as predicted by the COPES PSR models for all Phase I sections	272
139.	Actual PSR as determined by a panel of users versus PSR as predicted by the COPES PSR models for the dry-freeze region	276
140.	Actual PSR as determined by a panel of users versus PSR as predicted by the COPES JPCP PSR model for the dry-freeze region	278
141.	Actual PSR as determined by a panel of users versus PSR as predicted by the COPES JRCP PSR model for the dry-freeze region	279
142.	Actual PSR as determined by a panel of users versus PSR as predicted by the COPES PSR models for the dry-nonfreeze region	281
143.	Actual PSR as determined by a panel of users versus PSR as predicted by the COPES PSR models for the wet-freeze region	283
144.	Actual PSR as determined by a panel of users versus PSR as predicted by the COPES JPCP PSR model for the wet-freeze region	286
145.	Actual PSR as determined by a panel of users versus PSR as predicted by the COPES JRCP PSR model for the wet-freeze region	287
146.	Actual PSR as determined by a panel of users versus PSR as predicted by the COPES PSR models for the wet-nonfreeze region	289
147.	Actual field measured faulting versus faulting as predicted using the PFAULT models for all Phase I sections	291
148.	Actual field measured faulting versus faulting as predicted using the PFAULT models for the dry-freeze region	295
149.	Actual field measured faulting versus faulting as predicted using the PFAULT models for doweled pavements for the dry-freeze region	297
150.	Actual field measured faulting versus faulting as predicted using the PFAULT models for nondoweled pavements for the dry-freeze region	298
151.	Actual field measured faulting versus faulting as predicted using the PFAULT models for the dry-nonfreeze region	300
152.	Actual field measured faulting versus faulting as predicted using the PFAULT models for the wet-freeze region	302
153.	Actual field measured faulting versus faulting as predicted using the PFAULT models for doweled pavements for the wet-freeze region	305

LIST OF TABLES (continued)

VOLUME VI APPENDIX C AND APPENDIX D

APPENDIX D - SUMMARY OF ANALYSIS DATA FOR THE EVALUATION OF PREDICTIVE MODELS (continued)

Table	Title	Page
154.	Actual field measured faulting versus faulting as predicted using the PFAULT models for nondoweled pavements for the wet-freeze region	306
155.	Actual field measured faulting versus faulting as predicted using the PFAULT models for the wet-nonfreeze region	308
156.	Actual field measured faulting versus faulting as predicted using the PFAULT models for doweled pavements for the wet-nonfreeze region	310
157.	Actual field measured faulting versus faulting as predicted using the PFAULT models for nondoweled pavements for the wet-nonfreeze region	311
158.	Data used for the analysis of the PEARDARP, COPES, AND PFAULT predictive models	313

CHAPTER 1 INTRODUCTION

In a major national field and analytical research project conducted for the Federal Highway Administration (FHWA), the performance of jointed concrete pavements was studied. The effect of design, environmental, and service factors on jointed concrete performance was evaluated. This report is a summary of that study and is one volume of a six-volume series of reports. The other reports are:

FHWA Report No.	Vol. No.	Short Title
FHWA-RD-89-136	I	Evaluation of Concrete Pavement Performance and Design Features
FHWA-RD-89-137	II	Evaluation and Modification of Concrete Pavement Design and Analysis Models
FHWA-RD-89-139	IV	Appendix A—Project Summary Reports and Summary Tables
FHWA-RD-89-140	V	Appendix B—Data Collection and Analysis Procedures
FHWA-RD-89-141	VI	Appendix C—Synthesis of Concrete Pavement Design Methods and Analysis Models
		Appendix D—Summary of Analysis Data for the Evaluation of Predictive Models

STUDY OBJECTIVES

The specific objectives of the study were to:

- Evaluate the performance of different jointed concrete pavement design features on in-place pavement sections under similar environmental and traffic loading conditions.
- Determine the adequacy of available models and design procedures to predict the performance of in-place pavement sections.
- Improve the analysis and design procedures and guidance for the design of jointed concrete pavements to reflect the effects of sealing, drainage, and deflection on pavement performance.

The overall objective of the study can be summarized as the improvement of initial design procedures through consideration of existing analytical techniques and field performance observations.

BACKGROUND AND RESEARCH SCOPE

Several experimental concrete pavements constructed in the U.S. since the 1960's are old enough to have experienced sufficient traffic to provide some very significant insights about their performance. Many of these pavements were constructed to evaluate the effect of one or more design features on performance. It was believed that an in-depth evaluation of these sections could provide valuable inservice pavement performance information that could be used for improving concrete pavement design and construction procedures.

An extensive literature search was completed to identify experimental and research projects and regular construction pavement sections for which design, construction, and performance data were available. Sixteen experimental projects that totaled 80 sections were ultimately selected, along with 15 other sections not part of any experiment and representing newer designs, for a total of 95 concrete pavement sections.

Those sections included in the study consisted of both jointed reinforced and jointed plain designs and were the subject of a comprehensive condition survey in 1987. The performance data for each standard section and each group of experimental sections were documented and carefully analyzed. Many interesting and significant results were obtained from the initial performance analysis. The effects of the pavement design variables (thickness, joint spacing, base type, etc.) on performance were documented. Results from the study of field performance were then used in analytical evaluations to assess existing concrete design and analysis models and in the development of new prediction models.

DESCRIPTION OF REPORTS

The research results are documented in six volumes. Volume I presents a description and performance evaluation of the 95 pavement sections included in the study. Volume II investigates the accuracy of several concrete pavement performance models and presents new predictive models. Volume IV provides the detailed summary reports that document the design, construction, and performance of the 95 concrete pavement sections. Volume V provides the documentation of the data collection and analysis procedures used in the study. Volume VI contains a discussion of the analysis data for the evaluation of the prediction models. This particular volume, volume III, is an overall summary of the Phase I study. Consequently, it provides only the major highlights of the research.

CHAPTER 2 STUDY SECTIONS AND DATA COLLECTION

STUDY SECTIONS

More than 300 candidate sections were reviewed for possible inclusion in the study. These were sections, located all over the country, in which highway agencies made a concerted effort to investigate the performance of various concrete pavement design features. A partial listing of these sections is provided in appendix A.

Ninety-five jointed concrete pavement sections representing the four major climatic regions were ultimately selected and evaluated under this study. Figure 1 shows the States and Provinces that participated in the study, while table 1 provides general information on the selected study sections. The age of the pavement sections ranged from 1 to 36 years. Design features that were evaluated included slab thickness, pavement type, base type, joint spacing, method of load transfer, and shoulder type. A brief overview of the sections included in the study, and the design features that were evaluated, are provided in the following sections.

DRY-FREEZE ENVIRONMENTAL REGION

Twenty pavement sections were evaluated in the dry-freeze environmental region, including 17 experimental or older sections and 3 recently constructed sections. All of these sections were located in Minnesota.

Minnesota is actually located in a transition area between the wet-freeze and the dry-freeze environmental regions, but was included in the dry-freeze zone for purposes of categorization. However, an examination of the Thornthwaite Moisture Index, which represents the potential amount of (annual) free moisture available in an area, shows that Minnesota is certainly much drier than such States as Michigan or New York which are located in the wet-freeze environmental zone.

Table 2 provides a listing of the projects included from the dry-freeze environmental region. The pavements ranged in age from 1 to 17 years at the time of survey (1987). Such design features as slab thickness, pavement type, load transfer, shoulder type, and base type were included from this region.

DRY-NONFREEZE ENVIRONMENTAL REGION

Seventeen pavement sections were evaluated in the dry-nonfreeze environmental region, including 14 experimental or older sections and 3 recently constructed sections. All projects were located in either Arizona or California.

The projects included in the dry-nonfreeze environmental region are listed in table 3. The oldest sections were 16 years old and the youngest was 4 years old at

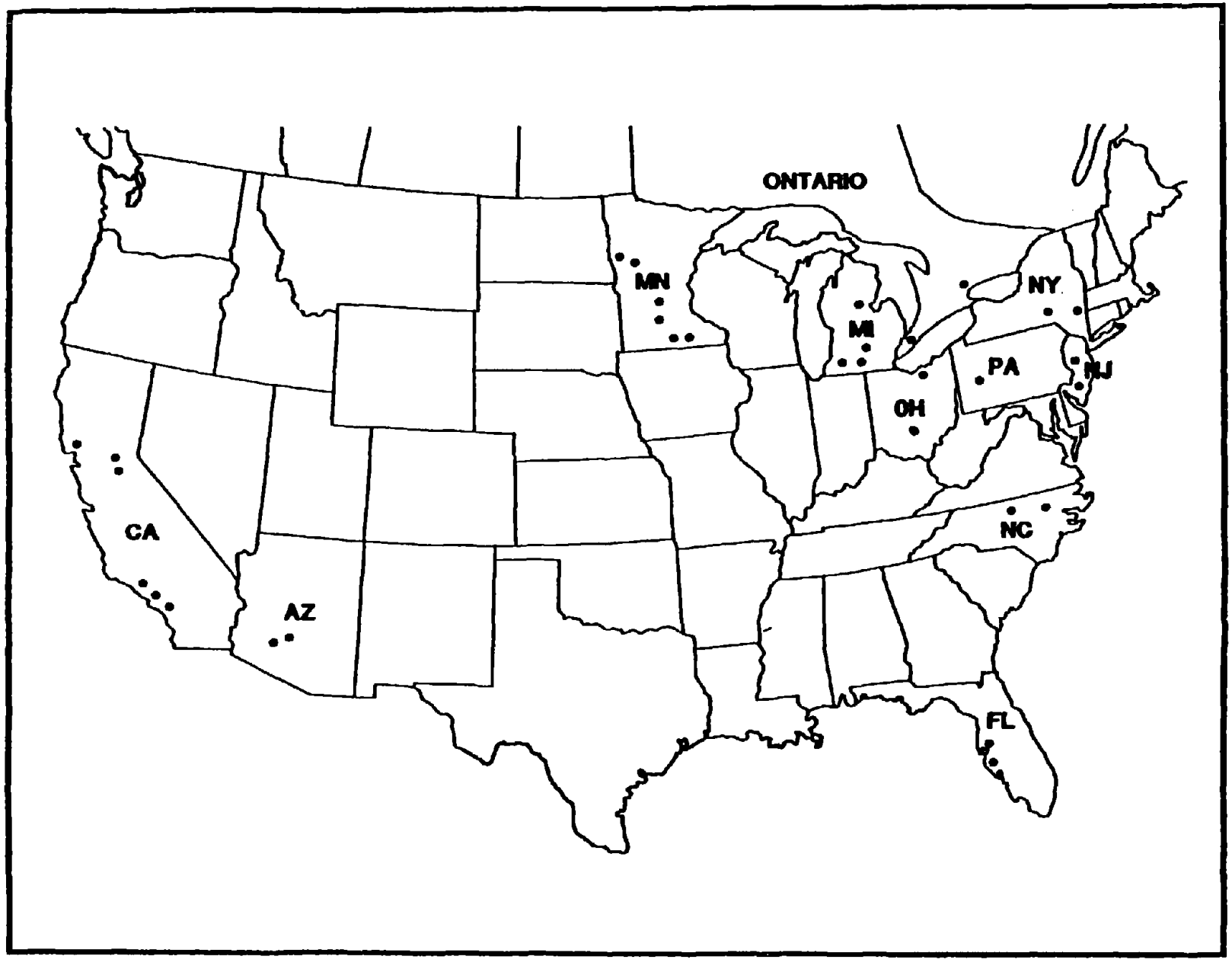

Figure 1. States participating in study.

Table 1. General information for pavements included in study.

ZONE	PROJECT LOCATION	Total Number of Exptl. Sects.	Number of Sects. Eval.	Project Average Section Length, FT	Thornthwaite Moisture Index	Corps of Engr. Freez. Index	No. of Freeze/ Thaw Cycles/ Year	Highest Average Daily Maximum Temp,°F	Lowest Average Daily Minimum Temp,°F	Average Max - Average Min, °F	Average Number of Days Precip/ Year	Annual Average Precip, IN	Design Features Evaluated (See Codes)
FREEZE ZONE	I-94 Rothsay, MN	24	12	729	0	2188	92	84	-3	87	109	23.4	1, 3, 6, 7
	I-94 Rothsay, MN	1	1	800	7	2188	92	84	-3	87	109	23.4	CONTROL
	I-90 Albert Lea, MN	4	4	1053	16	1688	90	85	6	79	106	29.7	1, 2, 4, 6, 7
	I-90 Austin, MN	1	1	1053	21	1250	90	83	2	81	110	31.2	NEW- 7
	TH 15 New Ulm, MN	1	1	1243	0	1800	80	86	2	84	105	28.1	NEW- 1,4,7,8
	TH 15 Truman, MN	1	1	1053	17	1800	88	83	1	82	105	30.2	NEW- 1,3,7,8
	RT 360 Phoenix, AZ	7	6	1059	-47	0	40	105	36	69	34	8.0	1, 3, 7, 8
	I-10 Phoenix, AZ	1	1	1041	-49	0	20	105	39	66	34	6.9	NEW- 3,4,6
DRY ZONE	I-5 Tracy, CA	9	5	1056	-42	0	40	94	37	57	61	9.7	1, 3, 4
	I-5 Sacramento, CA	1	1	1069	-31	0	40	93	38	55	58	17.2	CONTROL (8)
	I-210 Los Angeles, CA	2	2	988	-29	0	40	89	41	48	40	15.6	3, 8
	US 101 1000 Oaks, CA	1	1	1056	-25	0	40	76	43	33	40	14.6	NEW-1,3,4,7,8
	RT 14 Solemint, CA	1	1	1072	-43	0	40	98	32	66	40	7.3	NEW- 3,4,8
	US 10 Claro, MI	10	8	644	29	875	100	82	10	72	135	32.3	2,3,4,5,6,8
	I-69 Charlotte, MI	12	2	4068	22	563	100	84	13	71	144	31.8	7
	I-94 Marshall, MI	1	1	1066	27	563	100	83	15	68	144	34.0	NEW- 3,8
	I-94 Paw Paw, MI	1	1	1066	40	563	100	85	17	68	86	38.2	NEW- 3,8
	RT 23 Catskill, NY	30	6	599	54	500	80	82	9	73	136	38.9	2, 3, 4, 5, 6
	I-88 Otego, NY	4	4	1000	53	500	88	83	13	70	164	40.5	2, 4, 7
WET ZONE	RT 23 Chillicothe, OH	15	7	266	33	25	98	86	20	66	141	39.3	3, 4
	SR 2 Vermillion, OH	104	2	580	19	380	100	83	19	64	146	33.8	7
	HWY 3N Ruthven, ONT	4	4	1054	22	1000	100	80	19	61	128	32.3	1, 3, 7, 8
	HWY 427 Toronto, ONT	1	1	1054	13	1000	100	82	16	66	112	29.8	CONTROL
	RT 422 Kittanning, PA	5	5	965	53	300	100	83	15	68	162	41.2	3, 8
	RT 676 Camden, NJ	4	2	471	44	0	75	86	23	63	131	44.3	3, 8
	RT 130 Yardville, NJ	1	1	1099	37	0	80	85	25	60	131	42.5	CONTROL
NOWET ZONE	US 101 Geyserville, CA	6	3	933	49	0	50	91	37	54	75	43.7	7
	I-95 Rocky Mount, NC	9	8	1065	29	0	63	89	29	60	122	46.4	1,2,3,4,5,6
	I-85 Greensboro, NC	1	1	1057	25	0	70	87	27	60	120	42.0	NEW- 1,3,4
	I-75 Tampa, FL (Hill.)	1	1	1078	4	0	0	90	50	40	115	46.7	NEW- 1,4,7
	I-75 Tampa, FL (Man.)	1	1	1057	16	0	0	91	50	41	115	58.7	NEW- 3,4,8
	TOTAL	264	95										

Design Feature Codes:

1 = Slab Thickness
2 = Slab Type
3 = Base Type
4 = Joint Spacing
5 = Joint Configuration
6 = Load Transfer
7 = PCC Shoulder/Widened Lane
8 = Subdrainage

Table 2. Listing of pavement sections in dry-freeze environmental region.

Project ID	Location	Year Built	Number of Sections	Design Feature(s)
MN 1	I-94 Rothsay	1970	12	Base Type Slab Thickness Load Transfer Joint Spacing Shoulder Type
MN 2	I-90 Albert Lea	1977	4	Pavement Type Joint Spacing Slab Thickness Shoulder Type
MN 3	I-90 Austin	1984	1	Widened Lanes
MN 4	T.H. 15 New Ulm	1986	1	Widened Lanes
MN 5	I-94 Rothsay	1969	1	Joint Spacing
MN 6	T.H. 15 Truman	1983	1	Widened Lanes Permeable Base
TOTAL			20	

Table 3. Listing of pavement sections in dry-nonfreeze environmental region.

Project ID	Location	Year Built	Number of Sections	Design Feature(s)
AZ 1	S.R. 360 Phoenix	1972-1981	6	Base Type Slab Thickness Shoulder Type Drainage
AZ 2	I-10 Phoenix	1983	1	Load Transfer PCC Shoulder
CA 1	I-5 Tracy	1971	5	Base Type Slab Thickness Joint Spacing Concrete Strength
CA 2	I-210 Los Angeles	1980	2	Base Type
CA 6	Rte. 14 Solemint	1980	1	Base Type
CA 7	I-5 Sacramento	1979	1	Drainage
CA 8	U.S. 101 Thousand Oaks	1983	1	Widened Lanes
TOTAL			17	

the time of the survey. Design features from this environmental zone include base type, slab thickness, joint spacing, drainage, and widened lanes.

WET-FREEZE ENVIRONMENTAL REGION

The wet-freeze environmental region contributed by far the largest number of sections to the study. Forty-four pavement sections, consisting of 42 experimental or older sections and 2 recently constructed sections, were included for evaluation in this region. States and Provinces in the wet-freeze environmental region contributing sections include Michigan, New York, Ohio, Ontario, Pennsylvania, and New Jersey.

Table 4 lists the projects included in the study from the wet-freeze environmental region. Project age ranges from 1 to 36 years. Pavement design features in this environmental region include base type, slab thickness, joint spacing, pavement type, shoulder type, load transfer, joint orientation (skewed or perpendicular), and joint design.

WET-NONFREEZE ENVIRONMENTAL REGION

Fourteen pavement sections—11 experimental and older sections and 3 recently-constructed sections—were included from the wet-nonfreeze environmental region. California, North Carolina, and Florida contributed projects to the study. Table 5 lists the sections included in this environmental region. Projects range in age from 1 to 20 years. Design features in this region include base type, slab thickness, pavement type, load transfer, joint orientation, and shoulder type.

OVERALL DISTRIBUTION OF DESIGN FEATURES

To more fully present the overall distribution of design features contained in the 95 pavement sections included in the study, selected design features are described briefly in the following sections.

BASE TYPE

Six general types of base courses were included in the study: aggregate (AGG), cement-treated (CTB), asphalt-treated (ATB), permeable stabilized or permeable nonstabilized (PERM), lean concrete (LCB), and soil cement (SC). Some sections were constructed directly on subgrade without a base course (NONE). The distribution of base type by environmental region is shown in figure 2.

SLAB THICKNESS

Slab thickness ranged from a minimum of 7.5 in (191 mm) to a maximum of 15 in (381 mm). Thicker slabs (in excess of 11 in [279 mm]) were most often constructed

Table 4. Listing of pavement sections in wet-freeze environmental region.

Project ID	Location	Year Built	Number of Sections	Design Feature(s)
MI 1	U.S. 10 Clare	1975	8	Base Type Pavement Type Load Transfer Drainage
MI 3	I-94 Marshall	1986	1	Permeable Base Shoulder Type
MI 4	I-69 Charlotte	1970	2	Shoulder Type
MI 5	I-94 Paw Paw	1984	1	Permeable Base Shoulder Type
NY 1	Rte. 23 Catskill	1968	6	Base Type Pavement Type Load Transfer Joint Orientation
NY 2	I-88 Otego	1975	4	Joint Spacing Pavement Type Shoulder Type
OH 1	U.S. 23 Chillicothe	1973	7	Base Type Joint Spacing Dowel Coating
OH 2	S.R. 2 Vermilion	1974	2	Shoulder Type Thick Slab on Grade
ONT 1	HWY 3N Ruthven	1982	4	Base Type Slab Thickness Shoulder Type
ONT 2	HWY 427 Toronto	1971	1	Load Transfer
PA 1	Rte. 422 & 66 Kittanning	1980	5	Base Type
NJ 2	Rte. 130 Yardville	1951	1	Joint Spacing Joint Design
NJ 3	I-676 Camden	1979	2	Base Type Joint Design
TOTAL			44	

Table 5. Listing of pavement sections in wet-nonfreeze environmental region.

Project ID	Location	Year Built	Number of Sections	Design Feature(s)
CA 3	U.S. 101 Geyserville	1975	3	Shoulder Type Joint Sealing
NC 1	I-95 Rocky Mount	1967	8	Base Type Slab Thickness Pavement Type Joint Orientation Load Transfer
NC 2	I-85 Greensboro	1982	1	Load Transfer Shoulder Type
FL 2	I-75 Tampa (Hillsborough)	1986	1	Slab Thickness
FL 3	I-75 Tampa (Manatee)	1982	1	Base Type
TOTAL			14	

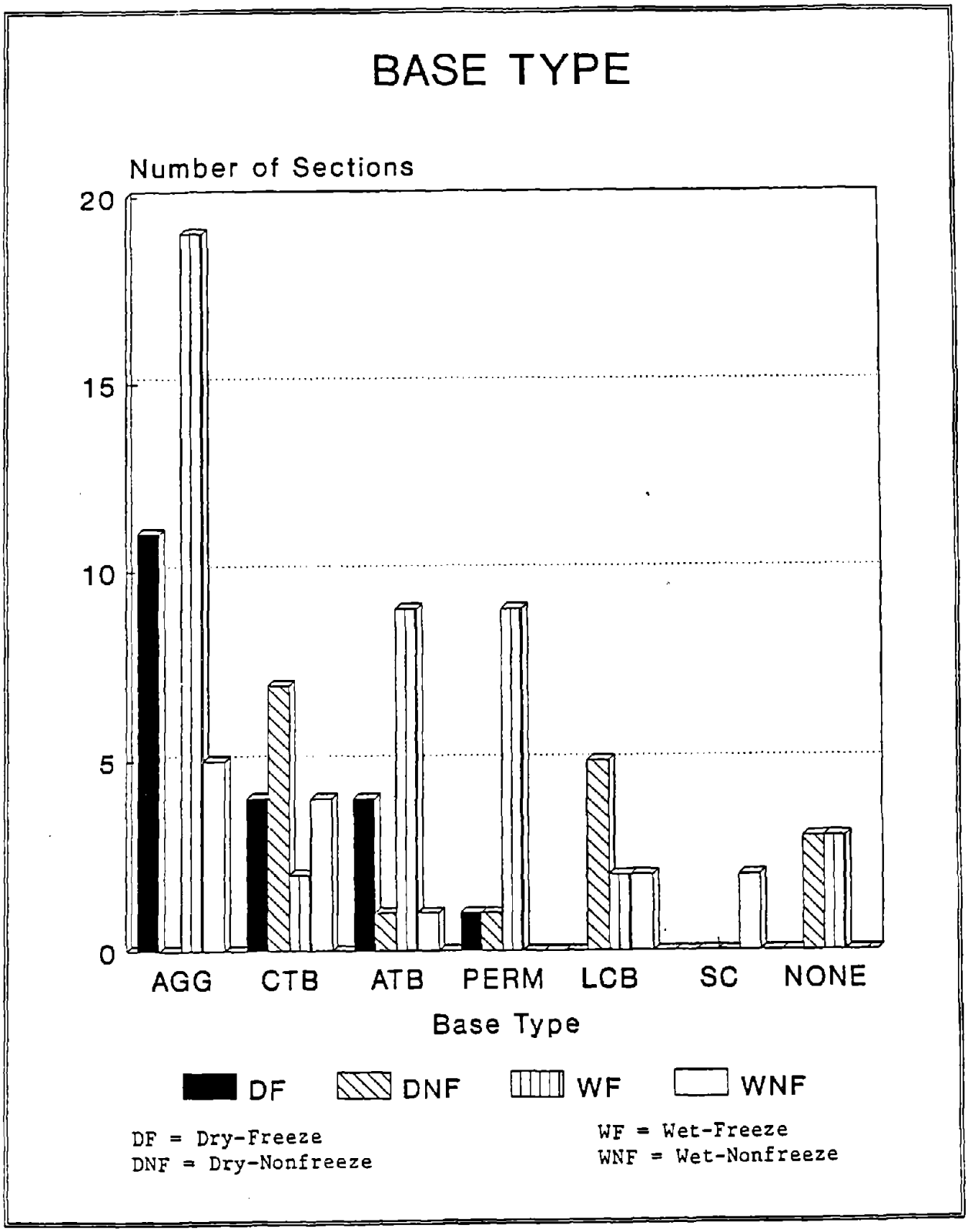

Figure 2. Distribution of base type by climatic region.

without a base course. The distribution of projects with slab thickness less than 10 in (254 mm) and greater than or equal to 10 in (254 mm) is shown in figure 3. The most common slab thickness was 9 in (229 mm).

JOINT SPACING/PAVEMENT TYPE

Both jointed plain concrete pavements (JPCP) and jointed reinforced concrete pavements (JRCP) were included in the study. By nature of the design characteristics inherent in each pavement type, a wide range of joint spacings was encountered. However, direct comparisons of joint spacings could very rarely be made within a pavement type, although relative comparisons of slab lengths could be made for sections with random joint spacing. The distribution of joint spacings by pavement type is illustrated in figure 4.

LOAD TRANSFER

Transverse joint load transfer is typically accomplished with aggregate interlock or mechanical load transfer devices. This study included a fair sampling of each type. The mechanical load transfer devices most commonly used in this study were dowel bars, although sections from New York utilized other devices (ACME two-part malleable iron load transfer devices and epoxy-coated I-beams). The distribution of load transfer methods is shown in figure 5.

SHOULDER TYPE/WIDENED LANES

Shoulder type was of interest to compare the structural benefits of portland cement concrete (PCC) shoulders with traditional asphalt concrete (AC) shoulders. A few sections with widened outside lanes were also included to evaluate their influence on pavement performance. The distribution of shoulder type (and widened lanes) is shown in figure 6.

SINGLE PAVEMENT SECTIONS

As previously mentioned, 15 single sections not part of any experiment were also included in the study. These were typically newer sections that contained unique design features (permeable base, widened lane, coated dowels, etc.). Other single pavement sections were included because they exhibited either very good or very poor performance, and it was believed that much could be learned from an in-depth evaluation of their performance.

FIELD DATA COLLECTION

This section provides a brief description of the data collection procedures used in the evaluation of the 95 inservice pavement sections. Every attempt was made to

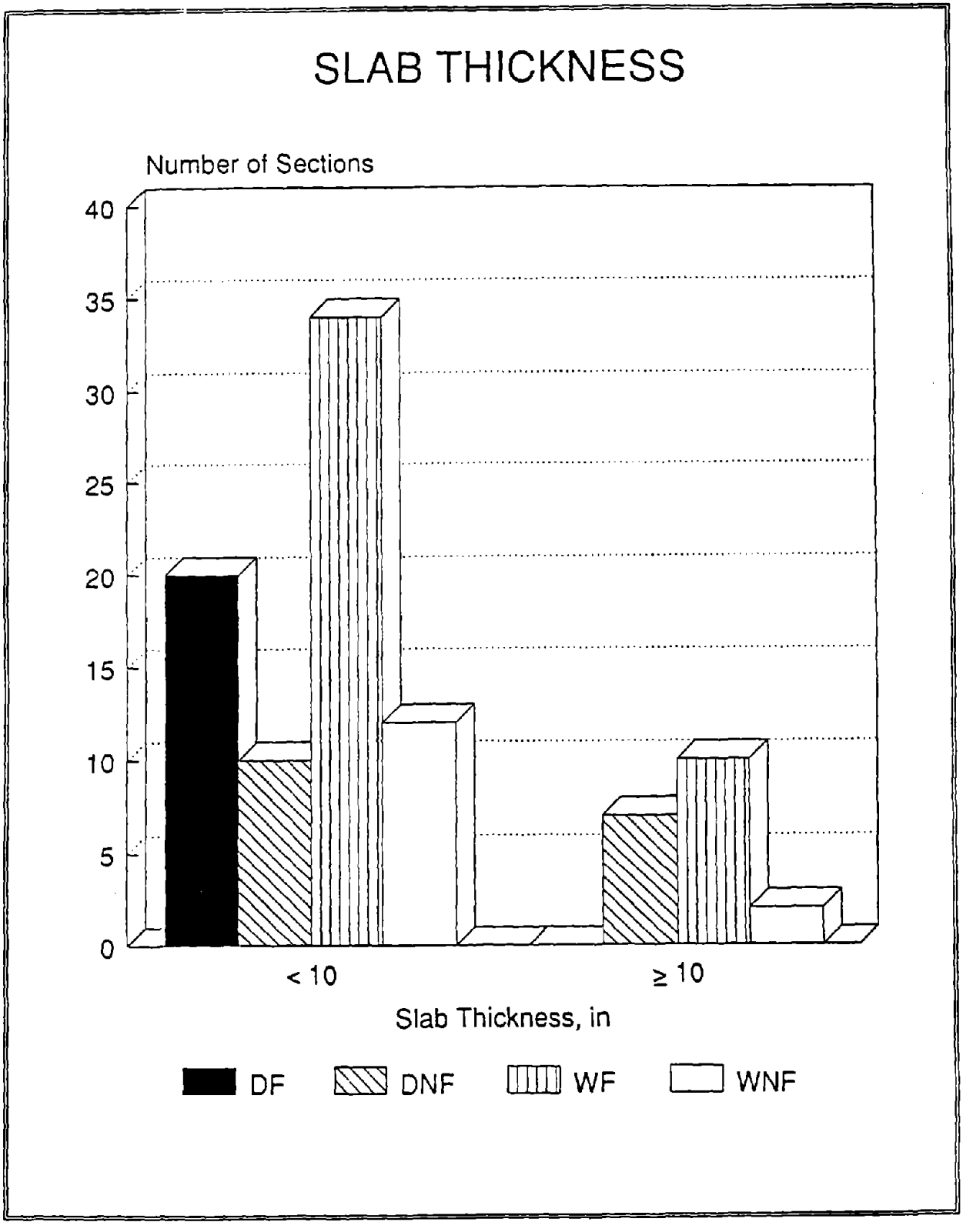

Figure 3. Distribution of slab thickness by climatic region.

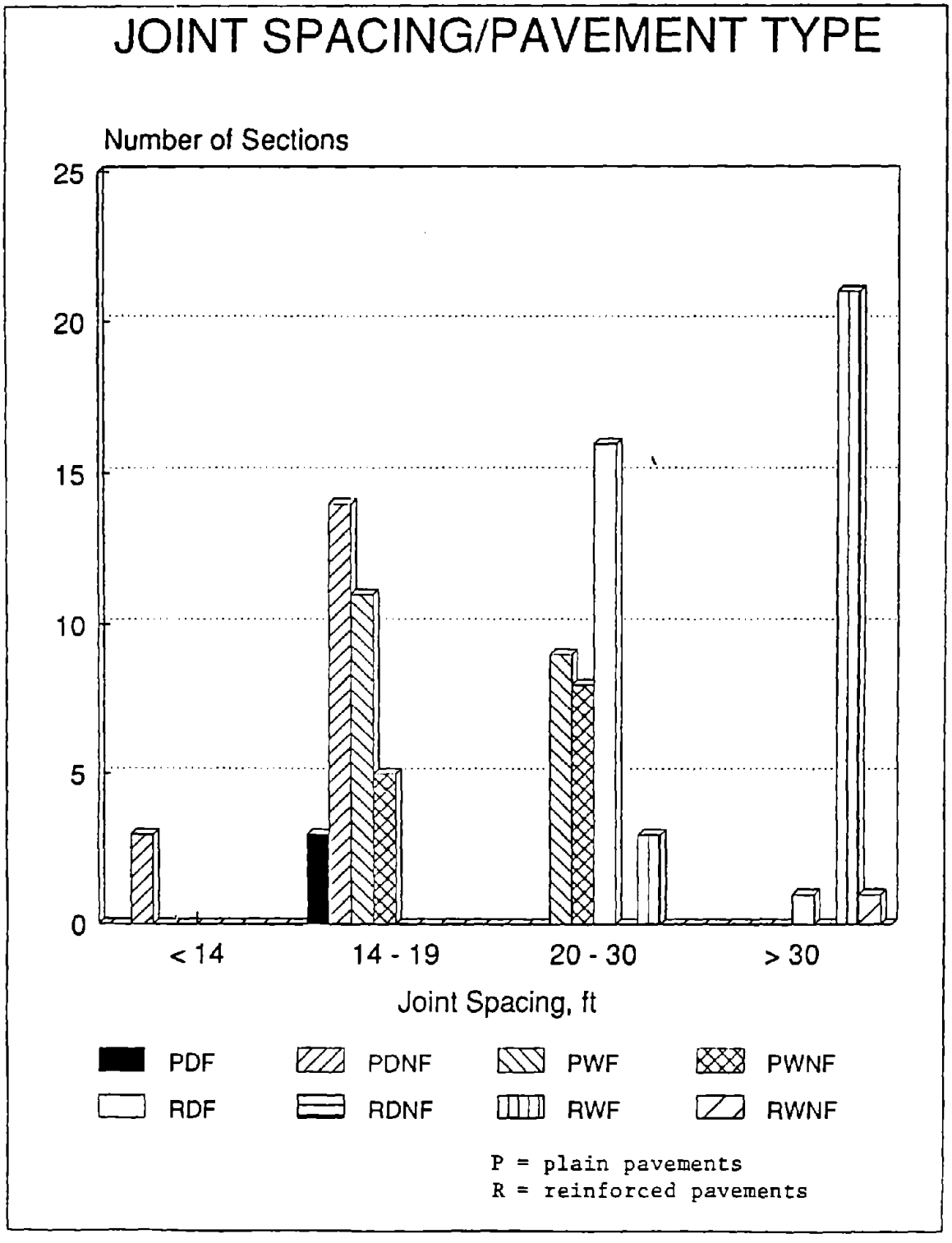

Figure 4. Distribution of joint spacing/pavement type by climatic region.

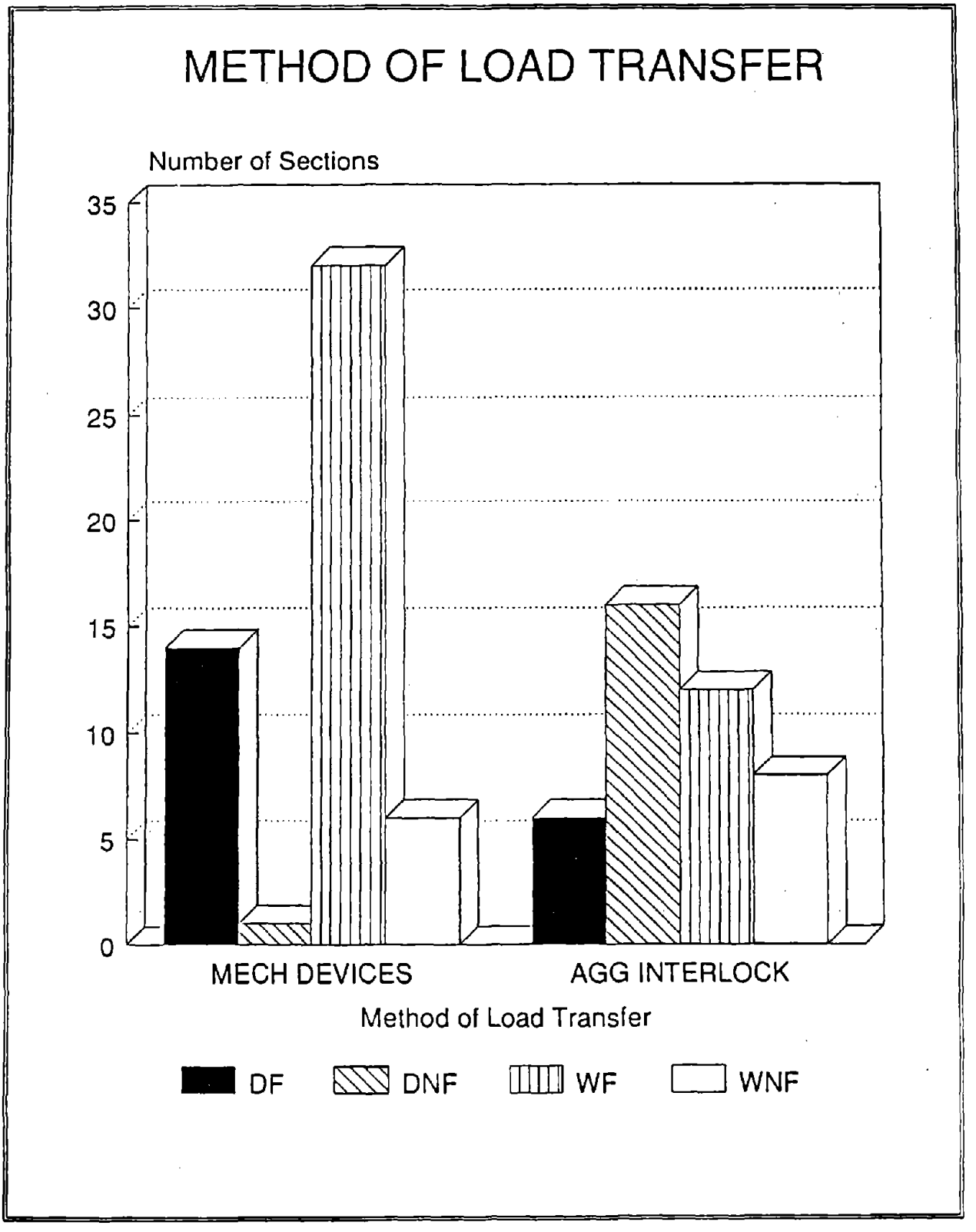

Figure 5. Distribution of load transfer mechanism by climatic region.

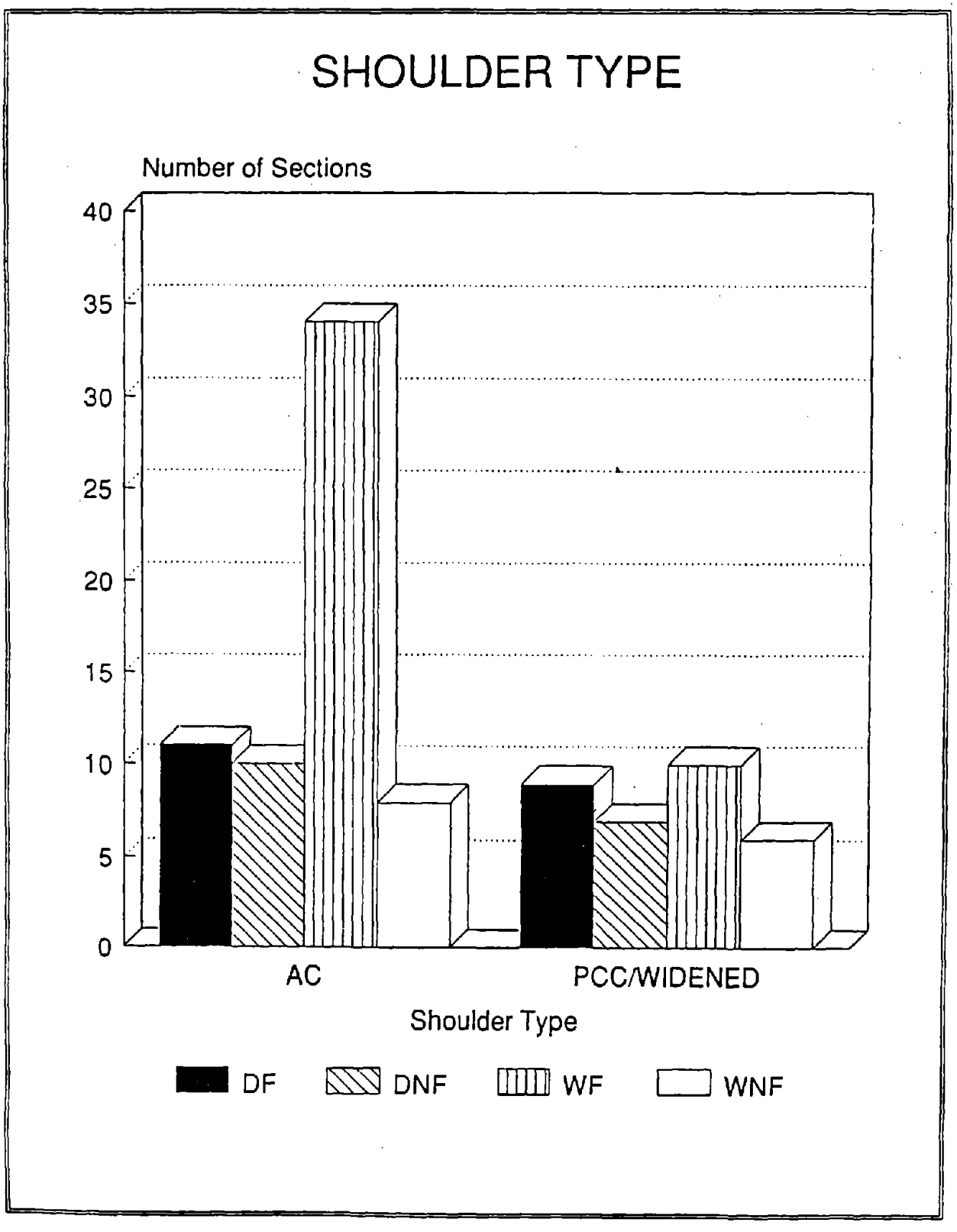

Figure 6. Distribution of shoulder type (and widened lanes) by climatic region.

collect information compatible with the Strategic Highway Research Program (SHRP) Long-Term Pavement Performance (LTPP) data base and to create as complete as possible a data record for each pavement section in this project.

To achieve a high level of reliability in the data collection process, the SHRP LTPP Data Collection Guide was followed to ensure the identification and collection of all key data elements.[1] In the field, pavement distresses were identified and quantified according to the Distress Identification Manual for Long-Term Pavement Performance (LTPP) Studies.[2] This manual provided a uniform basis for collecting distress data from survey to survey, and its use also ensured that the collected data was consistent with data collected for the LTPP studies.

The survey crews typically consisted of a senior project engineer and one or two other workers. Another member of the survey crew was a technician who was present on all of the field survey trips and participated in the survey of each section to ensure consistency in data collection.

The participating States assisted in the data collection activities by providing extensive design and construction information and by providing the traffic control necessary for the conduct of the field testing. Their assistance and cooperation in these and other areas are gratefully acknowledged.

PAVEMENT CONDITION SURVEY

Extensive measurements were made on each pavement section (e.g., cracking, spalling, joint seal deterioration). Data items collected include:

- Visible distress (cracking, joint spalling, etc.).
- Joint and crack faulting.
- Joint widths.
- Lane/shoulder drop-off and separation.
- Shoulder condition.
- Pavement slopes.

DRAINAGE SURVEY

A comprehensive drainage survey was conducted in order to perform a rational drainage analysis of each section. This consisted of the collection of:

- Depth and condition of drainage ditches.
- Examination of transverse and longitudinal joint sealant.
- Examination of drainage outlets.
- Identification of visible signs of pumping.
- Measurement of transverse and longitudinal slopes.

PHOTO SURVEY

The paper record of the condition survey was supported by a 35-mm photographic record of each section. This photo survey consisted of an initial set of photographs taken to provide an overview of the section, and subsequent photos of typical section features (e.g., transverse joints, slab condition, drainage features, etc.).

FALLING WEIGHT DEFLECTOMETER (FWD)

Nondestructive deflection testing was performed with a Dynatest Model 8000 FWD for purposes of modulus backcalculation, determination of load transfer efficiencies, and identification of voids. Generally, 10 mid-slab center deflections and 20 joint corner deflections were taken, although 10 mid-slab edge deflections were also obtained if a tied concrete shoulder existed. The FWD testing was performed while the temperature of the pavement was below 80 °F (27 °C) to avoid the influence of slab expansion on the measurement of load transfer and void detection.

PAVEMENT ROUGHNESS

Pavement surface roughness data were collected on all of the sections. A 1985 Buick Le Sabre was fitted with a rear-axle-mounted Mays Roughness Meter, which was run over each lane of each section twice and the results averaged. The test was run at a constant speed of 50 mi/h (80 km/h). During the first pass, the passengers in the car gave the section a present serviceability rating (PSR).

WEIGH-IN-MOTION (WIM)

WIM data was collected on selected study sections for 48 continuous hours. The weight data was obtained with a Streeter Richardson portable WIM system using a capacitive mat as its weight transducer placed in one wheelpath of the outside lane in the same direction of travel as the condition survey. Temporary inductive loops were placed both upstream and downstream of the capacitive mats. Vehicle classification data was acquired using automated vehicle classification (AVC) equipment in conjunction with pneumatic tube axle sensors. Two axle sensors were used with the AVC equipment to provide data from which to calculate vehicle speeds and axle spacings. The WIM equipment was calibrated by acquiring data from trucks of known weights and comparing those values to readings obtained for the same vehicles using the WIM equipment; adjustment factors were then developed and applied accordingly.

CORING AND BORING

Coring was performed with a portable drill equipped with a 6-in (152-mm) diameter bit. Center slab cores were retrieved from almost all of the sections and

tested in split tensile according to AASHTO T-198 (ASTM C 496). Stabilized base samples of sufficient dimensions were also retrieved and tested similarly. Cores were also retrieved from the transverse joints of most of the older sections and examined visually for any signs of deterioration along the underside of the joint core or for microcracking of the aggregate.

Base, subbase, and subgrade materials were retrieved from beneath the slab cores. The particle size distribution of granular materials was determined according to standard test methods. The liquid limit and plasticity index were also determined. This information was used to estimate a classification of the granular material according to procedures described in AASHTO M 145.

DATA BASE DESCRIPTION

A comprehensive data base was established for this research project to store the extensive design and performance data collected for each study section. The data base was created using the UNIFY Relational Data Base Management System.[3] The system resides on an IBM PC-AT with 640K RAM and a 30-Mb hard disk.

The data base includes projects from both Phase I (concrete pavement performance) and Phase II (structural overlay rehabilitation). The UNIFY software and the entire data base system occupy approximately 20 Mb of hard disk space. The Phase I projects occupy approximately 12 Mb.

The data elements included in the data base were based on the LTPP data collection guide.[1] Two data bases were created to accommodate the large amount of data that was collected for this research project: the "Inventory" data base and the "Monitoring" data base. The type of information included in each data base is listed in table 6.

The data base contains an error checking routine which checks for invalid character input for the field parameters on the screens. Each data base has its own data listing procedure and will list information from that particular data base only. This data can also be listed by individual sections, by individual projects, by each State, or by entire projects. The error checking routine and the data listing procedure can be output to the screen, to a specified file, or to the printer.

In addition to the UNIFY data base developed under this study, two additional data bases were established for the execution of statistical analyses. These data bases were developed for use with the personal computer (PC) version of SAS™. One separate SAS data base was developed for the sections included in this study, and one was developed for a collection of pavement sections from both this study and from other concrete pavement performance studies (i.e., COPES and the AASHO Road Test). Each of these data bases is available from the FHWA.

Table 6. Listing of major data items contained in the data base.

INVENTORY DATA BASE
Inventory Data
Geometric, Shoulder, and Drainage Information
General Survey Information
Layer Descriptions
Longitudinal and Transverse Joint Data
Concrete Mixture Data
Base and Subbase Material Properties
Subgrade Properties
Age and Major Improvements
Maintenance Data
Historical Maintenance Information
Rehabilitation Data
Historical Rehabilitation Data
Environmental Data
General Environmental Data
Annual Historical Environmental Data
Average Monthly Historical Data
MONITORING DATA BASE
Monitoring Data
Deflection Testing Data
Pavement Roughness Information
Distress Survey Information
Traffic Data
Average Daily Traffic
Percent Trucks
Equivalent Single-Axle Load Applications

CHAPTER 3 SUMMARY OF THE EFFECTS OF DESIGN FEATURES

PROJECT SUMMARIES

After the data collection and analysis phase, a large amount of information on the project sections had accumulated. With 95 project sections, the volume of data quickly created an extensive file of information. The researchers decided that each individual State project should be summarized and the salient findings documented. Each project was summarized in terms of the inventory features, drainage conditions, condition surveys, and a discussion of the effect on performance of the rigid pavement design features. The summaries were compiled in volume IV of this series. The reader is referred to that document for project-by-project details.

EFFECTS OF PAVEMENT DESIGN FEATURES

The performance of the jointed plain and reinforced concrete pavements based on the field data collection efforts was compiled for each of the design features. The conclusions are general in scope because the performance trends were based on the collective results of the 95 test sections.

SLAB THICKNESS

The effect of slab thickness on pavement performance was clear. Increasing the slab thickness helped to reduce transverse and longitudinal slab cracking in all cases in every climatic zone. This effect was much more noticeable when slab thicknesses were increased an inch on thinner pavements, e.g., from 8 to 9 in (203 to 229 mm), than when they were increased several inches, e.g., from 9 to 11 in (229 to 279 mm) or from 11 to 13 in (279 to 330 mm) on thicker pavements. It was impossible to directly compare the performance of the thinner slabs and the thicker slabs since all of the thick slabs were constructed directly on the subgrade and all of the thinner slabs were constructed on base courses.

Increasing the thickness of the slab did not appear to reduce joint spalling or joint faulting. Thick slabs on grade, especially those in wet climates and exposed to heavy traffic, faulted as much as thinner pavements constructed on a base course.

BASE TYPE

The base type seemed to have a significant effect on the performance of jointed concrete pavements. The aspects of base type that affected pavement performance included: base/slab interface friction, base stiffness, base erodibility, and base permeability or drainability. The major performance indicators that were affected by

variations in base type were transverse and longitudinal cracking, joint spalling, and faulting.

Cement-treated or soil-cement bases were the worst-performing base type. They tended to contribute to excessive pumping, faulting, and cracking in the associated slabs. This is most likely due to the use of an impermeable layer that traps moisture. Yet this impermeable layer can break down and contribute to the movement of fines beneath the slab.

The performance of lean concrete bases generally was poor, but ranged from poor to good. Large curling and warping stresses have been associated with slabs constructed over lean concrete bases. These stresses result in considerable transverse and longitudinal cracking of the slab. These bases can also contribute to a "bathtub" section in which moisture is trapped within the pavement cross section, particularly where there is poor subdrainage.

Dense-graded, asphalt-treated base courses ranged in performance from very poor to good. The fact that these type of bases were often constructed as a bathtub-type design contributed to their poor performance. This unsatisfactory design often resulted in severe cracking, faulting, and pumping of the slabs. However, a few sections displayed good performance, perhaps due to an adequate cross section. More investigation is required before any recommendations or guidelines for the use of asphalt-treated base courses can be proposed.

The construction of thicker, nondoweled slabs directly on the subgrade (no base) resulted in a pavement that performed marginally. These pavements were especially susceptible to faulting, even under low traffic levels. However, the performance of these pavements is not directly comparable to other pavement sections, as the slabs were thicker (11 to 15 in [279 to 381 mm]) than conventional pavements.

Pavements constructed over aggregate bases had varied performance, but were generally in the fair to very good category. In general, the more open the gradation of the aggregate in the base, the better the pavement performed. An advantage of the aggregate bases is that they contribute the least to the high curling and warping stresses in the slab. Also, even aggregate bases that are not open-graded tend to perform fairly well because they are more permeable and have a lower friction factor than stabilized base courses.

The best bases in terms of pavement performance were those designed to be permeable. Typical base courses have permeabilities ranging from 0 to less than 1 ft/day (0.3 m/day); good permeable bases have permeabilities upwards of 1000 ft/day (305 m/day). The highly permeable bases typically performed very well, although it should be noted that the sections are generally not very old and have not

been subjected to a significant amount of traffic. Specific areas of concern, however, were the high corner deflections and the low load transfer exhibited by the permeable base courses. Because these could impact their long-term performance, the use of dowel bars may be essential for pavements constructed on these types of bases.

The analysis of the effect of permeable base types is confounded by the presence of other design variables, but the limited data available suggests that the use of a permeable base layer may provide an effective means of improving pavement performance. An unexpected benefit of the use of permeable bases was the reduction in D-cracking on pavements susceptible to that distress.

A carefully-designed filter material is recommended beneath the permeable base course. Such a filter layer will prevent the intrusion of fines into the permeable base. If the permeable base becomes contaminated with fines, it will no longer efficiently remove water from the pavement structure. Regular maintenance of the drainage outlets is necessary to allow the water to be removed. Finally, the edge drains placed to remove the water from the permeable base layer must be located within the permeable base so that water can reach the drain and be removed.

SLAB LENGTH

Several experimental projects evaluated the effects on performance of different slab lengths. Slab lengths for JPCP ranged from an average of 8 to 30 ft (2.4 to 9.1 m). For JPCP, reducing the slab length reduces both the magnitude of joint faulting and the amount of transverse cracking. Shorter slabs may also reduce joint spalling, although there were insufficient data to support this conclusion. On sections with random joint spacing, researchers found that if slabs were 18 ft (5.5 m) or longer, they experienced more transverse cracking than the shorter slabs.

Jointed reinforced concrete pavement slabs included in this study ranged from 21 to 78 ft (6.4 to 23.8 m) long. Generally, the shorter joint spacings performed better, as measured by deteriorated transverse cracks, joint faulting, and joint spalling. However, several long-jointed JRCP slabs performed quite well. In particular, the 10-in (254 mm) JRCP, 78.5-ft (23.9 m) expansion-jointed pavement of NJ 2 performed very well. This pavement had 1.25-in (32 mm) diameter stainless steel wrapped dowels and displayed a PSR of 3.8 after 36 years and 35 million 18-kip (80 kN) equivalent single axle load (ESAL) applications.

The performance of ONT 2 in Toronto, Ontario, is also worth noting. This 9-in (229 mm) JPCP with skewed joints and 1-in (25 mm) diameter dowels is on a 6-in (152 mm) cement-treated base with joint spacing of 12-13-19-18 ft (3.7-4.0-5.8-5.5 m). The pavement has a PSR of 3.9 after 16 years and 36 million 18-kip (80 kN) ESAL applications. Longitudinal drains were retrofitted after 11 years of service.

Transverse cracking was noted only in the 19-ft (5.8-m) slabs. Factors to consider for enhanced JRCP performance are the amount of reinforcement, the dowel coating, the base type, the durability and top size of the aggregate, and the coefficient of expansion of the concrete.

For the JPCP sections, an examination of the stiffness of the foundation was made through the use of the radius of relative stiffness (l). The radius of relative stiffness is defined as:

$$l = \left[\frac{Eh^3}{12*k*(1 - u^2)} \right]^{0.25} \quad (1)$$

Where:

E	=	concrete elastic modulus, psi
h	=	slab thickness, in
k	=	modulus of subgrade reaction, psi/in
u	=	Poisson's ratio

It was found that as the ratio of slab length (L) to l increases, transverse cracking for JPCP was more likely to occur. Generally speaking, when L/l was greater than 5, transverse cracking occurred within the slab. This factor was further examined for different base types, and showed that stiffer base courses (e.g., CTB) required shorter joint spacing to reduce or eliminate transverse cracking. Figure 7 shows the observed relationship for aggregate bases and figure 8 shows the relationship for stabilized bases.

SLAB REINFORCEMENT

The amount of reinforcement appeared to influence the amount of deteriorated transverse cracking. Although often confounded by the presence of corrosion-resistant dowel bars, pavement sections that contained more than 0.1 percent reinforcing steel exhibited less deteriorated transverse cracking; sections with less than that amount often displayed a significant amount of transverse cracking, particularly in cold climates. A minimum of 0.1 percent reinforcing steel is therefore recommended, with larger amounts required for harsher climates and longer slabs. Corrosion-resistant dowel bars are also recommended. The combination of corrosion-resistant dowel bars, an adequate amount of reinforcement, and preformed compression seals appears to enhance the performance of jointed reinforced concrete pavements.

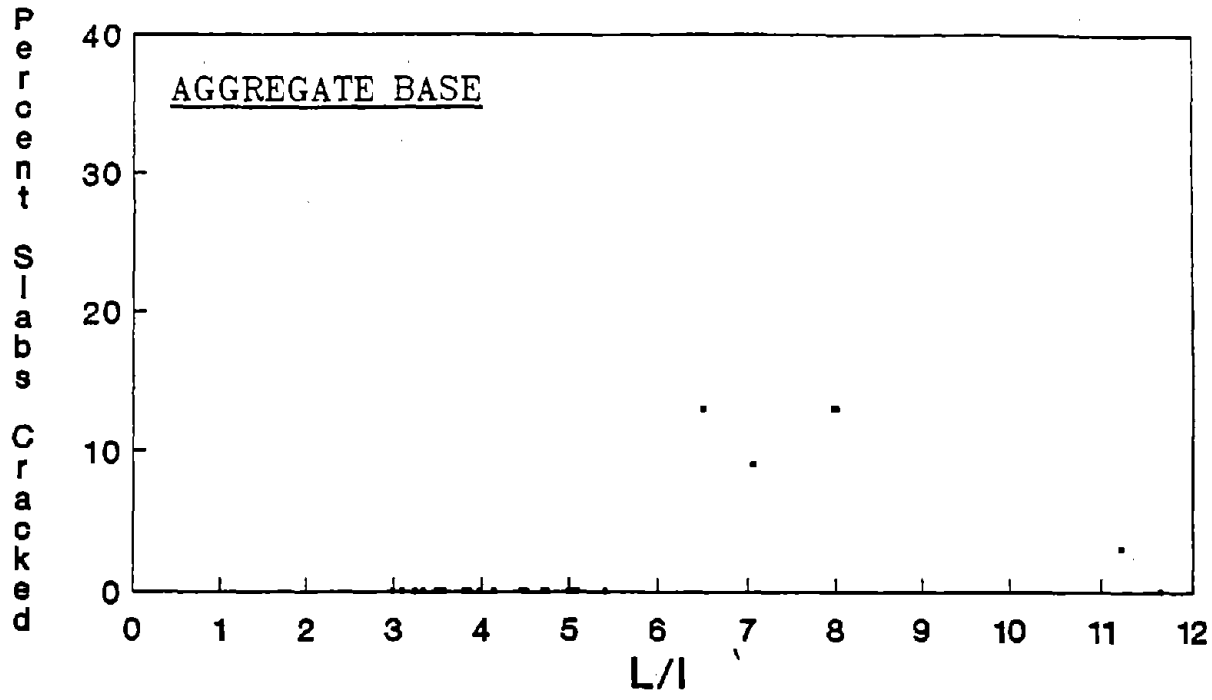

Figure 7. Percent slab cracking as a function of L/ℓ for sections with aggregate bases.

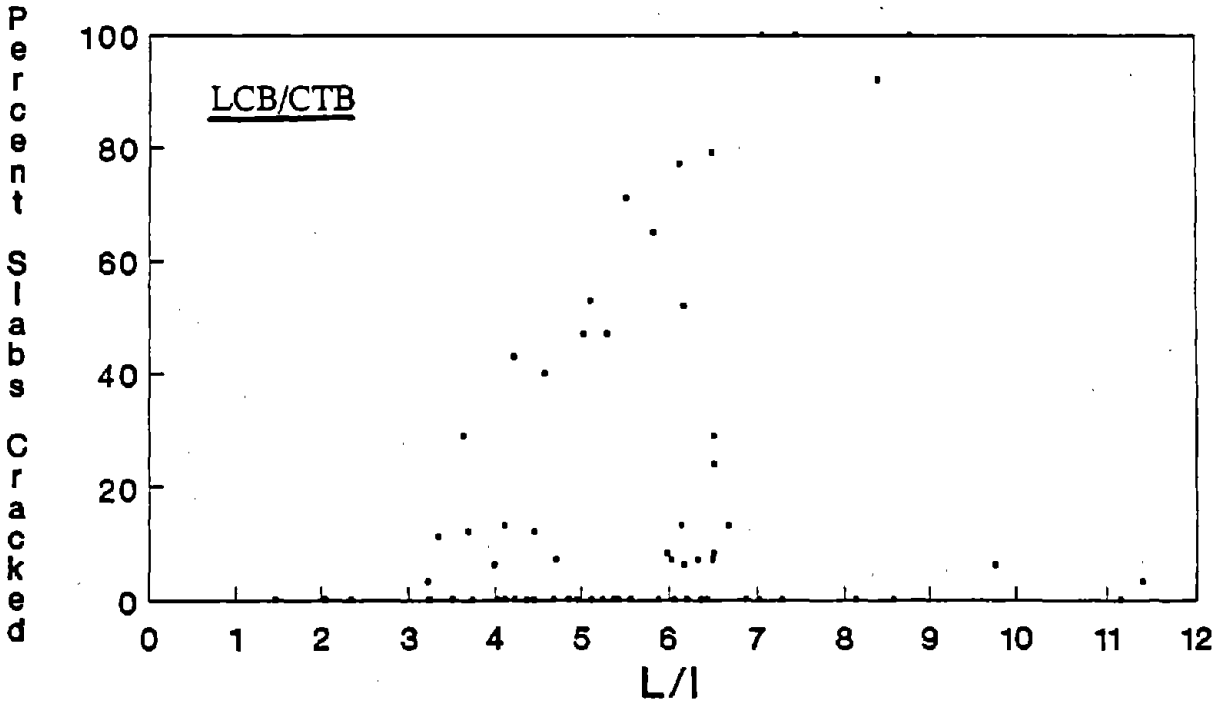

Figure 8. Percent slab cracking as a function of L/ℓ for sections with LCB and CTB bases.

JOINT ORIENTATION

The issue of joint orientation has been of interest in pavement design for many years. Conventional wisdom says that skewed joints reduce the number of wheel loads applied at the joint at one time to the pavement from two to one and, thus, may reduce load-associated distresses. While the results from the limited sample size in this study are ambiguous, all of the nondoweled sections with skewed joints had a lower PSR than similar designs with perpendicular joints. The available data provide no definitive conclusions on the effectiveness of skewing transverse joints for nondoweled slabs. Skewed joints (and random joint spacing for that matter) are not believed to provide any benefit to doweled slabs.

JOINT LOAD TRANSFER

Many sections in the study allowed for the direct comparison of the two methods of transverse joint load transfer. Dowel bars were found to substantially reduce the amount of joint faulting when compared directly with nondoweled sections of a similar design. The impact of load transfer devices on pavement performance becomes more significant at higher traffic levels.

It was observed that larger diameter bars provided better load transfer and control of faulting under heavy traffic than did smaller bars. It appeared that a dowel bar 1.25 in (32 mm) in diameter was necessary to provide good performance.

Nondoweled JPCP slabs generally developed significant faulting, regardless of pavement design or climate. This effect was somewhat mitigated by the use of permeable bases. However, the sections in this group had a much lower number of accumulated ESAL's, so no conclusions can be drawn yet.

Some sections with dowels displayed higher levels of joint spalling and more deteriorated cracks than sections of similar design without load transfer devices. It is suspected that the load transfer devices in these sections have corroded and locked up or were misaligned at the time of placement. This resulted in the development of working cracks instead of working joints. However, the use of dowel coatings that inhibit corrosion with effective bond breakers and the proper placement of the load transfer devices will certainly contribute to improved performance.

Two projects in New York involved the use of epoxy-coated I-beams for load transfer devices. On these particular projects, these unconventional devices performed fairly well, but the pavements have not been subjected to a large number of accumulated ESAL's. For instance, on other high-volume roadways, the ACME devices were unable to provide adequate load transfer and failed. At this time, corrosion-resistant dowel bars are believed to provide the best means of transverse joint load transfer.

DOWEL BAR COATINGS

Dowel bar coatings are applied to enhance resistance to corrosion due to moisture and deicing chemicals. While most of the sections in this study did not contain corrosion-resistant dowel bars, those that did generally exhibited superior performance. Very little deteriorated transverse cracking was identified on these sections, which would seem to indicate that the transverse joint was still functioning properly. In fact, one section in New Jersey with stainless-steel wrapped dowel bars was performing satisfactorily after 36 years of service. An effective bond breaker is also required.

LONGITUDINAL JOINT DESIGN

The longitudinal joint design was found to be a critical design element. Both inadequate forming techniques and insufficient longitudinal joint depths can contribute to the development of longitudinal cracking. There is evidence to support the advantage of sawing techniques over the use of inserts. However, no clear trend was identified regarding the minimum depth needed to ensure the formation of the longitudinal joint. The presence of stabilized base courses also contributed to the development of longitudinal cracking, and their use makes the timing of sawing operations even more critical since the joint must be established before a strong bond develops. It is generally recommended that the depth of the longitudinal joint be one-third of the actual (not plan) slab thickness, and it may have to be deeper when stabilized bases are included in the design.

JOINT SEALING

Joint sealing appeared to have a beneficial effect on the performance of concrete pavements. This was particularly true in harsh climates with excessive amounts of moisture. Preformed compression sealants were shown to perform for 15 years or more on heavily-trafficked pavements. Except where a D-cracking problem existed, the pavement sections containing the preformed sealants generally exhibited little joint spalling and were in good overall condition.

Rubberized asphalt joint sealants showed good performance for 3 to 7 years, although their performance was quite variable. Silicone joint sealants were included on a few projects and were performing well after as long as 5 years of service.

On short slabs, transverse joints should be sawed to a depth of 1/3 of the slab thickness and skip joint sawing should not be allowed. This will result in more uniform joint opening and will minimize the problem of preformed joint sealant pulling out of the joint.

TIED SHOULDERS

It is a widespread belief that the construction of tied shoulders on jointed concrete pavements serves to reduce edge stresses and edge and corner deflections by providing more lateral support to the mainline pavement. This is thought to improve pavement performance and increase pavement life. Surprisingly, this study showed that while PCC shoulders performed better than AC shoulders, many of the tied shoulder designs were deficient and actually contributed to poorer performance in the mainline pavement. Several factors are critical if the benefits of tied concrete shoulders are to be realized. Tiebars must not be spaced too far apart. A spacing of 40 in (1016 mm) on NY 2 was found to be too wide for the shoulder to provide support to the mainline pavement. Also, tiebars must be strategically located near slab corners to provide support. In areas susceptible to frost heave action, the shoulder should be as thick as the slab to avoid the effects of differential frost heave. Finally, the joint spacing of the concrete shoulder must match that of the mainline pavement to prevent the inducement of transverse cracking.

The use of tied shoulders on concrete pavements also allows the establishment of a sealable joint reservoir between the mainline pavement and the shoulder. This joint is the major source of moisture in a pavement and sealing this joint should help to reduce the frequency and deterioration of moisture-related distresses.

Tied PCC shoulders did not appear to have any effect on the faulting of the transverse joints in the mainline pavement, although on one project tied concrete shoulders were installed after 14 years for the specific purpose of reducing the rate of faulting. In some cases, tied PCC shoulders were constructed over a stabilized dense-graded base course in a bathtub design that resulted in the poor performance of the mainline pavement.

WIDENED TRAFFIC LANES

Widened traffic lanes are expected to enhance concrete pavement performance by reducing edge and corner loadings. By allowing for a more interior-loading condition, edge and corner stresses are reduced. However, the sections that incorporated widened lanes in their design were relatively new and had been subjected to low traffic loadings; hence, the effect of widened lanes on concrete pavement performance could not be evaluated. Nevertheless, it is believed that the use of widened lanes should be considered in the design of a concrete pavement. The traffic stripe should be placed at 12 ft (3.7 m) and the rumble strips included on the widened section to discourage shoulder encroachment in rural areas to reduce edge loadings by trucks. The maximum width of the lane should probably be no more than 14 ft (4.3 m).

SUBDRAINAGE

One area of pavement design for which little guidance exists is subdrainage. The provision of positive subdrainage, either in the form of longitudinal edge drains or the combination of a drainage layer and edge drains, generally resulted in a reduction in faulting and spalling related to D-cracking.

This study evaluated subdrainage indirectly by the rational calculation of a coefficient of drainage (C_d) for every pavement section. This coefficient not only takes into account the permeability of the layer directly beneath the slab, it also considers the permeability of the other layers, the presence of edge drains, the transverse and longitudinal slopes of the pavement surface, the drainage distance, and the climate.

The results showed that, with very few exceptions, as the drainage characteristics of the pavement sections improved, the load-related distresses decreased. This was especially true for faulting and transverse cracking. It appears that overall pavement performance can be improved by the construction of a base layer with a high permeability. Two major components of such a base are an open-graded material with a high permeability and the restriction of the percent fines. A filter layer must be provided below the permeable base, and a positive drainage system must be provided. Regular maintenance of the outlets must be performed.

SUMMARY

This study of the performance of 95 different pavement sections located around the country provided significant information on the effect of a large number of design variables on jointed concrete pavement performance. These results have been summarized by design variable in this chapter. However, it is clear that the performance of concrete pavements is a function of the interaction of many design features, and not just of a single feature. The enhancement of one feature at the expense of or without consideration of other features often seriously impaired the performance of the pavement. These design features do not constitute independent variables; as such, it is essential that all elements of a pavement design be considered together in order to obtain the best performance possible.

CHAPTER 4 CONCRETE PAVEMENT DESIGN AND ANALYSIS MODELS

SYNTHESIS AND SELECTION OF INITIAL MODELS

During the initial stages of the project, a number of the available pavement analysis models and design procedures were thoroughly reviewed and evaluated. Based upon this evaluation, models were selected for further investigation using the performance data collected under the study. This task was accomplished by obtaining the computer program and procedure documentation, analyzing the sensitivity of the models to changes in their variables, and documenting the capabilities and limitations of each model. Elements of the programs considered in the initial evaluation phase included memory requirements, run time, reasonableness of results, ease of use, and verification of the theory upon which the model is based. The models that were considered in the initial evaluation (along with appropriate references) are listed in table 7.

Table 7. Analysis and design models evaluated in this study.

Design	Structural Analysis	Prediction	Drainage/ Climatic
AASHTO (DNPS 86)*[4,5]	ILLISLAB*[16-18]	PEARDARP*[15,25-27]	CMS*[31,32]
CALTRANS[5,6]	JSLAB*[5,19]	PREDICT*[28-30]	Liu/Lytton*[33]
JCS-1*[5,7]	JRCP-4[20]		
BERM*[8]	H51[5,21,22]		
RPS-3[5,9,10]	RISC[5,23]		
PCA[5,11]	WESLAYER[5,24]		
JCP-1*[12,13]	WESLIQID[5,24]		
PMARP*[14,15]			

* Model selected for use in this project.

Those models selected for additional evaluation using the inservice performance data collected in the study are marked with an asterisk in table 7. Those that were not selected were found to have limitations in their applicability and approach.

ANALYSIS OF THE ACCURACY OF SELECTED PREDICTION MODELS

The prediction models selected for further evaluation include the AASHTO design equation, the PEARDARP models, the NCHRP 277 (COPES) models, and the PFAULT models. The models were analyzed using a combination of statistical

procedures and a graphical examination of the results. However, the accuracy of the existing models to predict the performance of pavements cannot be determined conclusively with the available data. It is only possible to determine whether the models can predict the actual performance of the sections that are included in this data base. Until a more comprehensive data base is developed that is considered representative of the entire population of pavements in the four environmental regions, it is impossible to determine the overall accuracy of the models or to develop models that accurately reflect the total population of pavements.

Each prediction model requires a unique set of inputs. The inputs for each individual section were obtained from the design and construction information, distress surveys, physical testing, and nondestructive testing. In addition, many of the models require the user to calculate or select inputs based on a set of recommendations that accompanies the model. A data set was created using the SAS, which includes all of the required inputs for each model.[34] The data set, containing all Phase I sections, is illustrated in table 94 of volume VI. A brief discussion of the various models evaluated, including the form of the model and a listing of required inputs, is presented in chapter 3 of volume II.

STATISTICAL ANALYSIS OF PREDICTION MODELS

The SAS statistical software was used to compare the actual, field-measured performance indicators to the performance indicators predicted by the various predictive models.[34] The paired t-test was conducted to examine the statistical similarity of the data sets. This test measures the mean difference of the measured and predicted performance indicator values; if the difference is 0.0, then the sample of field-collected performance indicator data comes from the same population as the sample of data generated by the predictive models.

A one-sample t-statistic is calculated for each data set, and then compared to a tabulated t-statistic (t_{table}) for a specified confidence level; 90 percent was used in this case. If $t_{calc} > t_{table}$, then the null hypothesis is rejected with a 10-percent chance of error, since the confidence level selected for this analysis is 90 percent. If the null hypothesis is rejected, then it can be inferred with 90-percent confidence that the sample of predicted performance indicators (from the models) is not statistically from the same population as the sample of measured performance indicators.

A brief summary of the results from the evaluation of the prediction models is presented here. A more detailed discussion of the analyses is provided in volume II.

AASHTO PAVEMENT DESIGN MODEL

Five sets of analyses were performed to examine the ability of the model to predict the amount of traffic actually sustained by each section. An analysis

containing all Phase I sections was performed to determine the predictive ability of the model for the entire data set. Additional analyses were performed for each of the four environmental regions.

The summary of the statistical analysis is presented in table 8. Note that t_{calc} is greater than t_{table} for every data set, which indicates that the AASHTO model does not adequately predict the ESAL's actually sustained by the pavement sections included in the study. This holds true when any environmental region is considered. This is most obvious in the wet-freeze region, where the predicted ESAL's are almost uniformly higher than the actual ESAL's. This suggests that the combination of available moisture and freeze-thaw cycling are not adequately considered in the AASHTO design process. Similarly, the model seemed to underpredict performance in the nonfreeze regions (actual ESAL's are greater than predicted ESAL's).

Table 8. Summary of the statistical analysis of the AASHTO design model.

Data Set	Number of Observations	t_{calc}	t_{table}	$t_{calc}>t_{table}$	Adequately Predict Performance
All Phase I	99	5.288	1.670	Yes	No
Dry-Freeze	20	4.871	1.729	Yes	No
Dry-Nonfreeze	17	2.915	1.746	Yes	No
Wet-Freeze	48	3.596	1.680	Yes	No
Wet-Nonfreeze	14	2.660	1.771	Yes	No

PEARDARP

PEARDARP incorporates models for PSI, roughness, spalling, faulting, and cracking. Each model was used to predict performance for all sections considered together and for sections within each climatic zone. Table 9 summarizes the statistical analysis of the PEARDARP predictive models.

It is observed from table 9 that none of the PEARDARP models adequately predict the performance of any of the pavement sections included in the study. This is true for all sections considered together and for sections within each climatic region.

Generally speaking, the following observations were noted from the evaluation of the PEARDARP models:

- The PSI model generally overpredicted serviceability for all regions.

Table 9. Summary of the statistical analyses of the PEARDARP prediction models.

Data Set	Number of Observations	t_{calc}	t_{table}*	$t_{calc} > t_{table}$	Adequately Predict Performance?
PSI					
All Phase I	99	17.276	1.670	YES	NO
Dry-Freeze	20	7.995	1.729	YES	NO
Dry-Nonfreeze	17	6.509	1.746	YES	NO
Wet-Freeze	48	12.047	1.680	YES	NO
Wet-Nonfreeze	14	7.120	1.771	YES	NO
ROUGHNESS					
All Phase I	99	16.882	1.670	YES	NO
Dry-Freeze	20	8.162	1.729	YES	NO
Dry-Nonfreeze	17	9.233	1.746	YES	NO
Wet-Freeze	48	10.828	1.680	YES	NO
Wet-Nonfreeze	14	13.429	1.771	YES	NO
SPALLING					
All Phase I	99	11.474	1.670	YES	NO
Dry-Freeze	20	6.924	1.729	YES	NO
Dry-Nonfreeze	17	3.413	1.746	YES	NO
Wet-Freeze	48	8.357	1.680	YES	NO
Wet-Nonfreeze	14	4.994	1.771	YES	NO

Table 9. Summary of the statistical analyses of the PEARDARP prediction models (continued).

Data Set	Number of Observations	t_{calc}	t_{table}*	$t_{calc} > t_{table}$	Adequately Predict Performance?
FAULTING					
All Phase I	99	7.825	1.670	YES	NO
Dry-Freeze					
All Sections	20	4.083	1.729	YES	NO
Doweled	14	5.465	1.771	YES	NO
Nondoweled	6	9.521	2.015	YES	NO
Dry-Nonfreeze	17	4.606	1.746	YES	NO
Wet-Freeze					
All Sections	48	8.598	1.680	YES	NO
Doweled	28	5.544	1.703	YES	NO
Nondoweled	20	7.109	1.729	YES	NO
Wet-Nonfreeze					
All Sections	14	5.325	1.771	YES	NO
Doweled	6	3.217	2.015	YES	NO
Nondoweled	8	5.942	1.895	YES	NO
CRACKING					
All Phase I	99	16.728	1.670	YES	NO
Dry-Freeze	20	11.855	1.729	YES	NO
Dry-Nonfreeze	17	6.958	1.746	YES	NO
Wet-Freeze	48	10.805	1.680	YES	NO
Wet-Nonfreeze	14	5.288	1.771	YES	NO

* t_{table} based on 90 percent confidence level.

- The roughness model overpredicted in the nonfreeze zones, but showed no trends in the other regions.
- The spalling model overpredicted for all regions.
- The doweled faulting model underpredicted faulting.
- The cracking model always predicted results between 320 and 420 linear ft (98 and 128 m) of cracking per 1000 ft^2 (93 m^2) for every section.

NCHRP 277 (COPES)

The NCHRP 277 (COPES) predictive models include pumping, faulting, spalling, cracking, and Present Serviceability Rating (PSR). The results of the statistical analysis of the COPES models are displayed in table 10. For all sections considered together, none of the COPES models were able to accurately predict the performance of the sections in the study. The table does show, however, that the model did accurately predict performance for certain climatic regions and pavement types, including:

- Pumping in the wet-nonfreeze region.
- Transverse joint faulting for JPCP in the dry-freeze region.
- Joint deterioration spalling for JPCP in the dry-freeze region.
- Joint deterioration spalling in the wet-nonfreeze region.

Other observations from the analysis include:

- The PSR models generally overpredicted in the freeze zones and underpredicted in the nonfreeze zones.
- No clear trend was observed for the prediction of pumping or faulting.
- The joint deterioration model and the cracking model generally overpredicted the occurrence of each distress type.

PFAULT FAULTING MODELS

Two PFAULT models were developed for transverse joint faulting prediction, one for doweled transverse joints and the other for nondoweled transverse joints. Both models contain mechanistic variables which are believed to influence the amount of faulting that occurs. Each of the models was evaluated by climatic zone.

Table 11 provides the summary of the statistical analysis for the PFAULT faulting model. The data indicates that the model was unable to adequately predict transverse joint faulting for all data sets but one (doweled sections in the wet-nonfreeze region). Generally speaking, however, there were no clear trends in the manner in which the model predicted performance.

Table 10. Summary of the statistical analyses of the COPES prediction models.

Data Set	Number of Observations	t_{calc}	t_{table}*	$t_{calc} > t_{table}$	Adequately Predict Performance?
PUMPING					
All Phase I	99	6.154	1.670	YES	NO
Dry-Freeze					
All Sections	20	4.498	1.729	YES	NO
JPCP	3	3.500	2.920	YES	NO
JRCP	17	4.243	1.746	YES	NO
Dry-Nonfreeze	17	1.951	1.746	YES	NO
Wet-Freeze					
All Sections	48	4.090	1.680	YES	NO
JPCP	22	4.125	1.721	YES	NO
JRCP	26	1.729	1.708	YES	NO
Wet-Nonfreeze	14	1.439	1.771	NO	YES
FAULTING					
All Phase I	99	4.181	1.670	YES	NO
Dry-Freeze					
All Sections	20	3.771	1.729	YES	NO
JPCP	3	2.910	2.920	NO	YES
JRCP	17	3.722	1.746	YES	NO
Dry-Nonfreeze	17	4.280	1.746	YES	NO
Wet-Freeze					
All Sections	48	8.532	1.680	YES	NO
JPCP	22	6.809	1.721	YES	NO
JRCP	26	5.459	1.708	YES	NO
Wet-Nonfreeze	14	5.421	1.771	YES	NO

Table 10. Summary of the statistical analyses of the COPES prediction models (continued).

Data Set	Number of Observations	t_{calc}	t_{table}*	$t_{calc} > t_{table}$	Adequately Predict Performance?
JOINT DETERIORATION					
All Phase I	99	6.633	1.670	YES	NO
Dry-Freeze					
All Sections	20	4.521	1.729	YES	NO
JPCP	3	1.220	2.920	NO	YES
JRCP	17	4.654	1.746	YES	NO
Dry-Nonfreeze	17	2.219	1.746	YES	NO
Wet-Freeze					
All Sections	48	4.938	1.680	YES	NO
JPCP	22	2.741	1.721	YES	NO
JRCP	26	4.806	1.708	YES	NO
Wet-Nonfreeze	14	1.558	1.771	NO	YES
CRACKING					
All Phase I	99	7.307	1.670	YES	NO
Dry-Freeze					
All Sections	20	2.925	1.729	YES	NO
JPCP	3	3.792	2.920	YES	NO
JRCP	17	7.110	1.746	YES	NO
Dry-Nonfreeze	17	1.899	1.746	YES	NO
Wet-Freeze					
All Sections	48	3.691	1.680	YES	NO
JPCP	22	3.898	1.721	YES	NO
JRCP	26	3.651	1.708	YES	NO
Wet-Nonfreeze	14	5.080	1.771	YES	NO

Table 10. Summary of the statistical analyses of the COPES prediction models (continued).

Data Set	Number of Observations	t_{calc}	t_{table}*	$t_{calc} > t_{table}$	Adequately Predict Performance?
PSR					
All Phase I	99	10.567	1.670	YES	NO
Dry-Freeze					
All Sections	20	4.782	1.729	YES	NO
JPCP	3	4.426	2.920	YES	NO
JRCP	17	4.534	1.746	YES	NO
Dry-Nonfreeze	17	5.833	1.746	YES	NO
Wet-Freeze					
All Sections	48	7.068	1.680	YES	NO
JPCP	22	3.514	1.721	YES	NO
JRCP	26	6.637	1.708	YES	NO
Wet-Nonfreeze	14	4.057	1.771	YES	NO

* t_{table} based on 90 percent confidence level.

Table 11. Summary of the statistical analyses of the PFAULT faulting prediction models.

Data Set	Number of Observations	t_{calc}	t_{table}*	$t_{calc} > t_{table}$	Adequately Predict Performance?
All Phase I	99	9.327	1.670	YES	NO
Dry-Freeze					
All Sections	20	4.986	1.729	YES	NO
Doweled	14	9.885	1.771	YES	NO
Nondoweled	6	3.836	2.015	YES	NO
Dry-Nonfreeze	17	3.569	1.746	YES	NO
Wet-Freeze					
All Sections	48	6.523	1.680	YES	NO
Doweled	28	3.997	1.703	YES	NO
Nondoweled	20	6.312	1.729	YES	NO
Wet-Nonfreeze					
All Sections	14	3.775	1.771	YES	NO
Doweled	6	1.281	2.015	NO	YES
Nondoweled	8	4.631	1.895	YES	NO

* t_{table} based on 90 percent confidence level.

OVERALL EVALUATION OF THE PREDICTION MODELS

This section documents an evaluation of the adequacy of several concrete pavement prediction models. In general, these models do not predict the distress (faulting, cracking, joint deterioration, pumping), serviceability, or roughness measured on the pavements included in this study to the 90 percent confidence level selected for this study. Therefore, it is clear that improved prediction models are needed for a variety of pavement analysis, design, and management purposes.

While each model may have specific limitations in its ability to predict performance, several general factors regarding the models' abilities to predict performance should be mentioned:

- Due to the large number of design, materials, climatic, and construction variables, it is extremely difficult to develop nationwide models. Regional models or general models calibrated to each State may be required.

- The COPES traffic data were based on W-4 truck factors that have been determined to be as much as 45 percent low for Interstate-type highways.

- Many combinations of design variables in the current data base did not exist at the AASHO Road Test or in the COPES data base (e.g., permeable bases, widened lanes, tied shoulders).

- Several of the projects in the current data base exhibited distresses that were the result of construction-related problems. Prediction models can never be expected to account for construction-related distress.

CASE STUDIES FOR SELECTED ANALYSIS MODELS

In addition to the predictive models, five specific analysis models were selected for detailed case study evaluations based upon the initial evaluation:

- A climatic model (CMS).
- A drainage characteristics model (Liu-Lytton).
- Structural analysis models (ILLISLAB, JSLAB, PMARP).
- A design method (JCP-1).
- Shoulder analysis and design models (JCS-1, BERM).

The models were investigated to determine their usefulness in the concrete pavement design process. They were evaluated using data from major experimental projects located in each of the four climatic zones. The experimental projects are

MN 1, I-94 Rothsay (dry-freeze), CA 1, I-5 Tracy (dry-nonfreeze), MI 1, US 10 Clare (wet-freeze), and NC 1, I-95 Rocky Mount (wet-nonfreeze). The analyses are presented in greater detail in chapter 4 of volume II.

EVALUATION OF THE CMS PROGRAM

The Climatic-Materials-Structural (CMS) program was developed to model the influence of climate on the behavior of pavement systems. Using the climatic and materials information from the region of a given pavement section, time-dependent temperature profiles, moisture profiles, and structural parameters of the pavement system are calculated.

The accuracy of the CMS program output largely depends on the quality of the input data. It is extremely important that the boundary conditions, climatic conditions, and material properties accurately represent the system to be analyzed. The theoretical validity of the individual models comprising the CMS model have been demonstrated, although the validity of the interaction of the models has not been proven.[31]

Although the program provides a tremendous amount of useful information, the inputs required for the program are obscure, difficult to obtain, and quite numerous. A listing of the input variables required for an execution of the program is provided in appendix C of volume VI.

Several problems were encountered in running the analyses:

1. The materials model did not execute. Input files that executed successfully when specifying the heat transfer model did not execute successfully when specifying the materials model.

2. For one section in which the moisture model was specified, the moisture content of the soil remained the same as the moisture content input into the program, meaning no moisture enters the pavement system through the surface of the pavement or through the edges of the pavement.

3. While each of the models contained in the CMS program is theoretically very rigorous and has been tested individually, the interaction between the models has never been tested.

Although somewhat overwhelming in its level of detail, the CMS program is believed to be useful in the pavement design process. CMS determines site-specific thermal gradients, which could otherwise only be determined by long-term pavement instrumentation and monitoring. These can aid the design engineer in the

determination of stresses due to thermal gradient and combination stresses due to thermal gradient and loading.

EVALUATION OF THE LIU-LYTTON DRAINAGE MODELS

The Liu-Lytton drainage models provide a method of computing the amount of rain water that penetrates into a pavement through cracks and joints and, subsequently, the rate of drainage out of the base course into the subgrade and into a lateral drainage system. The program's outputs can be used in the design process to examine deterioration of the paving layers based on moisture infiltration into those layers. Using site-specific climatic data and detailed information about the paving materials, the program calculates the percentage of the year that the lower paving layers will be in the weakened state.

The output of the program can be used as inputs to structural analysis models, fatigue analysis models, and predictive models that aid the engineer in the design of the pavement system. A detailed technical description of the program as well as a derivation of the models is presented in Environmental Effects on Pavements—Drainage Manual.[33]

As with the CMS model, the accuracy of the Liu-Lytton model largely depends on the input variables. To accurately characterize the pavement system in terms of the effectiveness of the drainage system, the probability of saturation, and determination of the structural properties of the paving layers, it is extremely important to use accurate climate data.

Several problems were encountered in the execution of the program. These problems are outlined below:

- The program will not accept impermeable base course layers. An option to choose à cement- or lime-stabilized layer exists, but the permeability must be greater than or equal to 0.0001 ft/day.

- The program only accepts a single base course layer beneath the slab, even though many concrete pavements are constructed with a base layer and a subbase layer.

- The material strengths are fixed for the types of materials that are allowable within the program (e.g., the modulus of a crushed limestone is fixed at 209.3 ksi [1443 MPa]).

- Only fine-grained (A-4 through A-7-6) subgrade materials can be analyzed.

- Only select input variables are echoed in the output file. It is valuable to the user to have a listing of all of the input variables used to calculate the program results.

- The format limits the number of consecutive dry-days to less than or equal to 99. However, in one case (Tracy, California) there were more than 140 consecutive dry-days in 1987.

- The sign convention for the transverse slope is not defined within the program documentation, user's guide, or input processor.

The Liu-Lytton program may be useful in the pavement design process by determining the potential for moisture influences on a pavement structure. The effect of changing material properties can then be incorporated into a structural analysis program or design procedure.

Work is currently underway on a separate FHWA contract to combine the U.S. Army Corps of Engineers Cold Regions Research and Environmental Laboratory frost heave/thaw weakening models, the CMS model, and the Liu-Lytton drainage models into a single, comprehensive program.

EVALUATION OF THE ILLISLAB PROGRAM

The ILLISLAB program is a finite element structural analysis program for the analysis of rigid pavements. Using design and material property information, the stresses, deflections, and moments are calculated for the given slab configuration. The program can model many design and analysis features, including, among others, various subgrade formulations, load transfer configurations, bonding conditions between layers, and axle load configurations. The program can examine any number of slabs in any arrangement and can also calculate stress due to a temperature difference between the top and bottom of the slab.

The ILLISLAB program was first developed in 1977 and has been under continuous revision, verification, and expansion at the University of Illinois. Through several research studies, the program's accuracy and ease of application have been improved. Revisions have also been made to facilitate meaningful interpretation of its results and to incorporate new foundation models.

The design information required to execute the program (slab thickness, joint spacing, PCC modulus of elasticity, k-value on top of the base, etc.) is readily obtainable. However, the user must carefully observe the recommendations on the development of the finite element mesh because this can have a large impact on the accuracy of the program's outputs.

The calculation of stresses due to thermal gradients is an important addition to the ILLISLAB program. The determination of the thermal stress is based on an internal iterative routine that eliminates the need for the user to manually determine the stress through successive executions of the program.

The ILLISLAB program is directly applicable to the design of rigid pavements. The accurate calculation of the stresses that develop in rigid pavements under loading (due to temperature or traffic) is critical for the determination of the life of a given pavement. Several design procedures have been developed that rely on the calculation of stresses induced by given axle loads and configurations. Relationships have been developed that relate the number of repeated loadings at a given stress level (relative to the strength of the material) to the life of a concrete pavement.

ANALYSIS OF JSLAB AND ILLISLAB

As part of the study, a comparative analysis of JSLAB and ILLISLAB was conducted. JSLAB and ILLISLAB are finite element programs that determine the stresses that develop in rigid pavements under various loading conditions. Both models are very similar, although each has several unique features:

1. ILLISLAB can model the subgrade with several different subgrade formulations (Winkler foundation, elastic solid formulation, a stress-dependent support model).

2. The JSLAB program requires the user to perform two separate executions of the program and manually subtract the results to determine the thermal stresses.

3. The JSLAB model does not calculate subgrade stresses.

4. The JSLAB program allows round or square dowel geometries; the ILLISLAB program only allows the use of round dowel bars.

5. Both models have the capability of modeling nonuniformly spaced dowel bars and hollow dowel bars.

6. JSLAB purports to be able to calculate moisture stresses, but actually guidelines are provided for the transformation of moisture gradients to equivalent thermal gradients.

The comparative evaluation of JSLAB and ILLISLAB was performed in this study on the MI 1 sections located on U.S. 10 near Clare, Michigan. The relative technical merits and the ease of use of each program were evaluated.

Each of the programs was run for the eight sections to determine the stresses and deflections for the edge and corner loading conditions. The effects of a temperature gradient through the slab were also determined. For a given section, exactly the same finite element mesh and load (or thermal gradient) was used for the execution of the programs.

Analysis of the Edge Loading Condition

Because all of the MI 1 sections have full-depth asphalt concrete shoulders, the edge loading condition was modeled as a free edge. The maximum stresses and deflections were determined beneath a 14.4-kip (64 kN) dual wheel load having a tire pressure of 120 psi (827 kPa). As expected, the point of maximum tensile stress and surface deflection was directly beneath the load at the outermost edge of the slab. The deflections, as calculated by both ILLISLAB and JSLAB, are shown in table 12. The deflections calculated by JSLAB are substantially higher than those calculated by ILLISLAB—over 20 percent higher in some cases. The edge stresses as calculated by the two programs differ by less than 10 percent. The only explanation for these differences is the stiffness matrix defined within the finite element programs. JSLAB was based on a very early version of ILLISLAB, one in which the stiffness matrix was in error.[17]

Table 12. Summary of maximum edge deflection as calculated by ILLISLAB and JSLAB.

	Deflection (mils)	
Section ID	ILLISLAB	JSLAB
MI 1-1a	24.0	25.6
MI 1-1b	25.4	28.2
MI 1-4a	17.3	22.0
MI 1-7a	24.3	30.1
MI 1-7b	25.7	31.6
MI 1-10a	20.8	23.1
MI 1-10b	19.0	22.0

Analysis of the Corner Loading Condition

In modeling the load transfer efficiency within the finite element models, every effort was made to match the deflection (δ) load transfer efficiency, as calculated from the FWD deflections, within 5 percent. The effect of voids beneath the slab was

not considered for this analysis. Again, the loading condition for the analysis was a 14.4-kip (64 kN) dual wheel with a tire pressure of 120 psi (827 kPa).

The errors in the JSLAB stiffness matrix yielded deflections and stresses that are significantly higher than those calculated using ILLISLAB. The deflections on either side of the joint (both approach and leave sides of the joint) as calculated by JSLAB are 10 to 20 percent higher than those calculated by ILLISLAB. The corner stresses as calculated by ILLISLAB and JSLAB differ by approximately 10 percent. However, the modeling of load transfer efficiency, which is a ratio of the unloaded deflection to the loaded deflection, is relatively unaffected by the consistently higher deflections.

Analysis of a Temperature Gradient Through the Slab

The stresses due to a temperature gradient through the slab as calculated by the two programs are shown in table 13. The programs were executed for the case of a single, unconstrained slab without a wheel load (temperature effects on multiple slabs can not be evaluated). The thermal stresses calculated by JSLAB are higher for positive thermal gradients and lower for negative thermal gradients. One explanation for this is that the JSLAB program ignores the effect of Poisson's ratio (u). This can account for 10 to 15 percent of the difference in the stresses.

Table 13. Summary of maximum thermal stress as calculated by ILLISLAB and JSLAB.

	MAXIMUM THERMAL STRESS (psi)			
	Positive Gradient (+3.0 °F/in [+1.67 °C/mm])		Negative Gradient (-1.0 °F/in [-0.56 °C/mm])	
Section ID	ILLISLAB	JSLAB	ILLISLAB	JSLAB
MI 1-1a	+479	+856	-173	-285
MI 1-1b	+509	+814	-182	-271
MI 1-4a	+165	+188	-114	-60.9
MI 1-7a	+146	+167	-107	-58.8
MI 1-7b	+143	+165	-103	-48.2
MI 1-10a	+162	+179	-116	-59.7
MI 1-10b	+166	+186	-111	-58.9

NOTE: MI 1-1 sections have 71-ft (22 m) slabs that are actually designed to crack. The actual thermal stresses will not be as high as indicated because of thermal cracks occurring in the pavement. Sign convention: (+) tension (-) compression

Conclusions

Based on the analyses, the ILLISLAB program had the following advantages over the JSLAB program:

1. The stiffness matrix in the current version of the ILLISLAB program has been shown to be correct.[17] The JSLAB stiffness matrix appears to be based on an earlier version of ILLISLAB that was later shown to contain an error in the stiffness matrix.

2. In modeling the effect of a thermal gradient through a slab, the ILLISLAB program accounts for the effect of the concrete Poisson's ratio, whereas the JSLAB program does not.

3. ILLISLAB calculates subgrade stresses.

4. Like JSLAB, ILLISLAB can model nonuniform dowel spacings.

5. ILLISLAB allows the engineer to choose from a variety of subgrade formulations.

6. The guidelines presented in the documentation on the JSLAB program concerning the development of moisture stresses are directly applicable to the ILLISLAB program.

EVALUATION OF THE PMARP PROGRAM

The PMARP program is a finite element program developed at Purdue University that accounts for the effects of fatigue on the performance of rigid pavements.[14,35] The PMARP program is based on an early version of the ILLISLAB program.[16] As stated previously, several errors have been found in the stiffness matrix in the early version of the ILLISLAB program and, therefore, are presumably repeated within the PMARP program.

The basic concept leading to the development of PMARP was that the structural integrity of a pavement system is continuously undergoing deterioration at various rates. That is, because of pavement deterioration, the structural characteristics of the pavement must be periodically reassessed and new estimates of the pavement's remaining life obtained.

Several technical problems and limitations with the PMARP program were encountered in addition to the stiffness matrix problem already mentioned:

1. For characterization of the subgrade, PMARP incorporates a resilient modulus of subgrade reaction (K_R), but eliminated four of the five broad soil categories (very soft, soft, medium, hard, and very hard) associated with it, retaining only the "medium" subgrade option.

2. Fatigue damage effects are accommodated in PMARP through the adjustment of the slab modulus value (E_c). However, the adjustments are made using unvalidated fatigue curves and statistical correlations.

3. The approach employed in PMARP to account for deterioration of load transfer efficiency as a function of the number of load repetitions has not been validated either theoretically or practically.

4. Two weaknesses of the pumping model include:

   a. The normalized pumping index (NPI) is determined using a regression equation of limited applicability and does not take into account important subbase and subgrade properties, such as gradation, permeability, and erodibility, among others.

   b. Determination of the void area hinges on the "average void depth," which is estimated by the user.

5. The mesh capabilities of the program are severely limiting.

Additional problems were encountered with the input processor used by the program:

1. The input processor misassigns several variables. For example, the reinforcement ratio in the x-direction is assigned to the reinforcement ratio in the y-direction.

2. The largest aggregate interlock factor that the input processor allows the user to input is 10×10^8; however, the input screen indicates that values of 10×10^{10} are to be used for keyed joints.

3. The input processor changes the user's values for the plate deflection versus resilient modulus inputs. The first two entries are accepted, while the third entry is changed to 0.0.

PMARP incorporates a compendium of individual concepts and solutions suggested over the last several decades to address some of the most difficult issues in rigid pavement analysis and design. While each one of these concepts reflected the state of the art at the time of their publication, most of the concepts also have widely-

recognized limitations, including appropriate conditions of applicability and their predominantly qualitative nature. The inclusion of many of these concepts in an overall model is neither especially accurate nor theoretically sound.

EVALUATION OF THE ZERO-MAINTENANCE DESIGN PROCEDURE

The Zero-Maintenance Design Procedure was developed in 1976 for use in the structural design of jointed plain concrete pavements for heavily trafficked highways.[12] The procedure was computerized at that time for use on a mainframe computer (entitled Jointed Concrete Pavements-1 [JCP-1]) and converted for use on a microcomputer in 1986.[36] The program consists of two different design approaches: serviceability and fatigue cracking. The serviceability prediction model was based on a very limited sample of data and was not evaluated in this study. The fatigue cracking model is based on fundamental mechanistic-empirical concepts.

The JCP-1 model requires a number of inputs, including slab dimensions, subgrade and base material data, PCC strength, traffic weight and volume data based on the axle load distribution, thermal gradient data, and other design information. Fatigue damage is computed over the specified design period with the user-supplied inputs. The mechanistically generated fatigue model was calibrated with a limited amount of JPCP field performance data. A reasonable correlation between transverse slab cracking and the fatigue damage number was found.

The JCP-1 program is based on mechanistic concepts calibrated to field conditions and appears to provide reasonable results for the design of jointed concrete pavements. It can directly and mechanistically consider several key design factors, including the stiffness of the base/subgrade, climatic data, axle load distributions, and slab thicknesses. However, at this time, the increased support provided by tied PCC shoulders cannot be evaluated using the existing program. Widened lanes can be evaluated by increasing the lateral distance of truck wheels. The incorporation of tied PCC shoulders as a design option would require the additional analysis of the effects of tied shoulders on stresses induced by traffic loading and thermal curling.

EVALUATION OF JCS-1

The Jointed Concrete Shoulder (JCS-1) program was developed to provide a method of designing jointed concrete shoulders based on a fatigue damage approach.[7] Traditionally, tied concrete shoulders have not been designed; standard thicknesses have been used instead. However, similar to the pavement design process, shoulders can be designed for a certain amount of traffic.

The inputs for this program are quite similar to the JCP-1 program because the two procedures are based on a fatigue damage approach. The required inputs

include the thickness of the mainline pavement, the expected load transfer efficiency across the tied shoulder, concrete strength properties, shoulder width, estimated shoulder thickness, axle load distribution, current and future year traffic volumes, and a foundation support (k-value) value. The program provides an estimate of the fatigue damage of a shoulder of a given thickness. An iterative approach is required to determine the minimum thickness to achieve a fatigue damage of approximately 1.0 over the life of the pavement.

The fatigue damage analysis was based on the following concepts and assumptions:

1. The two critical fatigue damage locations on the shoulder are at the lane-shoulder longitudinal joint and outer edge of the shoulder.

2. Reduction in critical edge stresses caused by traffic loading will diminish transverse cracking in the tied PCC shoulder.

3. A fatigue curve relating the ratio of repeated flexural stress to modulus of rupture and the number of stress applications to failure was developed.

4. The shoulder traffic is determined as a proportion of the mainline pavement traffic for encroaching traffic (lane-shoulder joint) and parked traffic (outer shoulder edge).

5. A relationship between computed fatigue damage and measured shoulder cracking was developed.

The JCS-1 program can be an integral part of the design process. By evaluating the structural requirements of the shoulder, the engineer can determine the structural thickness requirements of a tied concrete shoulder. However, other aspects of shoulder design must also be considered. For example, the shoulder must be thick enough to resist frost heave and the tiebars must be of sufficient size and proper spacing to provide support to the mainline pavement.

EVALUATION OF BERM

The BERM program was developed as part of a research project that focused on the structural design of shoulders.[8] The program is capable of designing both flexible and rigid shoulders; however, only the flexible shoulder design portion was evaluated under this study.

The BERM program was developed using the RISC finite element program and a cracking model that was based on results from the AASHO Road Test.[23]

Regression equations were developed to determine the critical stresses and strains within the shoulder. The stresses and strains are then related to the number of 18-kip (80 kN) ESAL's that the shoulder could sustain before cracking.

The fatigue damage analysis was based on the following set of concepts and assumptions:

1. The two critical fatigue damage locations on the shoulder are at the lane-shoulder longitudinal joint and outer edge of the shoulder.

2. Reduction in critical stresses and strains caused by traffic loading will diminish fatigue cracking in an asphalt concrete shoulder.

3. A fatigue curve relating the critical stresses and strains to the allowable number of 18-kip (80 kN) ESAL's was developed based on cracking observed at the AASHO Road Test.

4. The user is responsible for determining the number of 18-kip (80 kN) ESAL's expected on the shoulder over the life of the pavement.

The fatigue damage is manually determined as the ratio of the number of estimated ESAL's (percentage of the mainline traffic) to the number of allowable ESAL's (as calculated by the program).

The fatigue model used in the program was developed from AASHO Road Test data that consists of interior loading of asphalt concrete pavements. The lane-shoulder joint represents an edge condition, where the strain under load would be much higher. Because the Road Test was conducted in a single location with very controlled materials, the applicability of the data for use throughout the country is not known.

Nevertheless, the BERM program provides a method of determining asphalt shoulder thickness based on the materials' properties and estimated traffic and would be very useful in design.

SUMMARY AND CONCLUSIONS

This chapter has presented summaries of the accuracy of prediction models and of the usefulness of analysis models. On the whole, none of the available models were able to adequately predict the performance of the 95 inservice sections included in the study New or improved prediction models are clearly needed which can adequately predict the performance of concrete pavements.

Several analysis models were shown to have applicability for use in concrete pavement design. The CMS model uses site-specific climatic data to determine the material's response to daily, seasonal, and yearly changes in the environmental conditions. The Liu-Lytton drainage model analyzes the drainage capabilities of a given cross section subjected to specific environmental conditions. The outputs to these models may be used in conjunction with a structural model, such as ILLISLAB, to determine the stresses and deflections resulting from the environment and from the combination of load and environment. It should be noted, however, that both the CMS and the Liu-Lytton programs require a lot of input data.

The ILLISLAB, JSLAB, and PMARP programs can be used in the structural analysis of a specific pavement cross section. Each program has specific capabilities and applications to design. However, while performing the case studies several technical problems were discovered with the JSLAB and PMARP programs. The ILLISLAB program was shown to have broad application to rigid pavement analysis, through its ability to examine the stresses induced in a slab due to traffic loading, a temperature differential between the top and bottom of the slab, and the combination of these factors.

The Zero-Maintenance design procedure was developed based on mechanistic-empirical principles. The procedure accounts for the effect of thermal gradients and load stresses on the fatigue of rigid pavements. The procedure provides a useful tool in the design and analysis of rigid pavements.

In the past, design of pavement shoulders has been based on engineering judgement or policy decisions. Two design procedures have been developed which aid the engineer in determining the thickness required to support the estimated shoulder traffic. The JCS-1 program may be used to design the thickness and load transfer required for a tied PCC shoulder. The BERM program may be used to design the required thickness for an asphalt shoulder. With these programs, adequate shoulder designs can be achieved.

The potential benefits obtained through the use of accurate prediction models and analysis programs can contribute to the improvement of rigid pavement design. However, it must be realized that the procedures are only tools to assist in pavement design and analysis; they are intended to supplement, not replace, engineering judgment and knowledge.

CHAPTER 5 DEVELOPMENT OF NEW PREDICTION MODELS

INTRODUCTION

Acknowledging that the existing prediction models for concrete pavements have some deficiencies, new prediction models were developed in order to more accurately predict the performance of inservice concrete pavements (PSR, faulting, cracking, spalling). The 95 sections in this study (constituting the RIPPER data base) were combined with the over 400 concrete pavement sections from the NCHRP 277 (COPES) data base to allow for a large number of sections and a variety of different pavement designs and design features.

The use of models that can realistically project the condition or performance of a particular design under a variety of conditions (load, climate) would be extremely valuable in the pavement design process. A model that predicts performance, when applied to a specific design, would provide information about the modes of failure of that pavement. That information, fed back into the design process, could suggest which design inputs need to be reevaluated. However, the results of the models should be interpreted only as general indicators of performance and not as exact values.

Each of the models developed has been loaded onto Lotus 1-2-3™ spreadsheets for rapid evaluation of the effect of various input values on pavement performance. In addition, the FHWA is developing a microcomputer program that incorporates these new models.

The models developed in this study are briefly described in the following sections. More detailed information on the models is provided in volume II.

PRESENT SERVICEABILITY RATING (PSR)

The prediction of panel PSR ratings has been modeled several ways in the past. The original PSR equation from the AASHO Road Test was based upon both roughness and distress.[37] Many other models have been developed based solely on roughness (reference 38), or solely on visual distress (reference 39).

The best way to predict PSR for a given pavement is using roughness. However, a PSR model based only on key distress types is useful in mechanistic-empirical design of pavements to approximate physical deterioration (that can be estimated using other models) to serviceability, or user response.

PSR prediction models were developed for both JPCP and JRCP. Whereas all measured types of distress were initially considered, only three key distress types proved significant: joint faulting, joint deterioration (spalling), and transverse

cracking. The presence of full-depth patching also displayed some significance and hence is included in the equations.

The models developed for the prediction of PSR are provided in appendix B to this volume. Examination of the PSR models shows that reducing transverse joint faulting has the greatest effect on reducing the PSR. Spalling, transverse cracking and full-depth repairs have a much lesser effect on reducing PSR.

The primary limitation of these models is that they do not include all distress types nor "long wavelength" roughness, such as would be caused by settlements or heaves. These other sources of variation in PSR are not accounted for in the models.

These models are not intended to be used in place of roughness to predict PSR (or PSI), since it can be shown that measured roughness is the most economical way to predict serviceability. These models are useful in predicting serviceability when only key distress types are available to obtain an estimate of service life. Even then, the models should be used with caution, recognizing their limitations.

LONGITUDINAL CRACKING

Longitudinal cracks run parallel to the centerline of the pavement, in either lane. Longitudinal cracking may occur due to inadequate longitudinal joint forming practices, which include joint forming procedures, depth of formation, and timing of sawing; it may also be related to the presence of a stiff base (friction, bond). Major foundation movements from swelling or expansive soils can also cause random longitudinal slab cracking. Finally, longitudinal cracking that is located in the wheelpaths may be a result of concrete fatigue.

A number of factors were identified in the data base that might have an effect on the development of longitudinal cracking. These included the yearly mean temperature range, mean annual precipitation, mean freezing index, traffic loadings, pavement type (JPCP or JRCP), age, slab thickness, base type and type of joint forming technique (plastic tape insert or saw cutting).

However, all attempts to develop a prediction model were unsuccessful. One reason was the low proportion of sections with longitudinal cracking (17 percent), but it is believed that the major reason was that some of the key factors influencing longitudinal cracking are construction-related. Therefore, it was only possible to identify a few design factors that affected the occurrence of longitudinal cracking.

After numerous correlation and regression analyses that considered all variables in the data base, only two factors appeared to have a significant effect on longitudinal cracking. These factors were base type and joint forming method. The data base was averaged over these factors and the results are shown in table 14. The

plastic tape insert method results in far more longitudinal cracks than the saw cut method (215 ft/mi vs. 38 ft/mi).

Table 14 also shows the effect of base type on the occurrence of longitudinal cracking. Pavements constructed on aggregate bases or with no base type (slab on grade) appear to have fewer longitudinal cracks than those with stabilized bases, either with inserts or sawcut joints.

The base type is believed to be critical because of the friction produced between the slab and base course. Friction testing results generally show that slabs on grade or slabs on an aggregate base have much less sliding friction than a slab on a stabilized base. This data indicates that concrete pavements placed on any type of stabilized base are particularly susceptible to longitudinal crack development. The use of proper saw cutting techniques and the timing of the sawing are the most important factors in reducing the crack potential. While the depth of saw cut was not measured on any of the projects, the depth of the longitudinal joint from plans indicated that depths between 25 and 33 percent of the slab depth were generally adequate.

TRANSVERSE JOINT FAULTING

Transverse joint faulting is the major distress type that causes loss of serviceability in a jointed concrete pavement. Many different measures have been tried to reduce faulting, including the use of dowel bars, thick slabs, nonerodible bases, permeable bases, and short joint spacing. Many of these attempts have been unsuccessful or only partially successful. Procedures are urgently needed to assist designers in developing joint designs that will help to minimize faulting over the service life of the pavement, yet not result in large initial construction costs.

Several attempts have been made to develop prediction models for the faulting of transverse joints.[25,28] These attempts have been partially successful, in that prediction models were obtained that showed reasonable results. The major limitation of these models was in the limited data base of designs that was used to generate them and in the largely empirical development procedures employed.

The combined RIPPER and COPES data provide for a greatly expanded data base that includes pavement sections with new design features, such as permeable bases, thick slabs, and dowels in dry climates. There is a fairly good dispersion of pavement sections with only a few "holes" such as the lack of doweled sections in dry-nonfreeze areas (i.e., southwestern U.S.). There are also too few pavements with open-graded bases in certain areas.

Table 14. Mean longitudinal cracking for all sections included in COPES and RIPPER data bases.

LONG. JT. FORM TYPE	BASE TYPE	N CASES	AVERAGE LCRKS (FT/MILE)	AVERAGE LCRKS (FT/MILE)
INSERT	AGG	41	27	
INSERT	ATB	4	2051	215
INSERT	CTB	12	224	
INSERT	LCB	2	346	
SAW	None	17	17	
SAW	AGG	353	19	
SAW	ATB	65	58	38
SAW	CTB	136	73	
SAW	LCB	8	170	

Notes:

1. Longitudinal cracks (LCRKS) include all severities occurring in two adjacent traffic lanes.

2. Base types:
   None - slab on grade
   AGG - aggregate base
   ATB - asphalt-treated base
   CTB - cement-treated base
   LCB - lean concrete base

3. Joint forming type:
   INSERT - plastic tape insert
   SAW - saw cut in hardened concrete

Two comprehensive predictive models, one for doweled pavements and one for nondoweled pavements, were developed using the combined data bases. The models were developed using a combination of mechanistic and empirical approaches. The two models are provided in appendix B to this report. The individual models are discussed briefly in the following sections. More detailed information is found in chapter 5 of volume II.

DOWELED CONCRETE PAVEMENTS

The faulting prediction model for doweled concrete pavements includes many variables that have been shown by field investigations to affect faulting. These include repeated heavy traffic loadings, dowel bearing stress (which is greatly affected by dowel diameter), joint spacing, effective *k*-value, longitudinal drains, edge support from tied PCC shoulders or widened traffic lanes, and type of subgrade (since granular soils exhibit better drainage characteristics).

It should be pointed out that most of the sections on which this model is based contained noncoated dowel bars. It is inevitable, therefore, that the model will be biased in predicting faulting for pavements which contain coated dowels. Corrosion protection of dowel bars is considered essential for their long-term effectiveness.

A sensitivity of the doweled faulting model is shown in figures 9 and 10. Figure 9 shows that the dowel diameter (at a uniform dowel spacing of 12 in [305 mm]) had a marked effect on reducing faulting. For example, a 1.5 in (38 mm) diameter dowel can carry almost twice the number of axle loads as a 1 in (25 mm) bar to 0.20 in (5 mm) of faulting. Figure 10 indicates the beneficial effect of tied concrete shoulders and positive subdrainage in reducing joint faulting.

NONDOWELED CONCRETE PAVEMENTS

The faulting prediction model for nondoweled concrete pavements includes many variables that have been shown by field investigations to affect faulting of nondoweled joints. These include repeated heavy traffic loadings, base type, corner deflection (which is a function of slab thickness and effective *k*-values), joint opening (which is a function of temperature, joint spacing and slab/base friction), climate, longitudinal drains, edge support from tied PCC shoulders or widened traffic lanes, and type of subgrade (again because granular soils exhibit better drainage characteristics).

A sensitivity of the doweled and nondoweled faulting models is shown in figure 11. Base type, drainage, joint spacing and ESAL are observed to be the most critical design factors affecting transverse joint faulting.

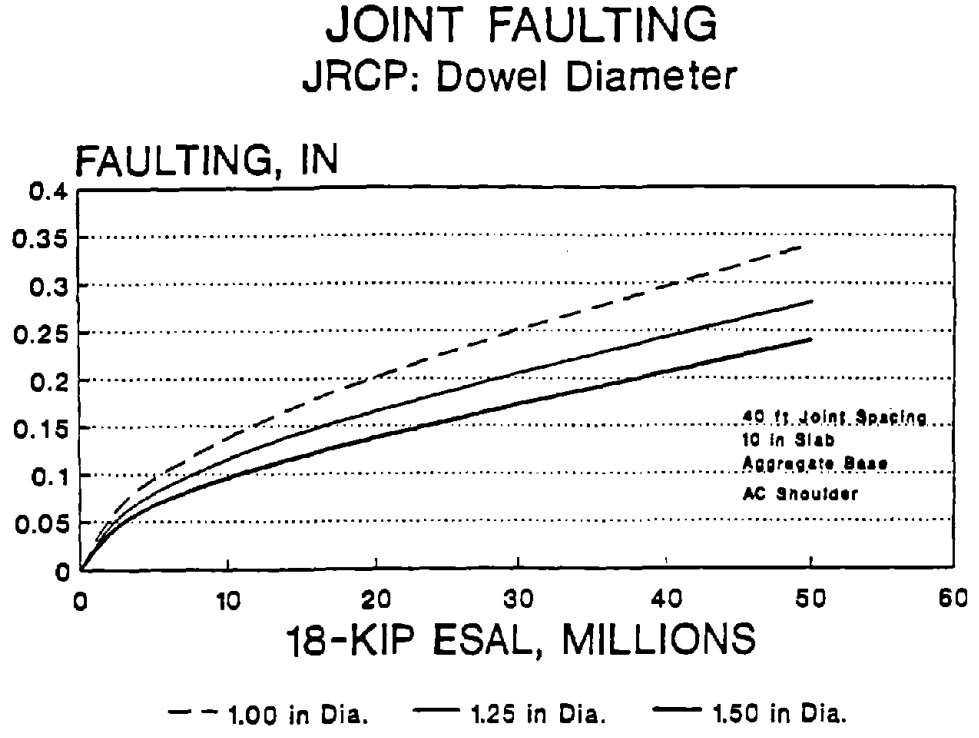

Figure 9. Sensitivity of doweled faulting model to dowel diameter.

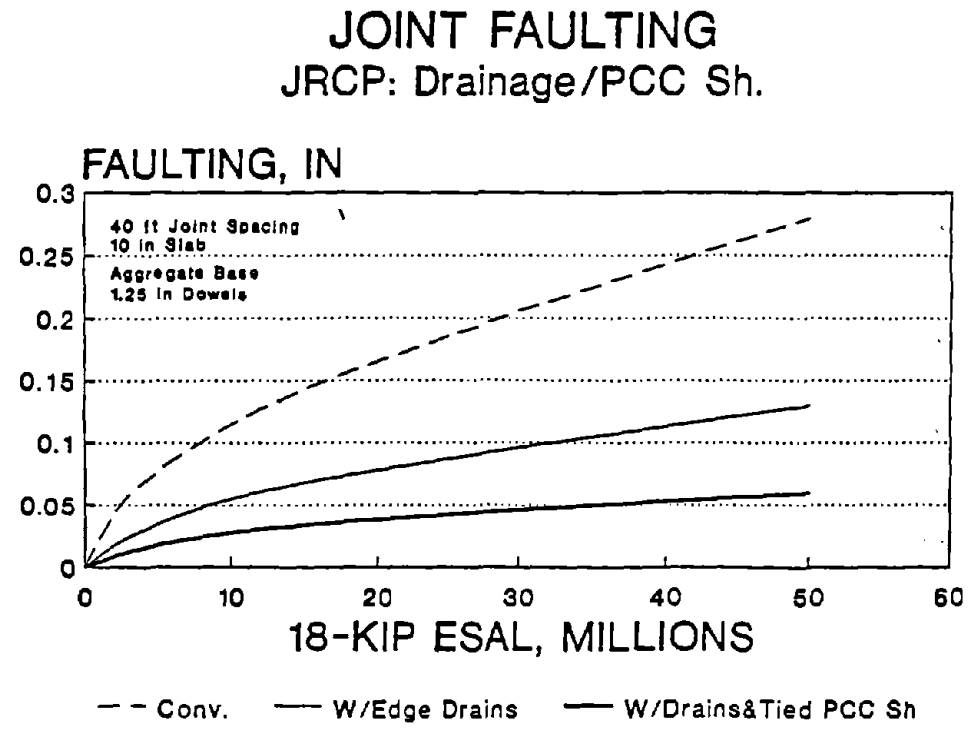

Figure 10. Sensitivity of doweled faulting model to drainage and shoulder type.

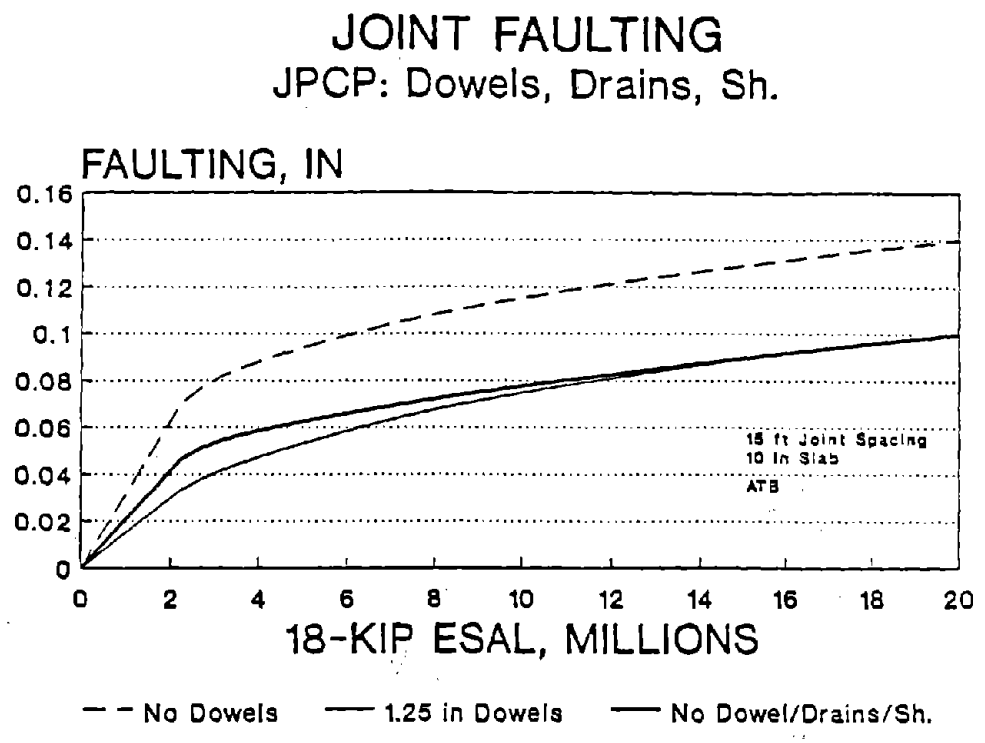

Figure 11. Sensitivity of faulting models to dowels, drainage, and shoulder type.

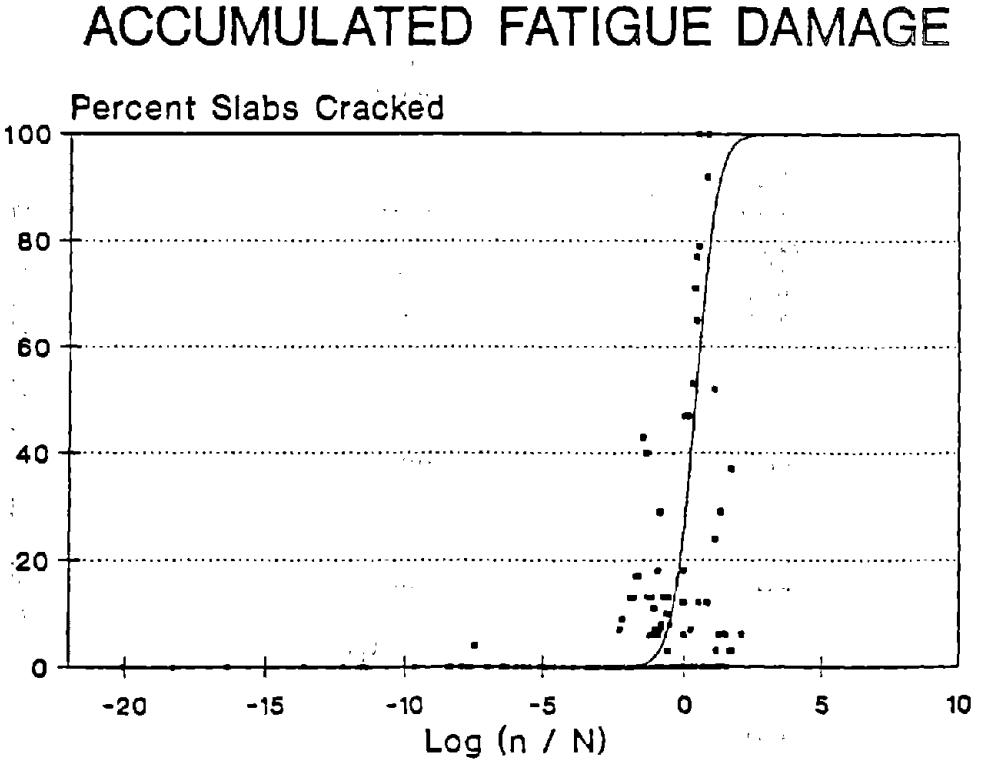

Figure 12. Percent slab cracking as a function of accumulated fatigue damage.

TRANSVERSE CRACKING

Transverse cracking in concrete slabs may occur for a number of reasons. Large temperature gradients through the slab, heavy truck loadings, and shrinkage of the concrete immediately after placement can all produce stresses in the slab which can result in transverse cracking. These can occur either singly or in combination.

Transverse cracks can occur in both jointed plain and jointed reinforced pavements. However, the mechanism influencing their occurrence in each pavement type is different. The long joint spacing generally associated with JRCP (on the order of 40 ft [12.2 m] or longer) produce excessive thermal stresses which result in transverse cracking. However, the slabs contain reinforcing steel which is expected to hold the cracks tight. Thus, because JRCP are expected to crack, no model was developed for JRCP. Instead, efforts were concentrated on developing a model for transverse cracking in jointed plain concrete pavements using the 52 JPCP sections from the RIPPER data base.

The model developed was based on a fatigue-consumption approach similar to the one used in reference 12. This concept assumes that a concrete pavement has a finite life and can withstand some maximum allowable number of repetitions, N, of a given traffic loading before failure. Every individual traffic loading applied, n, decreases the life of the pavement by an infinitesimal amount. Theoretically, when $\Sigma\, n/N = 1$, fracture of the concrete material would occur. However, because of the range in variability of materials, traffic loading, and other properties, fracture of the slab (due to fatigue) can occur at values less than 1.

Using historical traffic data, W-4 tables, and WIM data, the number of 18-kip (80 kN) ESAL applications (n) was estimated for each JPCP section. However, not all of these loadings would have been located at the slab edge, where the maximum tensile stress is developed. Studies have shown that trucks encroach into an edge loading condition (say, within 12 in [305 mm] of the slab edge) between 3 and 7 percent of the time.[40] Thus, it was assumed that an average of 5 percent of the trucks loaded the slab at the critical edge location. However, if a pavement section had a widened outside traffic lane, it was assumed that only 0.1 percent of the truck loadings produced an edge loading condition.

The maximum number of allowable number of repetitions, N, was computed using concrete fatigue damage considerations. First, stresses at the concrete slab edge were computed for a combination of traffic loading and thermal curling using section-specific design data, including slab thickness, composite *k*-value, and slab length. The stress at the slab edge was reduced if tied concrete shoulders were present.

It should be noted that, for sections with random slab lengths (e.g., 12-13-19-18 ft [3.7-4.0-5.8-5.5 m]), each slab length was considered individually as the stresses produced on each slab would be different. This also required that the percentage of slabs cracked be broken down according to slab length. Thus, there were actually 184 cases representing the 52 JPCP sections.

With the critical stress value calculated for the slab edge, the stress ratio was computed. The stress ratio is defined as the ratio of the edge stress to the 28-day modulus of rupture (third point). This value was then directly entered into the following fatigue equation:

$$\text{Log}_{10} N = 2.13 * [\ 1 / SR\ ]^{1.2} \quad (2)$$

where:

N = Allowable 18-kip (80 kN) applications
SR = Stress Ratio; the ratio of computed edge stress to 28-day modulus of rupture

With the determination of n and N, cumulative fatigue damage (n/N) was calculated for each JPCP section (or for each individual slab length for JPCP sections with random joint spacing). The base ten logarithm was taken of each fatigue damage value and plotted against the corresponding percent slabs cracked. This is illustrated by the individual data points shown in figure 12. This figure indicates that most transverse slab cracking occurs in a vertical band between -2 and +2. Thus, as fatigue damage approaches 1 ($\log_{10}$ [n/N] approaches 0), the likelihood of transverse slab cracking greatly increases.

Linear and nonlinear regression procedures were used to try to fit a model through the data. However, the large scatter of data prevented the development of a reasonable model. Therefore, à model was fit through the data for the sections exhibiting cracking. As such, this model would provide a conservative estimate of the development of transverse cracking. The model, which is plotted in figure 12, is given below:

$$P = \frac{1}{0.01 + 0.03 * [\ 20^{-\log (n/N)}\ ]} \quad (3)$$

where:

P = Percent of Slabs Cracked (transverse cracking)
n = Actual number of 18-kip (80 kN) ESAL applications at slab edge
N = Allowable 18-kip (80 kN) ESAL applications (from Eq. 2)

A sensitivity analysis was performed on the model for several key pavement design inputs. Figure 13 provides slab cracking as a function of 18-kip (80 kN) lane (not edge) ESAL applications for different shoulder types. It is observed that the sections with a tied PCC shoulder (20 percent stress load transfer efficiency assumed) and the sections with a widened outside traffic lane and AC shoulder exhibit very little, if any, transverse cracking. However, the sections with the AC shoulder display a significant amount of transverse cracking.

Figure 14 provides a similar sensitivity analysis for joint spacing. The positive influence of shorter slabs on reducing transverse cracking is clearly evident. The reduction in slab cracking between 20 ft (6.1 m) and 15 ft (4.6 m) slabs is quite significant, but additional benefit is also seen in reducing the joint spacing to 10 ft (3.0 m).

Figure 15 provides a sensitivity analysis of the transverse cracking model with respect to slab thickness. The 8-in (203 mm) slab is observed to exhibit extensive slab cracking very early in its life. Increasing the slab thickness from 8 in (203 mm) to 10 in (254 mm) has an enormous effect on reducing the development of fatigue cracking. Likewise, an increase in slab thickness from 10 in (254 mm) to 12 in (305 mm) reduces the amount of transverse slab cracking essentially to zero.

While the cracking model employs a mechanistic approach, there are other factors currently not incorporated (e.g., thermal coefficient of expansion, friction from the base) that also are believed to contribute to transverse cracking.

TRANSVERSE JOINT SPALLING

Joint and corner spalling are defined as any type of fracture or deterioration of the transverse joints, excluding corner breaks. Only medium- and high-severity joint spalling was considered in the development of the spalling prediction models.

A wide range of designs are included in this evaluation. The data was cleaned to remove any sections that had unusual load transfer mechanisms (e.g., ACME devices) or that were constructed using ineffective joint forming methods (e.g., Unitube joint inserts). This was done since these devices may actually contribute to joint spalling, and most new construction does not use these devices.

Prediction models were developed separately for JPCP and JRCP and are provided in appendix B. Extensive efforts to develop a single model for joint spalling were not successful. The relatively low R^2 values of the models indicate that not all of the variability is being accounted for. Often, the development of transverse joint spalling may be due to poor construction and maintenance practices, and these are difficult parameters to incorporate into a model.

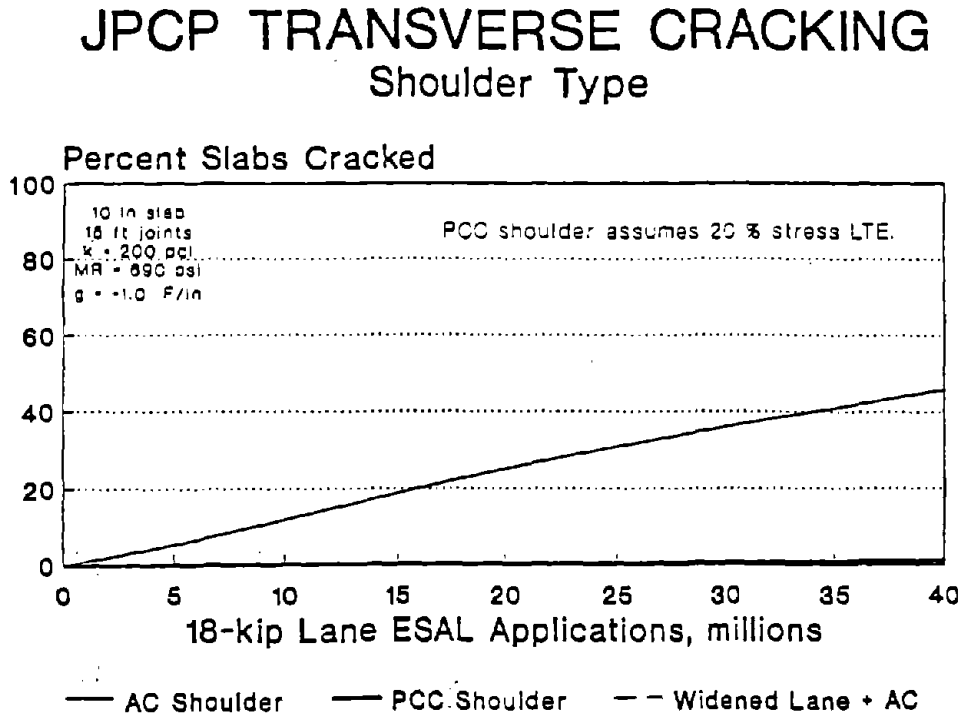

Figure 13. Sensitivity of JPCP cracking model to shoulder type.

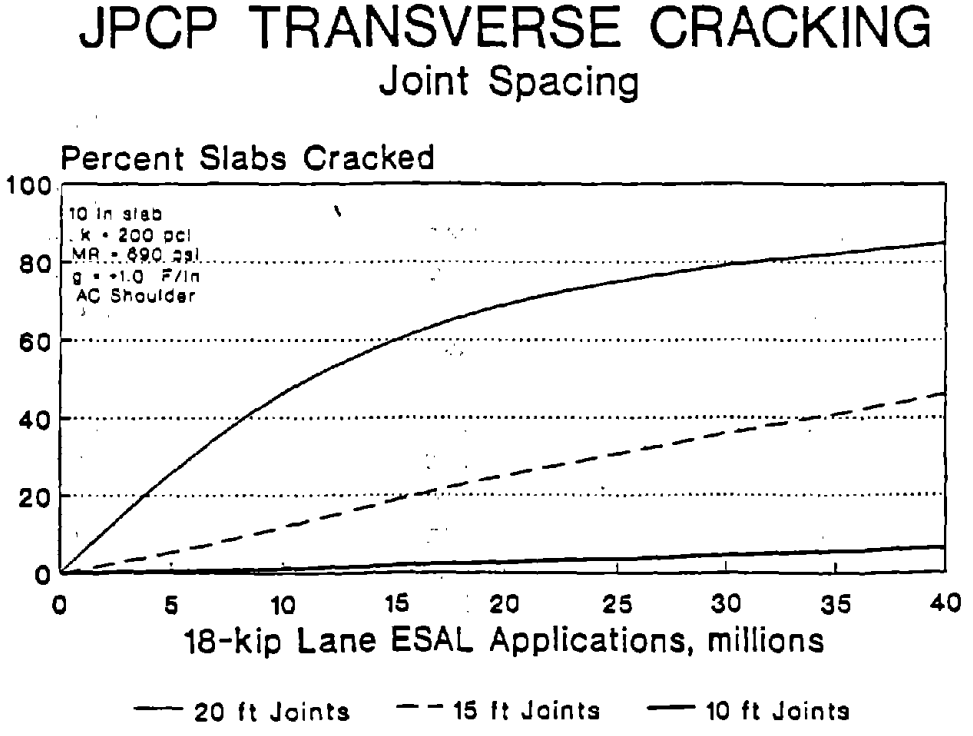

Figure 14. Sensitivity of JPCP cracking model to joint spacing.

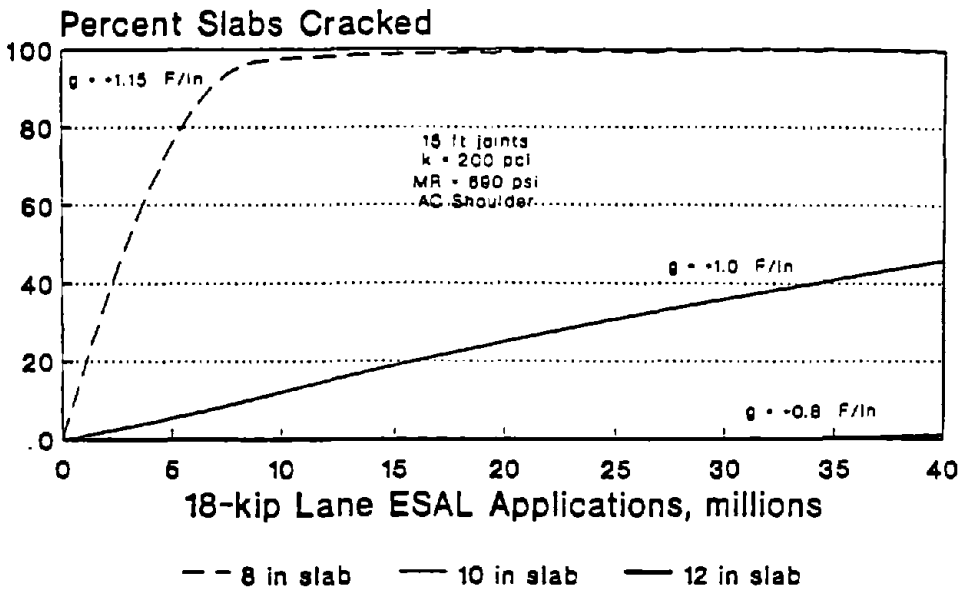

Figure 15. Sensitivity of JPCP cracking model to slab thickness.

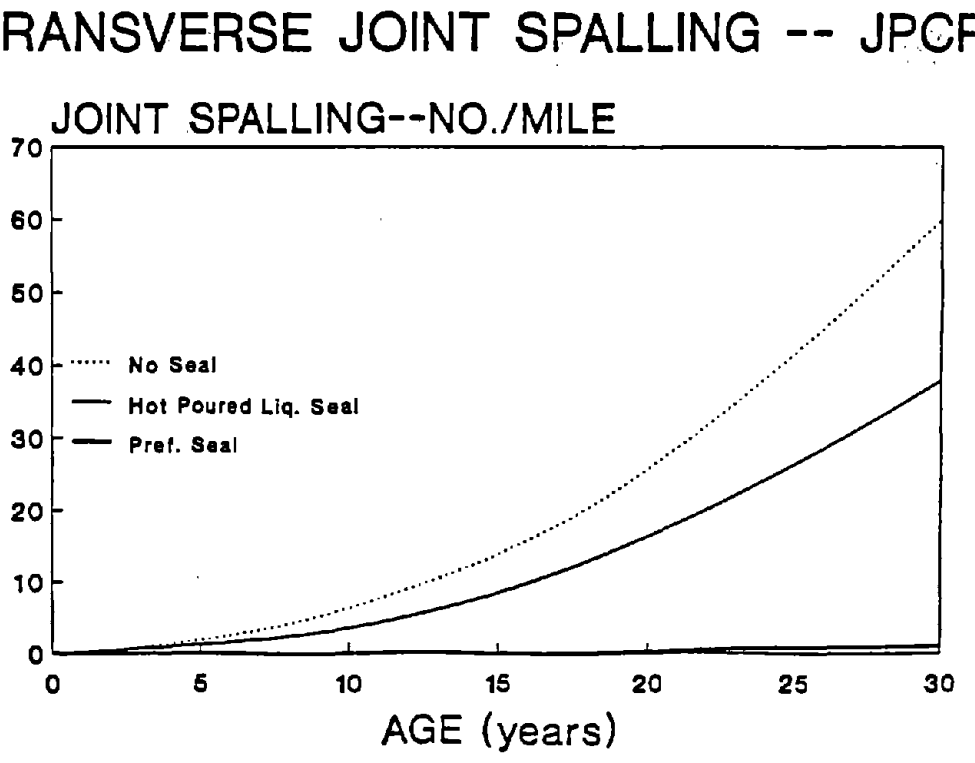

Figure 16. Sensitivity of JPCP spalling model to joint sealant type.

JPCP JOINT SPALLING MODEL

A sensitivity of the JPCP joint spalling model is shown in figures 16 and 17. Figure 16 shows the average effect that joint sealants have on a JPCP in a cold climate (FI = 400, no D-cracking). Having a (hot-poured) liquid joint sealant reduces the amount of spalling by nearly 50 percent over a 30-year period. A preformed sealant reduces the amount of joint spalling to essentially zero over a 30-year period. One such example of this was the ONT 2 section. This pavement section contained a preformed joint sealant and did not exhibit any joint spalling over a period of 15 years. Since it is believed that incompressibles are the major cause of joint spalling, it appears that preformed sealants are capable of keeping incompressibles from infiltrating the joints for a significant period of time.

Figure 17 shows the dramatic effect of D-cracking on joint spalling. In as little as 8 to 10 years, the spalling has reached levels approaching 100 deteriorated joints per mile. Figure 17 also shows the effect of a warm climate (FI = 0) and a freezing climate (FI = 400) on the development of joint spalling.

JRCP JOINT SPALLING MODEL

A sensitivity of the JRCP joint spalling model is shown in figure 18. This figure shows the average effect that joint sealants have on a JRCP in a cold climate (FI = 400, no D-cracking). Having a liquid (hot-poured) joint sealant reduces the amount of spalling by about 11 percent over a 30-year period. However, a preformed sealant reduces the amount of joint spalling to essentially zero over the same 30-year period.

One such example of this performance was MI 4-1 near Charlotte, Michigan. This pavement, whose joints were sealed with a preformed sealant, did not exhibit any joint spalling over a period of 15 years. Again, the preformed sealants are apparently quite successful in keeping out incompressibles, which are believed to be the major cause of joint spalling.

USE OF MODELS IN DESIGN

The use of models in the initial pavement design process can result in improved pavement designs by indicating potential problem areas that may exist in a design prior to its construction. Examples of applying models as design "checkers" include:

- Using the PSR model to estimate the total service life of the pavement from a users perspective.

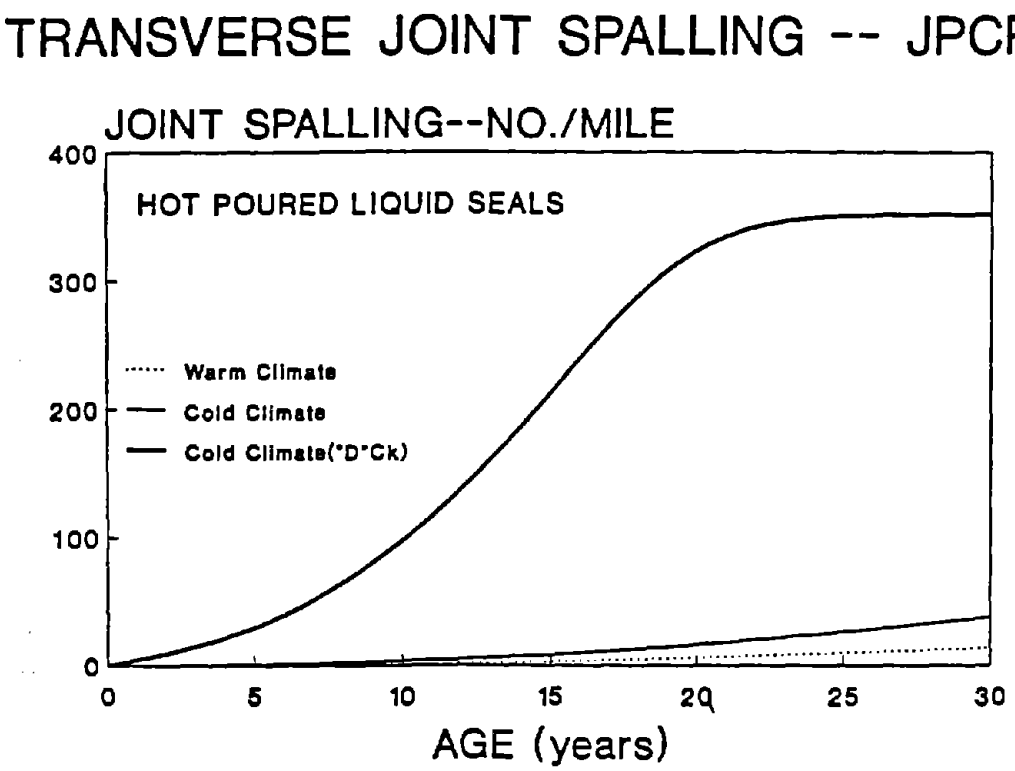

Figure 17. Sensitivity of JPCP spalling model to climate.

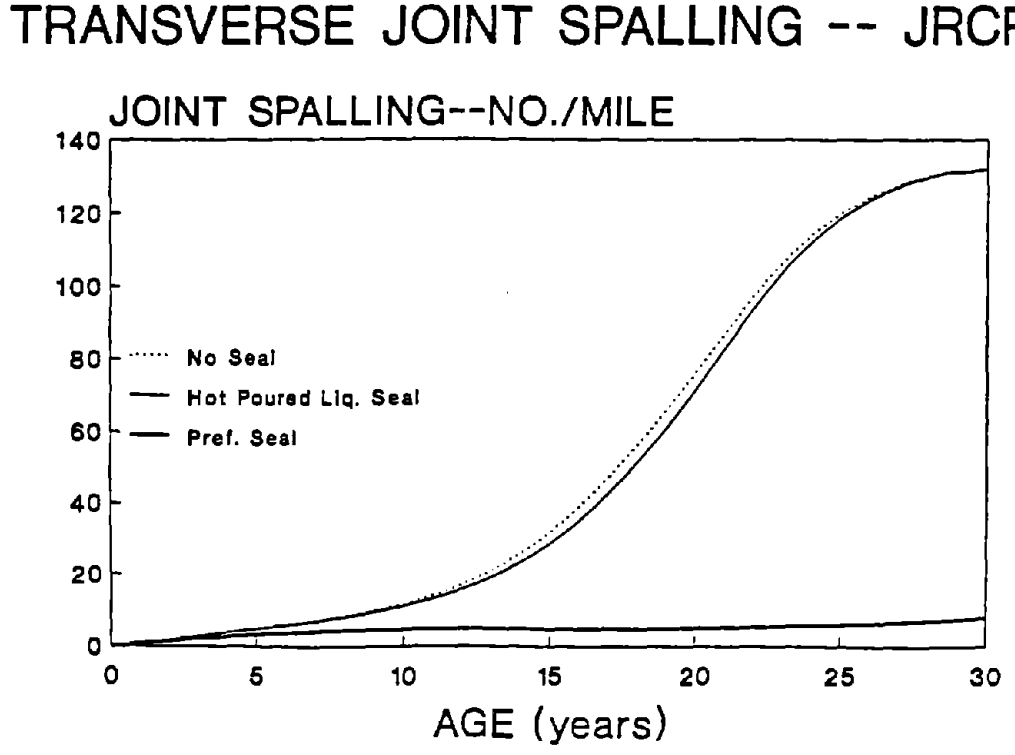

Figure 18. Sensitivity of JRCP spalling model to joint sealant type.

- Using the faulting models to check proposed joint designs. For example, if the models indicate that excessive faulting will occur prematurely in the life of the pavement, then the design engineer would want to more closely examine such features as load transfer, subdrainage, and base type. An excellent example of this application is provided in reference 5.

- Using the JPCP transverse slab cracking model to evaluate the proposed joint spacing. The model will indicate that excessive slab cracking may occur if too long of a joint spacing is used, allowing the engineer to modify the joint spacing accordingly.

The use of the prediction models in this manner require the selection of a design limit for each performance indicator. If, for a given design, the model indicates that certain design limits will be exceeded, the design will have to be reevaluated in terms of addressing those factors which influence the individual performance indicators. Suggested design limits, containing a factor of safety for additional reliability, are provided in table 15. Since these design limits have not been fully verified, these values should be considered advisory and should be applied with caution.

Table 15. Suggested design limits for use with prediction models.

PERFORMANCE INDICATOR	DESIGN LIMIT	
	JPCP	JRCP
Present Serviceability Rating (PSR) *	3.0	3.0
Joint Faulting, in	0.07	0.13
JPCP Transverse Slab Cracking, % of Slabs	10	- - -
Joint Spalling, # of joints per mile	25	15

* High-volume roadways assumed

ACCURACY OF MODELS

The use of the concrete pavement distress and serviceability prediction models developed under this study invariably raise the question of their accuracy. The R^2 and the standard error terms provide an indication of the ability of the models to represent the field data, but pavements are known to exhibit high levels of variability in performance. Two otherwise similar pavements exposed to the same traffic and environmental loadings will quite often display large differences in performance.

Several critical factors influence the accuracy of the prediction models. These factors include the following:

1. Each model represents an average "best fit" condition. Approximately one-half of the data lies above and one-half lies below the mean prediction. Use of the models for design purposes should consider application of a safety factor or the use of a lower critical distress level (as discussed in the previous section).

2. The accuracy of the prediction models can be evaluated in part by observing the residuals, or the difference between the actual value and the predicted value. These plots can graphically illustrate the ability (or inability) of the models to predict distress for individual projects. The overall error of the prediction models can be attributed to the following sources:

   - Pure error. Pure error is the difference in results that occurs between replicated or identical pavement sections. For example, if 10 identical JPCP projects were constructed in a given geographical area and all subjected to the same traffic and environmental loadings, they would exhibit different amounts of distress. Pure error has nothing to do with the accuracy of the prediction model and is the lowest possible variability between projects that can not be reduced (except perhaps through improved quality control of construction).

     Table 16 comes from reference 41 and shows how varied the performance can be for 12 pavement sections of approximate similarity. Table 17 also comes from reference 41 and shows the coefficient of variation (the mean divided by the standard deviation) for the primary performance indicators, demonstrating the "pure error" variation from project to project. The information for tables 16 and 17 come from the data collected under NCHRP Project 1-19.[28]

     To account for the "pure error" in the models, consider the case of transverse joint faulting. The prediction models developed in this study for doweled and nondoweled pavements had standard errors of 0.057 in (1.45 mm) and 0.028 in (0.72 mm), respectively. From the data collected

Table 16. Performance results for 12 "replicate" inservice pavement sections in Illinois.[41]

Section	Age (years)	ESAL (millions)	PSR	Faulting (inches)	Cracking (feet/mile)	Deteriorated Joints (no./mile)
1	18	5	4.2	0.11	0	0
2	18	5	4.0	0.05	0	0
3	18	5	3.4	0.25	0	0
4	22	5	3.8	0.06	950	1
5	22	5	3.6	0.10	1162	0
6	19	8	3.1	0.26	1214	0
7	19	8	2.5	0.39	1478	0
8	22	6	3.3	0.24	106	5
9	22	7	3.3	0.16	106	9
10	20	6	3.8	0.19	0	0
11	17	7	3.2	0.33	106	9
12	18	8	2.6	0.32	1426	18
Mean	19.4	6.3	3.4	0.20	545	4
COV	10	20	15	54	116	115

Pavement: JRCP, 10-inch slabs, 100-foot joint spacing, fine-grained subgrade, no "D" cracking, age between 17 and 22 years, ESAL between 5 and 9 million in design lane.

Table 17. Computed coefficients of variation for replicate pavement sections.[41]

State	Pavement Type	Number of Replicates	COEFFICIENT OF VARIATION (COV) PSR	Faulting	Cracking	Deteriorated Joints
IL	JRCP	16	5	49	183	- - -
		18	9	58	227	178
		3	21	81	151	86
		18	16	45	110	158
		7	11	41	52	137
		19	12	37	116	173
MN	JRCP	4	6	60	111	129
		3	3	22	53	15
LA	JRCP	15	8	38	273	154
		13	6	50	123	77
		2	2	70	54	7
GA	JPCP	5	7	31	121	142
		5	9	13	88	157
		6	13	41	81	94
CA	JPCP	7	5	41	97	171
		4	6	17	30	200
		5	6	17	70	224
		3	9	45	104	173
		9	13	38	77	133
UT	JPCP	2	7	71	141	0
		15	4	33	107	195
		5	7	34	149	129
MEAN COV			8	42	115	130

in reference 28, the mean faulting for a doweled pavement was 0.15 in (3.80 mm). Using the mean coefficient of variation for faulting from table 17, a standard deviation of 0.063 in (1.60 mm) would be expected (standard deviation is equal to the mean faulting times the coefficient of variation for faulting, i.e., 0.15 * 0.42). This value, representing the performance of actual replicate sections, is slightly higher than the 0.057 in (1.45 mm) obtained for the doweled joint faulting prediction model. For the case of nondoweled pavements, the mean faulting (from reference 28) was 0.08 in (2.03 mm) and therefore a standard deviation of 0.08 * 0.42 = 0.034 in (0.85 mm) would be expected. This value is again slightly higher than the 0.028 in (0.72 mm) obtained for the nondoweled joint faulting prediction model. Since both of the values representing actual replicate sections are about the same as the total error of prediction for the two prediction models, it appears that the models are predicting about as good as they will ever be able to predict.

Similar analyses could be performed on the other models to illustrate that there is a set amount of "pure error" associated with actual field performance that simply can not be reduced below a certain level.

- Data error. Data error is the result of errors in traffic estimation, slab thickness, dowel diameter, distress measurement, or any other variable included in the prediction model. Although the data was collected and stored with great care, there are undoubtedly some errors in the data.

- Lack of fit error. This error is the result of selecting the form of the prediction model that does not represent the underlying mechanistic processes for the development of each distress type.

- Error due to missing variables. While there are many important variables included in each prediction model, there are likely several other variables that were not included in the models that may influence joint faulting. Their absence from the prediction model will increase the error associated with the predictions.

SUMMARY

The incorporation of the results from the field performance evaluations into meaningful guidelines for pavement design was accomplished in the form of both generalized guidelines and improved prediction models. New prediction models were developed for Present Serviceability Rating (PSR), transverse joint faulting, transverse slab cracking (JPCP only), and transverse joint faulting. These models were developed using the combined RIPPER and COPES data bases, consisting of approximately 500 pavement sections.

The models and the performance evaluation presented in chapter 3 provide some interesting insights into concrete pavement performance. This was particularly true for three specific topics of concern: transverse joint sealing, drainage, and deflection.

From the performance evaluation, transverse joint sealing appeared to have a beneficial effect on reducing joint spalling and other joint-related distresses. Although joint sealing in general appeared to enhance concrete pavement performance, preformed compression seals and silicone sealants appeared to provide for longer and more effective service than hot-poured sealants. These findings were supported by the joint spalling models, which clearly indicate the effect of sealed joints on reducing concrete joint spalling. The joint spalling models also show the tremendous impact of preformed compression seals on reducing joint spalling.

The beneficial effect of positive subdrainage on concrete pavement performance was also evident from the performance evaluation and the models. The performance evaluation demonstrated that pavements with better drainage characteristics (quantified in terms of the AASHTO drainage coefficient, C_d) exhibited enhanced pavement performance, particularly in terms of less joint faulting. It was also observed from the performance evaluation how positive subdrainage slowed the progression of D-cracking. The faulting models indicated that the presence of positive subdrainage, either in the form of an open-graded base or longitudinal edge drains, had a positive effect in reducing joint faulting.

The critical importance of reduced deflections on concrete pavement performance was noted in the field surveys where deflections were measured at slab corners. Corners exhibiting high deflections and corresponding low load transfer efficiencies often exhibited extensive joint-related distress, including faulting, pumping, and loss of support. The nondoweled faulting model supports these findings by illustrating how high corner deflections result in the rapid development of joint faulting for nondoweled joints. The doweled faulting model indicates that the corner deflection for a doweled joint was about one-half that of a corner deflection for a nondoweled joint. Finally, the JPCP cracking model indicates that if edge deflections were reduced through the use of a widened lane or tied shoulder, then transverse cracking would be reduced or eliminated.

The new models developed under this study are believed to be more accurate than any other prediction models currently available, due to the extensive amount of inservice performance data and the mechanistic-empirical approach utilized. However, it is recommended that these models be reevaluated when the data from the Strategic Highway Research Program (SHRP) Long-Term Pavement Performance (LTPP) study becomes available.

CHAPTER 6 COST EFFECTIVENESS EVALUATION OF SELECTED PAVEMENT DESIGN FEATURES

INTRODUCTION

There are a number of design features that can be included as options in a given pavement design. This study has examined the performance of many of these features, such as base type, the use of load transfer devices, and construction of tied concrete shoulders. Performance data have supported findings such as the beneficial effect of dowel bars on reducing faulting and the effect of short joint spacing in reducing transverse cracking. However, including any of these design features as options invariably increases the construction cost of the pavement.

To fully evaluate the effectiveness of these design features, it is necessary to know the improved performance from their use and also to quantify the costs of these features. This can be accomplished by estimating the increased costs and the additional life that is gained from the use of the design feature and comparing those to the costs and life of a similar pavement that did not contain the design feature. The following design features were evaluated for their cost effectiveness:

- Dowel bars.
- Base types.
- Joint spacing.
- Widened lanes.
- Thick slabs.
- Joint sealants.
- Edge drains.
- Pavement type.
- Tied shoulders.
- Joint orientation.

These features were evaluated based on data collected at one or more locations on project sections in Minnesota, Michigan, North Carolina, Arizona, and California.

ANALYSIS PROCEDURE

The evaluation of the design features is possible because each feature is included in a project where an adjacent section exists without the feature. The long-term performance of pavements with each of the features was estimated using the new distress models for faulting, transverse cracking, and spalling discussed in chapter 5. The traffic that the pavement would carry before reaching critical levels was calculated and compared to the pavement without that feature. The critical levels that were utilized are shown in table 18.

Table 18. Critical distress levels by pavement type.[39]

Pavement Distress	JPCP	JRCP
Transverse joint spalling, % of joints	15-20	20-30
Transverse joint faulting, in	0.10	0.20
Transverse cracks/mi	67	70

NOTES: Transverse joint spalling is defined as only medium- and high-severity levels for both pavement types.

All transverse cracks are counted for JPCP; only deteriorated (medium- and high-severity) cracks are counted for JRCP.

Actual construction costs were requested and rèceived from each of the States participating in this part of the study. Current (1989) costs were requested on a two-lane-mile basis, including shoulders. The respondents were asked to assume that all of the pavements were rural Interstate highways with two lanes in each direction. The pavements were assumed to be constructed at grade, with a 6-ft (1.8 m) inner shoulder and a 10-ft (3.0 m) outer shoulder. Only the initial construction costs were considered. This approach was used for the sake of simplicity; it is not a life-cycle cost analysis, but rather a comparative initial cost analysis only. A summary of those costs is found in appendix A of volume II.

Each of the prediction models developed relates key distress types with appropriate contributory factors, including traffic. Thus, it was possible to predict the traffic carried by the pavement to reach the critical distress level. The traffic to reach the critical distress level was calculated for each of the three distresses shown in table 18. The lowest traffic calculated for each design identifies which distress will control "failure" of the pavement and is the traffic level used in the cost-effectiveness calculation.

The cost effectiveness of each design feature (or combination of design features in some cases) was evaluated in a direct comparison between the design without the feature (conventional design) and the design with the feature (new design). The percent cost increase of the new design over the conventional design can be calculated as:

$$\Delta P = [(\text{New costs}/\text{Conventional costs}) - 1] * 100 \quad (4)$$

The percent life increase of the new design over the conventional design can be calculated as:

$$\Delta L = [(x \text{ ESAL's}/y \text{ ESAL's}) - 1]^* 100 \quad (5)$$

where x is the life (in ESAL's) of the new design and y the life of the conventional design. If the percent life increase of the new design over the conventional design is greater than the percent cost increase, the new design (incorporation of the design feature) is considered to be more cost effective, or worth the additional costs. This assumes that all other costs will be the same, which most likely will not always be the case.

RESULTS

Different concrete pavement design features were evaluated for pavements in each of the study areas, and the results were tabulated in volume II. Appendix A of volume II provides design information for the sections evaluated. Table 19 provides an example of the results of the analysis.

SUMMARY OF COST EVALUATION

The cost effectiveness of new design features was evaluated by comparing the predicted performance of the pavements with these features to the predicted performance of similar pavements at the same location without the features. The models developed under this contract were used to predict performance. This approach was used because the pavements with the new design features have not, in most cases, carried enough traffic to have developed critical distress levels. Therefore, it was not possible to evaluate the cost effectiveness of the design features with actual data.

It is clear that this approach has several drawbacks. The models that were used may not be good predictors for the specific designs that were selected. An example would be the evaluation of the cost effectiveness of skewed joints where the available models do not differentiate in performance by joint orientation. Additionally, pavement failure may also occur through some distress for which a model was not developed and applied. This is especially possible with materials problems or construction problems, which were not covered by the models.

Another problem is that the models are applied to predict the performance of pavements that are actually constructed and carrying traffic. The models have, in some cases, predicted failure by a given distress when the actual pavement has carried more traffic and has still not failed.

Finally, while reaching the critical level of any distress was used as a trigger to identify failure, failure of the different distresses is probably not equal. Rehabilitation of a faulted pavement would probably be much less expensive than rehabilitation of

Table 19. Example of the cost-effectiveness evaluation for Arizona projects.

	DESIGN 1		DESIGN 2		DESIGN 3	
	New Design	Conventional Design	New Design	Conventional Design	New Design	Conventional Design
	13 in PCC No Base	9 in PCC CTB	9 in PCC LCB	9 in PCC CTB	Dowels PCC Shld	No Dowels AC Shoulders
FAULTING (ESAL's, millions)	12	15	17	15	55	18
TRANSVERSE CRACKING (ESAL's, millions)	14000000	5.3	3.1	5.3	7000	47
TRANSVERSE SPALLING (ESAL's, millions)	23.1	23.1	23.1	23.1	43.5	43.5
COSTS	$425,340	$478,140	$460,540	$478,140	$538,636	$495,740
LIFE (critical ESAL's)	12	5.3	3.1	5.3	43.5	18
Percent Increase in Costs	-11%		-4%		9%	
Percent Increase in Life	126%		-42%		142%	
COST-EFFECTIVE (Yes/No)	Yes		No		Yes	

a cracked or spalled pavement. For the sake of simplicity, however, these failure modes were all considered to be equal.

While there are problems with the methodology selected for this analysis, the approach is useful for comparing the performance of these design features at specific locations although the pavements have not carried sufficient loads to allow an analysis of cost effectiveness with actual data. It would be desirable to look at these designs in the future when they have carried a significantly large volume of traffic.

Only a few comparisons could be carried across several of the different sections. However, those that could showed some interesting results. They are discussed below.

The inclusion of dowels was generally cost effective. The inclusion of dowels in the design greatly reduced transverse joint faulting. Designs without dowel bars failed prematurely in terms of excessive joint faulting.

For nondoweled pavements, the construction of thicker slabs was cost effective. The thicker slabs resisted cracking and faulting, but it is believed that a more effective design might have been achieved with the inclusion of dowel bars.

Shorter joint spacing was observed to be cost effective on both JPCP and JRCP. The shorter joint spacings reduced transverse joint faulting, slab cracking and joint spalling.

The cost effectiveness of base types were often dependent upon other factors in the design. For example, in one case, the use of a lean concrete base instead of a cement-treated base was cost effective, but this did not hold true on another design with different features. Also, the selection of a permeable aggregate base instead of a regular aggregate base was cost effective in one case, but the use of an asphalt-treated base rather than an aggregate base was not cost effective.

In general, the addition of drainage was cost effective. This included the addition of permeable bases. In particular, pavements with provision for drainage displayed less transverse joint faulting.

It should be emphasized that the evaluation of the effectiveness of the pavement designs must be conducted on a project-wide basis. The inclusion of one design feature at the expense of another may not provide the expected results. All of the design features must be considered together in order to fully comprehend their influence on pavement performance.

APPENDIX A PARTIAL LISTING OF CANDIDATE SECTIONS

Climatic Zone	Section Number	Location	Const. Date	Section Length	Pavement Type	Pavement Thickness	Base Type	Joint Spacing	Joints Skewed	Dowels	Joint Sealing	Shoulder/ Widened	Drainage
Dry Freeze	MN 1-1	Rothsay, MN	1970	675	JRCP	9.0	AGG	27	Yes	No	Preformed	AC	None
	MN 1-2	Rothsay, MN	1970	6075	JRCP	9.0	AGG	27	Yes	Yes	Preformed	AC	None
	MN 1-3	Rothsay, MN	1970	675	JRCP	8.0	AGG	27	Yes	No	Preformed	AC	None
	MN 1-4	Rothsay, MN	1970	675	JRCP	8.0	AGG	27	Yes	Yes	Preformed	AC	None
	MN 1-5	Rothsay, MN	1970	675	JRCP	8.0	ATB	27	Yes	No	Preformed	AC	None
	MN 1-6	Rothsay, MN	1970	675	JRCP	8.0	ATB	27	Yes	Yes	Preformed	AC	None
	MN 1-7	Rothsay, MN	1970	675	JRCP	9.0	ATB	27	Yes	No	Preformed	AC	None
	MN 1-8	Rothsay, MN	1970	6075	JRCP	9.0	ATB	27	Yes	Yes	Preformed	AC	None
	MN 1-9	Rothsay, MN	1970	675	JRCP	9.0	CTB	27	Yes	No	Preformed	AC	None
	MN 1-10	Rothsay, MN	1970	6075	JRCP	9.0	CTB	27	Yes	Yes	Preformed	AC	None
	MN 1-11	Rothsay, MN	1970	675	JRCP	8.0	CTB	27	Yes	No	Preformed	AC	None
	MN 1-12	Rothsay, MN	1970	675	JRCP	8.0	CTB	27	Yes	Yes	Preformed	AC	None
	MN 1-13	Rothsay, MN	1970	675	JRCP	9.0	ATB	27	Yes	No	Preformed	AC	None
	MN 1-14	Rothsay, MN	1970	6075	JRCP	9.0	ATB	27	Yes	Yes	Preformed	AC	None
	MN 1-15	Rothsay, MN	1970	675	JRCP	8.0	ATB	27	Yes	No	Preformed	AC	None
	MN 1-16	Rothsay, MN	1970	675	JRCP	8.0	ATB	27	Yes	Yes	Preformed	AC	None
	MN 1-17	Rothsay, MN	1970	675	JRCP	8.0	CTB	27	Yes	No	Preformed	AC	None
	MN 1-18	Rothsay, MN	1970	675	JRCP	8.0	CTB	27	Yes	Yes	Preformed	AC	None
	MN 1-19	Rothsay, MN	1970	675	JRCP	9.0	CTB	27	Yes	No	Preformed	AC	None
	MN 1-20	Rothsay, MN	1970	6075	JRCP	9.0	CTB	27	Yes	Yes	Preformed	AC	None
	MN 1-21	Rothsay, MN	1970	675	JRCP	9.0	AGG	27	Yes	No	Preformed	AC	None
	MN 1-22	Rothsay, MN	1970	6075	JRCP	9.0	AGG	27	Yes	Yes	Preformed	AC	None
	MN 1-23	Rothsay, MN	1970	675	JRCP	8.0	AGG	27	Yes	No	Preformed	AC	None
	MN 1-24	Rothsay, MN	1970	675	JRCP	8.0	AGG	27	Yes	Yes	Preformed	AC	None
	MN 2-1	Albert Lea, MN	1977	37594	JPCP	9.0	AGG	13-16-14-19	Yes	Outer	HP	Wid. Inner	None
	MN 2-2	Albert Lea, MN	1977	3010	JPCP	8.0	AGG	13-16-14-19	Yes	Outer	HP	Wid. Inner	None
	MN 2-3	Albert Lea, MN	1977	20011	JRCP	9.0	AGG	27	Yes	Yes	Preformed	Wid. Inner	None
	MN 2-4	Albert Lea, MN	1977	22018	JRCP	9.0	AGG	27	Yes	Yes	Preformed	Wid. Inner	None
	ND 1-1	Rugby, ND	1977	?	JPCP	9.0	None	14-18-14-18	Yes	Yes	?	?	?
	ND 1-2	Rugby, ND	1977	?	JPCP	3.0/6.0	LCB	14-18-14-18	Yes	No	?	?	?
Dry Nonfreeze	AZ 1-1	Phoenix, AZ	1972	9504	JPCP	9.0	CTB	15-13-15-17	Yes	No	HP	AC	None
	AZ 1-2	Phoenix, AZ	1975	9715	JPCP	13.0	None	15-13-15-17	Yes	No	HP	PCC	None
	AZ 1-4	Phoenix, AZ	1979	6996	JPCP	13.0	None	15-13-15-17	Yes	No	HP	PCC	None
	AZ 1-5	Phoenix, AZ	1979	6996	JPCP	11.0	None	15-13-15-17	Yes	No	HP	PCC	None
	AZ 1-6	Phoenix, AZ	1982	8976	JPCP	9.0	LCB	15-13-15-17	Yes	No	HP	PCC	None
	AZ 1-7	Phoenix, AZ	1982	5280	JPCP	9.0	LCB	15-13-15-17	Yes	No	HP	PCC	Edge Drains
	CA 1-1	Tracy, CA	1971	2900	JPCP	8.4	CTB	8-11-7-5	Yes	No	None	AC	None
	CA 1-2	Tracy, CA	1971	2138	JPCP	8.4	CTB	8-11-7-5	Yes	No	None	AC	None
	CA 1-3	Tracy, CA	1971	10556	JPCP	8.4	CTB	12-13-19-18	Yes	No	None	AC	None
	CA 1-4	Tracy, CA	1971	16199	JPCP	8.4	CTB	12-13-19-18	Yes	No	None	AC	None
	CA 1-5	Tracy, CA	1971	2800	JPCP	11.4	CTB	12-13-19-18	Yes	No	None	AC	None
	CA 1-6	Tracy, CA	1971	2354	JPCP	11.4	CTB	12-13-19-18	Yes	No	None	AC	None
	CA 1-7	Tracy, CA	1971	2903	JPCP	8.4	LCB	12-13-19-18	Yes	No	None	AC	None
	CA 1-8	Tracy, CA	1971	2378	JPCP	8.4	LCB	12-13-19-18	Yes	No	None	AC	None
	CA 1-9	Tracy, CA	1971	2900	JPCP	8.4	CTB	12-13-19-18	Yes	No	None	AC	None
	CA 1-10	Tracy, CA	1971	3152	JPCP	8.4	CTB	12-13-19-18	Yes	No	None	AC	None
	CA 2-1	Los Angles, CA	1980	3500	JPCP	8.4	PLCB	13-19-18-12	Yes	No	None	AC	Edge Drains
	CA 2-2	Los Angles, CA	1980	3500	JPCP	8.4	PLCB	13-19-18-12	Yes	No	None	AC	Edge Drains
	CA 2-3	Los Angles, CA	1980	26400	JPCP	8.4	LCB	13-19-18-12	Yes	No	None	AC	None
	CA 4-1	San Jose, CA	1974	1000	JPCP	9.0	CTB	13-19-18-12	Yes	No	HP	AC	None
	CA 4-2	San Jose, CA	1974	1000	JPCP	9.0	CTB	13-19-18-12	Yes	No	Polyurethane	AC	None
	CA 4-3	San Jose, CA	1974	1000	JPCP	9.0	CTB	13-19-18-12	Yes	No	Polymer	AC	None
	CA 4-4	San Jose, CA	1974	1000	JPCP	9.0	CTB	13-19-18-12	Yes	No	Preformed	AC	None
	CA 4-5	San Jose, CA	1974	5280	JPCP	9.0	CTB	13-19-18-12	Yes	No	None	AC	None
	CA 4-6	San Jose, CA	1974	1000	JPCP	9.0	CTB	13-19-18-12	Yes	No	None	AC	Edge Drains

Climate Zone	Section Number	Location	Const. Date	Section Length	Pavement Type	Pavement Thickness	Base Type	Joint Spacing	Joints Skewed	Dowels	Joint Sealing	Shoulder/ Widened	Drainage
Wet Freeze	MI 1-1a	Clare, MI	1975	1320	JRCP	9.0	AGG	71.2	No	Yes	Preformed	AC	Edge Drains
	MI 1-1b	Clare, MI	1975	1320	JRCP	9.0	AGG	71.2	No	Yes	Preformed	AC	None
	MI 1-2a	Clare, MI	1975	1320	JRCP	9.0	AGG	71.2	No	Yes	Preformed	AC	Edge Drains
	MI 1-2b	Clare, MI	1975	1320	JRCP	9.0	AGG	71.2	No	Yes	Preformed	AC	None
	MI 1-3a	Clare, MI	1975	1320	JRCP	9.0	AGG	71.2	No	Yes	Preformed	AC	Edge Drains
	MI 1-3b	Clare, MI	1975	1320	JRCP	9.0	AGG	71.2	No	Yes	Preformed	AC	None
	MI 1-4a	Clare, MI	1975	1320	JPCP	9.0	PATB	12-18-19-13	Yes	No	Preformed	AC	Edge Drains
	MI 1-4b	Clare, MI	1975	1320	JPCP	9.0	PATB	12-18-19-13	Yes	No	Preformed	AC	None
	MI 1-5a	Clare, MI	1975	1320	JPCP	9.0	PATB	12-18-19-13	Yes	No	Preformed	AC	Edge Drains
	MI 1-5b	Clare, MI	1975	1320	JPCP	9.0	PATB	12-18-19-13	Yes	No	Preformed	AC	None
	MI 1-6a	Clare, MI	1975	1320	JPCP	9.0	PATB	12-18-19-13	Yes	No	Preformed	AC	Edge Drains
	MI 1-6b	Clare, MI	1975	1320	JPCP	9.0	PATB	12-18-19-13	Yes	No	Preformed	AC	None
	MI 1-7a	Clare, MI	1975	1320	JPCP	9.0	AGG	12-16-17-13	No	Yes	Preformed	AC	Edge Drains
	MI 1-7b	Clare, MI	1975	1320	JPCP	9.0	AGG	12-16-17-13	No	Yes	Preformed	AC	None
	MI 1-8a	Clare, MI	1975	1320	JPCP	9.0	AGG	12-16-17-13	No	Yes	Preformed	AC	Edge Drains
	MI 1-8b	Clare, MI	1975	1320	JPCP	9.0	AGG	12-16-17-13	No	Yes	Preformed	AC	None
	MI 1-9a	Clare, MI	1975	1320	JPCP	9.0	AGG	12-16-17-13	No	Yes	Preformed	AC	Edge Drains
	MI 1-9b	Clare, MI	1975	1320	JPCP	9.0	AGG	12-16-17-13	No	Yes	Preformed	AC	None
	MI 1-10a	Clare, MI	1975	1320	JPCP	9.0	ATB	12-18-19-13	Yes	Yes	Preformed	AC	Edge Drains
	MI 1-10b	Clare, MI	1975	1320	JPCP	9.0	ATB	12-18-19-13	Yes	Yes	Preformed	AC	None
	MI 1-11a	Clare, MI	1975	1320	JPCP	9.0	ATB	12-18-19-13	Yes	Yes	Preformed	AC	Edge Drains
	MI 1-11b	Clare, MI	1975	1320	JPCP	9.0	ATB	12-18-19-13	Yes	Yes	Preformed	AC	None
	MI 1-12a	Clare, MI	1975	1320	JPCP	9.0	ATB	12-18-19-13	Yes	Yes	Preformed	AC	Edge Drains
	MI 1-12b	Clare, MI	1975	1320	JPCP	9.0	ATB	12-18-19-13	Yes	Yes	Preformed	AC	None
	MI 1-25	Clare, MI	1975	>1000	JPCP	9.0	ATB	12-18-19-18	Yes	No	Preformed	PCC	None
	MI 4-1	Charlotte, MI	1971	2640	JRCP	9.0	AGG	71.2	No	Yes	Preformed	PCC	Edge Drains
	MI 4-2	Charlotte, MI	1971	2640	JRCP	9.0	AGG	71.2	No	Yes	Preformed	AC	Edge Drains
	MO 1-1	Bethany, MO	1977	922.5	JRCP	9.0	AGG	61.5	No	Yes	HP	AC	None
	MO 1-2	Bethany, MO	1977	922.5	JRCP	9.0	AGG	61.5	No	Yes	HP	AC	None
	MO 1-3	Bethany, MO	1977	922.5	JRCP	9.0	AGG	61.5	No	Yes	HP	AC	None
	MO 1-4	Bethany, MO	1977	922.5	JRCP	9.0	AGG	61.5	No	Yes	HP	AC	None
	MO 1-5	Bethany, MO	1977	922.5	JRCP	9.0	ATB	61.5	No	Yes	HP	AC	None
	MO 1-6	Bethany, MO	1977	922.5	JRCP	9.0	PATB	61.5	No	Yes	HP	AC	None
	MO 1-7	Bethany, MO	1977	922.5	JRCP	9.0	CTB	61.5	No	Yes	HP	AC	None
	MO 1-8	Bethany, MO	1977	922.5	JRCP	9.0	AGG	61.5	No	Yes	HP	AC	None
	MO 2-1	Caldwell Co, MO	1964	1450	JPCP	7.0	AGG	30.0	No	Yes	?	AGG	None
	MO 2-3	Caldwell Co, MO	1964	1100	JPCP	9.0	AGG	30.0	No	Yes	?	AGG	None
	MO 2-5	Caldwell Co, MO	1964	3770	JRCP	9.0	AGG	61.5	No	Yes	?	AGG	None
	Mo 2-6	Caldwell Co, MO	1964	1200	JRCP	7.0	AGG	61.5	No	Yes	?	AGG	None
	MO 3-1	Daviess Co, MO	1963	700	JPCP	7.0	AGG	30.0	Yes	No	?	None	None
	MO 3-5	Daviess Co, MO	1963	811	JPCP	6.0	AGG	30.0	No	Yes	?	None	None
	MO 3-7	Daviess Co, MO	1963	930	JPCP	6.0	AGG	30.0	Yes	No	?	None	None
	MO 3-9	Daviess Co, MO	1963	591	JPCP	8.0	AGG	30.0	No	Yes	?	None	None
	NJ 1	I-80, NJ	1973	25000	JPCP	9.0	AGG	15	No	Yes	None	AC	None
	NJ 2	Yardville, NJ	1947	15840	JRCP	10.0	AGG	78.5	No	Yes	HP	AC	None
	NJ 3-1	Camden, NJ	1979	519	JRCP	9.0	NSOG	78.5	No	Yes	HP	AC	DB/LD
	NJ 3-2	Camden, NJ	1979	438	JRCP	9.0	PATB	78.5	No	Yes	HP	AC	DB/LD
	NY 1-1	Catskill, NY	1968	1800	JPCP	9.0	ATB	20.0	No	Yes	Preformed	AC	None
	NY 1-2	Catskill, NY	1968	1800	JRCP	9.0	ATB	60.8	No	Yes	Preformed	AC	None
	NY 1-3	Catskill, NY	1968	2400	JRCP	9.0	ATB	60.8	No	Yes	Preformed	AC	None
	NY 1-4	Catskill, NY	1968	2400	JRCP	9.0	AGG	60.8	No	Yes	Preformed	AC	None
	NY 1-5a	Catskill, NY	1968	1200	JPCP	9.0	Soil Cement	20.0	No	No	Preformed	AC	None
	NY 1-5b	Catskill, NY	1968	1200	JPCP	9.0	Soil Cement	20.0	No	No	Preformed	AC	None
	NY 1-6	Catskill, NY	1968	2400	JPCP	9.0	AGG	20.0	No	Yes	Preformed	AC	None
	NY 1-7	Catskill, NY	1968	2400	JPCP	9.0	ATB	20.0	No	No	Preformed	AC	None
	NY 1-8a	Catskill, NY	1968	1200	JPCP	9.0	ATB	20.0	Yes	No	Preformed	AC	None
	NY 1-8b	Catskill, NY	1968	1200	JPCP	9.0	ATB	20.0	No	No	Preformed	AC	None
	NY 2-1	Otego, NY	1975	600	JPCP	7.0	AGG	18-22-16-20	Yes	No	HP	?	None
	NY 2-2	Otego, NY	1975	600	JPCP	7.0	AGG	18-22-16-20	Yes	No	HP	?	None
	NY 2-3	Otego, NY	1975	1920	JPCP	9.0	AGG	20.0	No	Yes	HP	PCC	None
	NY 2-4	Otego, NY	1975	700	JPCP	9.0	AGG	25.3	No	Yes	HP	PCC	None

Climatic Zone	Section Number	Location	Const. Date	Section Length	Pavement Type	Pavement Thickness	Base Type	Joint Spacing	Joints Skewed	Dowels	Joint Sealing	Shoulder/ Widened	Drainage
Wet Freeze (cont.)	NY 2-5	Otego, NY	1975	800	JPCP	9.0	AGG	26.7	No	Yes	HP	PCC	None
	NY 2-6	Otego, NY	1975	1920	JPCP	9.0	AGG	20.0	No	Yes	HP	PCC	None
	NY 2-7	Otego, NY	1975	700	JPCP	9.0	AGG	23.3	No	Yes	HP	PCC	None
	NY 2-8	Otego, NY	1975	800	JPCP	9.0	AGG	26.7	No	Yes	HP	PCC	None
	NY 2-9	Otego, NY	1975	30180	JPCP	9.0	AGG	20.0	No	Yes	HP	PCC	None
	NY 2-10	Otego, NY	1975	700	JPCP	9.0	AGG	23.3	No	Yes	HP	PCC	None
	NY 2-11	Otego, NY	1975	800	JPCP	9.0	AGG	26.7	No	Yes	HP	PCC	None
	NY 2-12	Otego, NY	1975	30180	JPCP	9.0	AGG	20.0	No	Yes	HP	PCC	None
	NY 2-13	Otego, NY	1975	700	JPCP	9.0	AGG	23.3	No	Yes	HP	PCC	None
	NY 2-14	Otego, NY	1975	800	JPCP	9.0	AGG	26.7	No	Yes	HP	PCC	None
	NY 2-15	Otego, NY	1975	31680	JRCP	9.0	AGG	63.5	No	Yes	HP	AC	None
	OH 1-1	Chillicothe, OH	1973	240	JRCP	9.0	AGG	40	No	Yes	Preformed	AC	None
	OH 1-2	Chillicothe, OH	1973	320	JRCP	9.0	AGG	40	No	Yes	Preformed	AC	None
	OH 1-3	Chillicothe, OH	1973	147	JRCP	9.0	ATB	21	No	Yes	Preformed	AC	None
	OH 1-4	Chillicothe, OH	1973	360	JRCP	9.0	ATB	40	No	Yes	Preformed	AC	None
	OH 1-5	Chillicothe, OH	1973	153	JPCP	9.0	ATB	17	Yes	No	Preformed	AC	None
	OH 1-6	Chillicothe, OH	1973	168	JRCP	9.0	AGG	21	No	Yes	Preformed	AC	None
	OH 1-7	Chillicothe, OH	1973	360	JRCP	9.0	AGG	40	No	Yes	Preformed	AC	None
	OH 1-8	Chillicothe, OH	1973	360	JRCP	9.0	AGG	40	No	Yes	Preformed	AC	None
	OH 1-9	Chillicothe, OH	1973	400	JRCP	9.0	AGG	40	No	Yes	Preformed	AC	None
	OH 1-10	Chillicothe, OH	1973	189	JRCP	9.0	AGG	21	No	Yes	Preformed	AC	None
	OH 1-11	Chillicothe, OH	1973	40	JRCP	9.0	AGG	40	No	Yes	Preformed	AC	None
	OH 1-12	Chillicothe, OH	1973	120	JRCP	9.0	AGG	40	No	Yes	Preformed	AC	None
	OH 2-1	Vermillion, OH	1974	1072	JRCP	9.0	ATB	40	No	Yes	HP	AC	Edge Drains
	OH 2-2	Vermillion, OH	1974	663	JRCP	9.0	ATB	40	No	Yes	HP	AC	None
	OH 2-3	Vermillion, OH	1974	191	JRCP	9.0	ATB	40	No	Yes	None	AC	None
	OH 2-4	Vermillion, OH	1974	149	JRCP	9.0	ATB	40	No	Yes	Preformed	AC	None
	OH 2-5	Vermillion, OH	1974	945	JRCP	9.0	AGG	40	No	Yes	HP	AC	Edge Drains
	OH 2-9	Vermillion, OH	1974	705	JRCP	9.0	AGG	40	No	Yes	HP	AC	Edge Drains
	OH 2-11	Vermillion, OH	1974	224	JRCP	9.0	AGG	40	No	Yes	None	AC	Edge Drains
	OH 2-15	Vermillion, OH	1974	221	JRCP	9.0	AGG	40	No	Yes	Preformed	AC	Edge Drains
	OH 2-17	Vermillion, OH	1974	222	JRCP	9.0	AGG	40	No	Yes	None	AC	Edge Drains
	OH 2-18	Vermillion, OH	1974	463	JRCP	9.0	AGG	40	No	Yes	HP	AC	Edge Drains
	OH 2-19	Vermillion, OH	1974	705	JRCP	9.0	AGG	40	No	Yes	HP	AC	Edge Drains
	OH 2-20	Vermillion, OH	1974	681	JRCP	9.0	AGG	60	No	Yes	HP	AC	Edge Drains
	OH 2-21	Vermillion, OH	1974	170	JRCP	9.0	AGG	20	No	Yes	HP	AC	Edge Drains
	OH 2-22	Vermillion, OH	1974	231	JRCP	9.0	AGG	40	No	Yes	None	AC	Edge Drains
	OH 2-23	Vermillion, OH	1974	248	JRCP	9.0	AGG	40	No	Yes	Preformed	AC	Edge Drains
	OH 2-24	Vermillion, OH	1974	210	JRCP	9.0	AGG	20	No	Yes	Preformed	AC	Edge Drains
	OH 2-24b	Vermillion, OH	1974	226	JRCP	9.0	AGG	20	No	Yes	Preformed	AC	Edge Drains
	OH 2-25	Vermillion, OH	1974	216	JRCP	9.0	AGG	20	No	Yes	None	AC	Edge Drains
	OH 2-26	Vermillion, OH	1974	229	JRCP	9.0	AGG	20	No	Yes	HP	AC	Edge Drains
	OH 2-27	Vermillion, OH	1974	299	JRCP	9.0	AGG	60	No	Yes	HP	AC	Edge Drains
	OH 2-28	Vermillion, OH	1974	397	JRCP	9.0	AGG	60	No	Yes	None	AC	Edge Drains
	OH 2-29	Vermillion, OH	1974	433	JRCP	9.0	AGG	60	No	Yes	Preformed	AC	Edge Drains
	OH 2-30	Vermillion, OH	1974	400	JRCP	9.0	No Base	40	No	Yes	HP	AC	None
	OH 2-32	Vermillion, OH	1974	212	JRCP	9.0	No Base	40	No	Yes	HP	AC	None
	OH 2-33a	Vermillion, OH	1974	660	JRCP	15.0	No Base	20	No	No	HP	PCC	None
	OH 2-33b	Vermillion, OH	1974	500	JRCP	15.0	No Base	20	No	NO	HP	AC	None
	OH 2-34	Vermillion, OH	1974	220	JRCP	9.0	AGG	40	No	Yes	Preformed	AC	None
	OH 2-35	Vermillion, OH	1974	221	JRCP	9.0	AGG	40	No	Yes	None	AC	None
	OH 2-38	Vermillion, OH	1974	223	JRCP	9.0	AGG	40	No	Yes	HP	AC	None
	OH 2-39	Vermillion, OH	1974	534	JRCP	9.0	AGG	40	No	Yes	None	AC	None
	OH 2-42	Vermillion, OH	1974	423	JRCP	9.0	AGG	40	No	Yes	HP	AC	Edge Drains
	ONT 1-1	Ruthven, ONT	1982	15840	JPCP	12.0	No Base	12-13-18-19	Yes	No	HP	AC	Edge Drains
	ONT 1-2	Ruthven, ONT	1982	16896	JPCP	8.0	PATB	12-13-18-19	Yes	No	HP	AC	Edge Drains
	ONT 1-3	Ruthven, ONT	1982	2640	JPCP	8.0	LCB	12-13-18-19	Yes	No	HP	PCC	Edge Drains
	ONT 1-4	Ruthven, ONT	1982	15840	JPCP	7.0	LCB	12-13-18-19	Yes	No	HP	PCC	Edge Drains
	ONT 2	Toronto, ONT	1971	6234	JPCP	9.0	CTB	12-13-18-19	Yes	Yes	Preformed	AC	Edge Drains
	PA 1-1	Kittanning, PA	1980	1414	JRCP	10.0	AGG-Cement	46.5	No	Yes	HP	AC	Edge Drains
	PA 1-2	Kittanning, PA	1980	1450	JRCP	10.0	PATB	46.5	No	Yes	HP	AC	Edge Drains
	PA 1-3	Kittanning, PA	1980	1000	JRCP	10.0	PAGG	46.5	No	Yes	HP	AC	Edge Drains
	PA 1-4	Kittanning, PA	1980	1850	JRCP	10.0	PAGG	46.5	No	Yes	HP	AC	Edge Drains
	PA 1-5	Kittanning, PA	1980	1600	JRCP	10.0	AGG	46.5	No	Yes	HP	AC	Edge Drains

Climate Zone	Section Number	Location	Const. Date	Section Length	Pavement Type	Pavement Thickness	Base Type	Joint Spacing	Joints Skewed	Dowels	Joint Sealing	Shoulder/ Widened	Drainage
Wet Nonfreeze	CA 3-1	Geyserville, CA	1975	1000	JPCP	9.0	CTB	13-19-18-12	Yes	No	HP	PCC-Tied	None
	CA 3-2	Geyserville, CA	1975	1000	JPCP	9.0	CTB	13-19-18-12	Yes	No	None	PCC-Tied	None
	CA 3-3	Geyserville, CA	1975	1000	JPCP	9.0	CTB	13-19-18-12	Yes	No	Preformed	PCC-Untied	None
	CA 3-4	Geyserville, CA	1975	5280	JPCP	9.0	CTB	13-19-18-12	Yes	No	None	AC	None
	CA 3-5	Geyserville, CA	1975	1000	JPCP	9.0	CTB	13-19-18-12	Yes	No	None	PCC-Untied	None
	CA 3-6	Geyserville, CA	1975	5280	JPCP	9.0	CTB	13-19-18-12	Yes	No	None	AC	None
	FL 1-1	Fort Meyers, FL	1978	2000	JPCP	9.0	CTB	20	No	No	Preformed	AC	None
	FL 1-2	Fort Meyers, FL	1978	2000	JPCP	3.0/9.0	LCB-A	15	Yes	No	Preformed	AC	None
	FL 1-3	Fort Meyers, FL	1978	900	JPCP	3.0/9.0	LCB-B	15	Yes	No	Preformed	PCC	None
	FL 1-4	Fort Meyers, FL	1978	1000	JPCP	3.0/9.0	LCB-B	15	Yes	No	Preformed	AC	None
	FL 1-5	Fort Meyers, FL	1978	1000	JPCP	3.0/9.0	LCB-B	15	Yes	No	Preformed	AC	None
	FL 1-6	Fort Meyers, FL	1978	1700	JPCP	3.0/9.0	LCB-C	15	Yes	No	Preformed	AC	None
	FL 1-7	Fort Meyers, FL	1978	2000	JPCP	3.0/9.0	LCB-A	15	No	No	Preformed	AC	None
	FL 1-8	Fort Meyers, FL	1978	2000	JPCP	3.0/9.0	LCB-B	15	No	No	Preformed	AC	None
	FL 1-9	Fort Meyers, FL	1978	2000	JPCP	3.0/9.0	LCB-C	15	No	No	Preformed	AC	None
	FL 1-10	Fort Meyers, FL	1978	2000	JPCP	3.0/9.0	LCB-A	20	No	Yes	Preformed	AC	None
	FL 1-11	Fort Meyers, FL	1978	2000	JPCP	3.0/9.0	LCB-B	20	No	Yes	Preformed	AC	None
	GA 1	Treutlen Co, GA	1979	64706	JPCP	10.0	AC	20	No	Yes	HP	PCC-Tied	?
	GA 2	Haralson Co, GA	1980	61169	JPCP	11.0	AC	20	No	Yes	HP	PCC-Tied	?
	GA 3	Troup Co, GA	1979	57446	JPCP	10.0	LCB	20	No	Yes	HP	PCC-Tied	?
	LA 2	?	1961	?	?	9.5	Sand	20	?	?	?	?	?
	LA 5	?	1960	?	?	9.5	Soil Cement	20	?	?	?	?	?
	LA 21	?	1961	?	?	8.75	Sand	20	?	?	?	?	?
	LA 28	?	1964	?	?	9.33	Sel. Soil	20	?	?	?	?	?
	LA 29	?	1964	?	?	8.75	Sel. Soil	20	?	?	?	?	?
	LA 32	?	1961	?	?	7.6	Sel. Soil	20	?	?	?	?	?
	LA 36	?	1965	?	?	9.0	Sand	20	?	?	?	?	?
	LA 37	?	1965	?	?	9.0	Sand	20	?	?	?	?	?
	LA 50	?	1961	?	?	9.88	Sel. Soil	20	?	?	?	?	?
	LA 60-1	Calcasieu PA, LA	1964	17424	JRCP	10.0	Sand Shell	58.5	No	Yes	?	?	?
	LA 60-2	Calcasieu PA, LA	1964	20064	JRCP	10.0	Sand Shell	58.5	No	Yes	?	?	?
	LA 61-1	Calcasieu PA, LA	1964	10560	JRCP	10.0	Sand Asphalt	58.5	No	Yes	?	?	?
	LA 61-2	Calcasieu PA, LA	1964	?	JRCP	10.0	Sand Asphalt	58.5	No	Yes	?	?	?
	LA 62-1	Ouachita PA, LA	1961	16315	JRCP	10.0	Sand	58.5	No	Yes	?	?	?
	LA 62-2	Ouachita PA, LA	1960	15840	JRCP	10.0	Sand	58.5	No	Yes	?	?	?
	LA 63-1	Lincoln PA, LA	1961	10032	JRCP	10.0	Soil Cement	58.5	No	Yes	?	?	?
	LA 63-2	Lincoln PA, LA	1960	13253	JRCP	10.0	Sand	58.5	No	Yes	?	?	?
	LA 64-1	St. Landry PA, LA	1963	19378	JRCP	10.0	Sand	58.5	No	Yes	?	?	?
	LA 64-2	St. Landry PA, LA	1964	14256	JRCP	10.0	Sand Asphalt	58.5	No	Yes	?	?	?
	MS 1-1	Jackson, MS	1980	195	JPCP	6.5	?	15	Yes	Yes	Silicone	?	?
	MS 1-2	Jackson, MS	1980	195	JPCP	6.5	?	15	No	Yes	Silicone	?	?
	MS 1-3	Jackson, MS	1980	180	JPCP	6.5	?	20	Yes	Yes	Silicone	?	?
	MS 1-4	Jackson, MS	1980	180	JPCP	6.5	?	20	No	Yes	Silicone	?	?
	NC 1-1	Rocky Mount, NC	1967	7339	JPCP	9.0	AGG	30	Yes	No	AC	AC	None
	NC 1-2	Rocky Mount, NC	1967	10507	JPCP	9.0	Soil Cement	30	No	Yes	AC	AC	None
	NC 1-3	Rocky Mount, NC	1967	10243	JPCP	9.0	Soil Cement	30	No	No	AC	AC	None
	NC 1-4	Rocky Mount, NC	1967	9979	JPCP	9.0	AGG	30	No	Yes	AC	AC	None
	NC 1-5	Rocky Mount, NC	1967	10243	JPCP	9.0	CTB	30	No	No	AC	AC	None
	NC 1-6	Rocky Mount, NC	1967	11669	JPCP	9.0	ATB	30	No	No	AC	AC	None
	NC 1-7	Rocky Mount, NC	1967	11986	JRCP	8.0	AGG	60	No	Yes	AC	AC	None
	NC 1-8	Rocky Mount, NC	1967	83530	JPCP	9.0	AGG	30	No	No	AC	AC	None

APPENDIX B NEW PREDICTION MODELS

PRESENT SERVICEABILITY RATING

PSR prediction models were developed for both JPCP and JRCP. Whereas all measured types of distress were initially considered, only three key distress types proved significant: joint faulting, joint deterioration (spalling), and transverse cracking. The presence of full-depth patching also displayed some significance and hence is included in the equations.

JOINTED PLAIN CONCRETE PAVEMENTS

$$PSR = 4.356 - 0.0182\ TFAULT - 0.00313\ SPALL - 0.00162\ TCRKS - 0.00317\ FDR \quad (6)$$

Where:

PSR = Mean panel rating of pavement (0 to 5 AASHTO Scale)

TFAULT = Cumulative transverse joint faulting, in/mi

SPALL = Number of deteriorated (medium- and high-severity) transverse joints per mile

TCRKS = Number of transverse cracks (all severities) per mile

FDR = Number of full-depth repairs per mile

Statistics:

R^2 = 0.58
SEE = 0.31 (units of PSR)
n = 282

JOINTED REINFORCED CONCRETE PAVEMENTS

$$PSR = 4.333 - 0.0539\ TFAULT - 0.00372\ SPALL - 0.00425\ MHTCRKS - 0.000531\ FDR \quad (7)$$

Where:

PSR = Mean panel rating of pavement (0 to 5 AASHTO Scale)

TFAULT = Cumulative transverse joint faulting, in/mi

SPALL = Number of deteriorated (medium- and high-severity) transverse joints per mile

MHTCRKS = Number of medium- and high-severity cracks per mile

FDR = Number of full-depth repairs per mile

Statistics:

R^2 = 0.64
SEE = 0.37 (units of PSR)
n = 434

TRANSVERSE JOINT FAULTING

Two predictive models were developed using the combined data bases; one for nondoweled pavements and one for doweled pavements. Because of the mechanisms involved in faulting, it was not possible to combine these two design types into one model. The models were developed using a combination of mechanistic and empirical approaches.

DOWELED CONCRETE PAVEMENTS

$$FAULT = ESAL^{0.5280} * [\ 0.1204 + 0.04048 * (BSTRESS1 / 1000)^{0.3388} + 0.007353 * (AVJSPACE / 10)^{0.6725}) - 0.1492 * (KSTAT / 100)^{0.05911} - 0.01868 * DRAIN - 0.00879 * EDGESUP - 0.00959 * STYPE\ ] \quad (8)$$

Where:

FAULT = Mean transverse joint faulting, in;

ESAL = Cumulative equivalent 18-kip (80 kN) single-axle loads in lane, millions;

BSTRESS = Maximum concrete bearing stress using closed-form equation, psi;

$$= f_d * P * T * [\ K_d * (2 + BETA * OPENING) / (4 * E_s * I * BETA^3)\ ]$$

$$BETA = [\ K_d * DOWEL / (4 * E_s * I)\ ]^{0.25}$$

f_d = Distribution factor;
$= 2 * 12 / (l + 12)$

l = Radius of relative stiffness, in;
$= [\ E_c * THICK^3 / (12 * (1 - u^2) * KSTAT)\ ]^{0.25}$

E_c = Concrete modulus of elasticity, psi;
$= 14.4 * 150^{1.5} * MR_{28}^{0.77}$

I	=	Moment of inertia of dowel bar cross section, in^4;
	=	0.25 * 3.1416 * (DOWEL / 2)^4
THICK	=	Slab thickness, in;
MR_{28}	=	Concrete modulus of rupture at 28 days, psi;
u	=	Poisson's Ratio, set to 0.15;
P	=	Applied wheel load, set to 9000 lb;
T	=	Percent transferred load, set to 0.45;
K_d	=	Modulus of dowel support, set to 1,500,000 pci;
BETA	=	Relative stiffness of the dowel-concrete system;
DOWEL	=	Dowel diameter, in;
E_s	=	Modulus of elasticity of the dowel bar, set to 29,000,000 psi;
KSTAT	=	Effective modulus of subgrade reaction, on the top of base, psi/in;
OPENING	=	Average transverse joint opening, in
	=	CON * AVJSPACE * 12 * (ALPHA * TRANGE / 2 + e)
AVJSPACE	=	Average transverse joint spacing, ft;
CON	=	Adjustment factor due to base/slab frictional restraint,
	=	0.65 if stabilized base,
	=	0.80 if aggregate base or lean concrete base with bond breaker
ALPHA	=	Thermal coefficient of contraction of PCC, set to 0.000006 /°F;
TRANGE	=	Annual temperature range, °F;
e	=	Drying shrinkage coefficient of PCC, set to 0.00015 in/in;
DRAIN	=	Index for drainage condition,
	=	0, if no edge subdrain exists,
	=	1, if edge subdrain exists;

EDGESUP = Index for edge support,
= 0, if no edge support exists,
= 1, if edge support exists;

STYPE = Index for AASHTO subgrade soil classification,
= 0, if A-4 to A-7,
= 1, if A-1 to A-3;

Statistics:

R^2 = 0.67
SEE = 0.0571 in
n = 559

NONDOWELED CONCRETE PAVEMENTS

$$FAULT = ESAL^{0.2500} * [\ 0.000038 + 0.01830 * (\ 100 * OPENING\ )^{0.5585} + 0.000619 * (\ 100 * DEFLAMI\ )^{1.7229} + 0.0400 * (\ FI / 1000\ )^{1.9840} + 0.00565 * BTERM - 0.00770 * EDGESUP - 0.00263 * STYPE - 0.00891 * DRAIN\ ] \quad (9)$$

Where:

FAULT = Mean faulting across the transverse joints, in;

ESAL = Cumulative 18-kip (80 kN) equivalent single-axle loads in traffic lane, millions;

OPENING = Average transverse joint opening, in;
= CON * AVJSPACE * 12 * (ALPHA * TRANGE / 2 + e)

CON = Adjustment factor due to base/slab frictional restraint,
= 0.65 if stabilized base,
= 0.80 if aggregate base;

AVJSPACE = Average transverse joint spacing, ft;

ALPHA = Thermal coefficient of contraction of PCC, set to 0.000006 /°F;

TRANGE = Annual temperature range, °F; (Minimum average January temperature - Maximum average July temperature)

e = Drying shrinkage coefficient of PCC, set to 0.00015 in/in;

DEFLAMI = Ioannides' corner deflection, in;[42]
= $P * (\ 1.2 - 0.88 * 1.4142 * a / l\ ) / (KSTAT * l^2)$

l = Radius of relative stiffness, in;
= $[\ E_c * THICK^3 / (\ 12 * (\ 1 - u^2\ ) * KSTAT\ )\ ]^{0.25}$

E_c = Concrete modulus of elasticity, psi;
= $14.4 * 150^{1.5} * MR_{28}^{0.77}$

P = Applied wheel load, set to 9000 lb;

a	=	Radius of the applied load, set to 5.64 in, assuming tire pressure = 90 psi;
KSTAT	=	Modulus of subgrade reaction, on the top of base, psi/in;
THICK	=	Slab thickness, in;
u	=	Poisson's Ratio, set to 0.15;
MR_{28}	=	Concrete modulus of rupture at 28 days, psi;
BTERM	=	Base type factor;
	=	$10 * [ESAL^{0.2076} * (0.04546 + 0.05115 * GB + 0.007279 * CTB + 0.003183 * ATB - 0.003714 * OGB - 0.006441 * LCB)]$
GB	=	Dummy variable for dense-graded aggregate base,
	=	1 if aggregate base,
	=	0 otherwise;
CTB	=	Dummy variable for dense-graded, cement-treated base,
	=	1 if cement-treated base,
	=	0 otherwise;
ATB	=	Dummy variable for dense-graded, asphalt-treated base,
	=	1 if asphalt-treated base,
	=	0 otherwise;
OGB	=	Dummy variable for open-graded aggregate base or open-graded asphalt-treated base,
	=	1 if open-graded base,
	=	0 otherwise; and
LCB	=	Dummy variable for lean concrete base,
	=	1 if lean concrete base,
	=	0 otherwise.
FI	=	Freezing index, Degree-Days;
DRAIN	=	Index for drainage condition,
	=	0, if no edge subdrain exists,
	=	1, if edge subdrain exists;

EDGESUP = Index for edge support,
= 0, if no edge support exists,
= 1, if edge support exists;

STYPE = Index for AASHTO subgrade soil classification,
= 0, if A-4 to A-7,
= 1, if A-1 to A-3;

Statistics:

R^2 = 0.81
SEE = 0.028 in
n = 398

TRANSVERSE CRACKING - JOINTED PLAIN CONCRETE PAVEMENTS

Using the concept of fatigue consumption, a mechanistic model was developed for transverse cracking in jointed plain concrete pavements. The form of the model is in the classical S-shape curve, which is thought of as representing actual cracking development.

$$P = \frac{1}{0.01 + 0.03 * [\ 20^{-\log (n/N)}\ ]} \qquad (10)$$

where:

P = Percent of Slabs Cracked
n = Actual number of 18-kip (80 kN) ESAL applications at slab edge
N = Allowable 18-kip (80 kN) ESAL applications

(11)

in which:

$\text{Log}_{10}\ N = 2.13 * [\ 1\ /\ SR\ ]^{1.2}$

SR = Stress Ratio, ratio of computed edge stress to 28-day modulus of rupture

TRANSVERSE JOINT SPALLING

Prediction models were developed separately for JPCP and JRCP. Extensive efforts to develop a single model for joint spalling were not successful. One reason may be that most of the joint spalling for JPCP was of medium-severity, with very few joints with high-severity spalling. JRCP sections, however, had a much greater proportion of joints exhibiting high-severity joint spalling.

JPCP JOINT SPALLING MODEL

$$JTSPALL = AGE^{2.178} * [\ 0.0221 + 0.5494\ DCRACK - 0.0135\ LIQSEAL - 0.0419\ PREFSEAL + 0.0000362\ FI\ ] \quad (12)$$

Where:

JTSPALL = Number of medium-high joint spalls/mile

AGE = Age since original construction, years

DCRACK = 0, if no D-cracking exists
= 1, if D-cracking exists

LIQSEAL = 0, if no liquid sealant exists in joint
= 1, if liquid sealant exists in joint

PREFSEAL = 0, if no preformed compression seal exists
= 1, if preformed compression seal exists

FI = Freezing Index, degree days below freezing

Statistics:

R^2	=	0.59
SEE	=	15 joints/mi
n	=	262

JRCP JOINT SPALLING MODEL

$$JTSPALL = AGE^{4.1232} * [\ 0.00024 + 0.0000269\ DCRACK + 0.000307\ REACTAGG - 0.000033\ LIQSEAL - 0.0003\ PREFSEAL + 0.00000014\ FI\ ] \quad (13)$$

Where:

JTSPALL = Number of medium-high joint spalls/mile

AGE = Age since original construction, years

DCRACK = 0, if no D-cracking exists
= 1, if D-cracking exists

LIQSEAL = 0, if no liquid sealant exists in joint
= 1, if liquid sealant exists in joint

PREFSEAL = 0, if no preformed compression seal exists
= 1, if preformed compression seal exists

FI = Freezing Index, degree days below freezing

REACTAGG = 0, if no reactive aggregate exists
= 1, if no reactive aggregate exists

Statistics:

R^2 = 0.47
SEE = 13 joints/mi
n = 280

REFERENCES

1. J. B. Rauhut, M. I. Darter, R. L. Lytton, P. R. Jordahl, M. P. Gardner, G. L. Fitts, and K. D. Smith, Data Collection Guide for Long-Term Pavement Performance Studies, Draft Report Prepared for the Strategic Highway Research Program (Washington, DC: SHRP, January 1988).

2. K. D. Smith, M. I. Darter, J. B. Rauhut, and K. T. Hall, Distress Identification Manual for the Long-Term Pavement Performance (LTPP) Studies, Draft Report Prepared for the Strategic Highway Research Program (Washington, DC: SHRP, December 1987).

3. UNIFY Relational Database Management System, Version 3.2 (Unify Corporation, 1985).

4. American Association of Highway and Transportation Officials, AASHTO Guide for Design of Pavement Structures (Washington, DC: AASHTO, 1986).

5. K. W. Heinrichs, M. J. Lui, M. I. Darter, S. H. Carpenter, and A. M. Ionnides, Rigid Pavement Analysis and Design, Report No. FHWA-RD-88-068 (Washington, DC: Federal Highway Administration, July 1989).

6. California Department of Transportation, Highway Design Manual (California: CALTRANS, 1975).

7. J. S. Sawan, M. I. Darter, and B. J. Dempsey, Structural Analysis and Design of Portland Cement Concrete Highway Shoulders, Report No. FHWA/RD-81/122 (Washington, DC: Federal Highway Administration, 1982).

8. K. Majidzadeh and G. J. Ilves, Structural Design of Roadway Shoulders—Final Report, Report No. FHWA/RD-86/089 (Washington, DC: Federal Highway Administration, May 1986).

9. R. K. Kher, W. R. Hudson, and B. F. McCullough, A Systems Analysis of Rigid Pavement Design, Research Report No. 123-5 (Austin, TX: University of Texas at Austin, January 1975).

10. R. F. Carmichael and B. F. McCullough, Modification and Implementation of Rigid Pavement Design System, Research Report 123-26 (Austin, TX: University of Texas at Austin, January 1975).

11. Portland Cement Association, Thickness Design for Concrete Highway and Street Pavements, 1984.

12. M. I. Darter and E. J. Barenberg, Design of Zero-Maintenance Plain Jointed Pavement, Vol. 1—Development of Design Procedures, Report No. FHWA-RD-77-111 (Washington, DC: Federal Highway Administration, April 1977).

13. M. I. Darter and E. J. Barenberg, Design of Zero-Maintenance Plain Jointed Pavement, Vol. II—Design Manual, Report No. FHWA-RD-77-112 (Washington, DC: Federal Highway Administration, April 1977).

14. J. Larralde, PMARP User's Manual, FHWA Contract No. DTFH61-85-C-00051 (Purdue, IN: Purdue University, 1985).

15. S. Kopperman, G. Tiller, and M. Tseng, Purdue Pumping Model: PMARP and PEARDARP Interactive Microcomputer Version, FHWA Contract No. DTFH61-85-C-00051 (SRA Technologies, 1986).

16. A. M. Tabatabaie, E. J. Barenberg, and R. E. Smith, Longitudinal Joint Systems in Slip-Formed Rigid Pavements, Vol. II—Analysis of Load Transfer Systems for Concrete Pavements, Report No. FAA-RD-79-4,II (Washington, DC: Federal Aviation Administration, November 1979).

17. A. M. Ioannides, Analysis of Slab-on-Grade for a Variety of Loading and Support Conditions, Ph.D. thesis, University of Illinois at Urbana, 1984.

18. A. M. Ioannides, E. J. Barenberg, and M. R. Thompson, "Finite Element Model with Stress Dependent Support," *Transportation Research Record 954*, Transportation Research Board, 1984.

19. S. D. Tayabji and B. E. Colley, Analysis of Jointed Concrete Pavements, Report No. FHWA/RD-86/041 (Washington, DC: Federal Highway Administration, February 1986).

20. N. F. Robertson, Report on a Study of a Computer Program for Cracking Analysis of Jointed Reinforced Concrete Pavements, Technical Memorandum 472-4 (Austin, TX: University of Texas at Austin, 1985).

21. W. C. Kreger, Computerized Aircraft Ground Flotation Analysis—Edge Loaded Rigid Pavement, Research Report No. ERR-FW-572 (Fort Worth, TX: General Dynamics Corp., January 1967).

22. G. Pickett and G. K. Ray, "Influence Charts for Concrete Pavements," *Transactions, Vol. 116*, ASCE, 1951.

23. K. Majidzadeh, G. J. Ilves, and H. Sklyut, Mechanistic Design of Rigid Pavements, Vol. I—Development of the Design Procedure, Vol. II—Design and Implementation Manual, FHWA Contract No. DOT-FH-11-9568 (Washington, DC: Federal Highway Administration, June 1984).

24. Y. T. Chou, Structural Analysis Computer Programs for Rigid Multicomponent Pavement Structures with Discontinuities—WESLIQID and WESLAYER, Report 1: Program Development and Numerical Presentations; Report 2: Manual for the WESLIQID Finite Element Program; Report 3: Manual for the WESLAYER Finite Element Program, Technical Report GL-81-6 (U.S. Army Engineer Waterways Experiment Station, May 1981).

25. A. J. van Wijk, Purdue Economic Analysis of Rehabilitation and Design Alternatives in Rigid Pavements: A User's Manual for PEARDARP, FHWA Contract No. DTFH61-85-C-00051 (Purdue, IN: Purdue University, 1985).

26. A. J. van Wijk, Rigid Pavement Pumping: 1. Subbase Erosion, 2. Economic Modeling, Final Report, FHWA Contract No. DTFH61-82-C-00035 (Washington, DC: Federal Highway Administration, September 1985).

27. A. J. van Wijk et al., "Pumping Prediction Model for Highway Concrete Pavements," *Journal of Transportation Engineering, Vol. 115, No. 2*, ASCE, March 1989.

28. M. I. Darter, J. M. Becker, and M. B. Snyder, Development of a Concrete Pavement Evaluation System (COPES), Vol. I—Research Report, NCHRP Report 277 (Washington, DC: National Cooperative Highway Research Program, 1984).

29. M. I. Darter, J. M. Becker, and M. B. Snyder, Development of a Concrete Pavement Evaluation System (COPES), Vol.II—User's Manual, NCHRP Project 1-19 (Urbana, IL: University of Illinois, 1984).

30. M. T. Darter, PREDICT program written in Microsoft Basic for the IBM Personal Computer, Urbana, IL.

31. B. J. Dempsey, W. A. Herlache, and A. J. Patel, The Climatic-Materials-Structural Pavement Analysis Program User's Manual, Report No. FHWA/RD-82/126 (Washington, DC: Federal Highway Administration, 1986).

32. B. J. Dempsey, W. A. Herlache, and A. J. Patel, Environmental Effect on Pavements—Vol. III: Theory Manual, Report No. FHWA/RD-84/115 (Washington, DC: Federal Highway Administration, 1986).

33. S. J. Liu and R. L. Lytton, Environmental Effects on Pavements—Vol. IV: Drainage Manual, Report No. FHWA/RD-84/116 (Washington, DC: Federal Highway Administration, 1986).

34. Statistical Analysis System (SAS), Version 6.03 (Cary, NC: SAS Institute, Inc., 1987).

35. J. Larralde, Structural Analysis of Rigid Pavements with Pumping, Final Report, FHWA Contract No. DTFH61-82-C-00035 (Washington, DC: Federal Highway Administration, September 1985).

36. S. Kopperman, G. Tiller, and M. Tseng, ICP-1: Interactive Microcomputer Version, User's Manual: IBM-PC and Compatible Version, Report No. FHWA-TS-87-205 (Washington, DC: Federal Highway Administration, January 1986).

37. "The AASHO Road Test, Report 5—Pavement Research," Highway Research Board, Special Report 61E, Publication No. 954, 1962.

38. M. I. Darter and E. J. Barenberg, Zero-Maintenance Pavement: Results of Field Studies on the Performance Requirements and Capabilities of Conventional Pavement Systems, Report No. FHWA-RD-76-105 (Washington, DC: Federal Highway Administration, 1976).

39. K. T. Hall, J. M. Connor, M. I. Darter, and S. H. Carpenter, Rehabilitation of Concrete Pavements, Volume III—Concrete Pavement Evaluation and Rehabilitation System, Report No. FHWA-RD-88-073 (Washington, DC: Federal Highway Administration, July 1989).

40. R. F. Benekohal and K. T. Hall, "Effect of Lane Widening on Lateral Distribution of Truck Wheels," Paper prepared for presentation at the 69th Annual Meeting of the Transportation Research Board, January 1990.

41. R. B. Rauhut, M. I. Darter, R. L. Lytton, and R. E. DeVor, "Technical Research Area #2, Long-Term Pavement Performance Pre-Implementation Activities," NCHRP Project 20-20, January 1986.

42. A. M. Ioannides, M. R. Thompson, and E. J. Barenberg, "Westergaard Solutions Reconsidered," *Transportation Research Record 1043*, Transportation Research Board, 1985.